



## BOOK OF ABSTRACTS

### Nowelties' Final Conference

*New Materials and Inventive Waste Water Treatment Technologies.  
Harnessing resources effectively through innovation*

**11-12 May 2022, Inter-University Centre Dubrovnik, CROATIA**



University of Zagreb  
Faculty of Chemical  
Engineering and Technology



**Publisher**

Faculty of Chemical Engineering and Technology, University of Zagreb, Croatia

**For the publisher**

Ante Jukić

**Editors**

Sandra Babić, Dragana Mutavdžić-Pavlović, Hrvoje Kušić, Mira Petrović

**Text prepared by**

AUTHORS, who are fully responsible for the abstracts

**Organizers**

Faculty of Chemical Engineering and Technology, University of Zagreb, Croatia

The Catalan Institute for Water Research, Girona, Spain

The Croatian Society of Chemical Engineers

**Organizing committee:**

Prof. Sandra Babić

Faculty of Chemical Engineering and Technology, University of Zagreb, Croatia

Prof. Hrvoje Kušić

Faculty of Chemical Engineering and Technology, University of Zagreb, Croatia

Prof. Dragana Mutavdžić-Pavlović

Faculty of Chemical Engineering and Technology, University of Zagreb, Croatia

Prof. Mira Petrović

The Catalan Institute for Water Research, Girona, Spain

Miyako Nitta

The Catalan Institute for Water Research, Girona, Spain

**Sponsors**

Shimadzu d.o.o.

Labtım Adria d.o.o.

AlphaChrom d.o.o.

**ISBN: 978-953-6470-94-5**

## PREFACE

NOWELTIES is a MSCA European Joint Doctorate (EJD) that provides cutting edge training opportunities for the education of tomorrow's water treatment experts. The core activity is the research programme (composed of 14 individual research projects) aimed at development of inventive water treatment technologies (advanced biological treatments, innovative oxidation processes, hybrid systems) that allow catering for the varied treatment demands for a plethora of interconnected streams arising from recycling loops.

The main objective of the Final Conference is to present the results of NOWELTIES' research program, as well as new achievements in the field of the development and application of new materials and inventive processes for waste water treatment, with specific emphasis on the technologies able to control contamination by organic micropollutants (OMPs) and therefore help overcoming barriers for water reclamation.

Conference will present some recent technological and methodological developments that offer a range of opportunities for transitioning to smart water management and adopting treatment approaches capable of significantly enhancing the degradation of OMPs, whilst exhibiting a low energy footprint and residual stream.

The Conference is intended to be an informal venue that encourages an exchange of the latest information and ideas among scientist and is not limited to NOWELTIES members, but it is open for a wide scientific community, industry and end users.

## TOPICS COVERED

### **Advances in biological treatment of WW**

Biological treatment systems contain a variety of active microorganisms and may operate under different redox conditions. Consequently, there is huge versatility of designs and operations whose optimization may lead to an improvement in process efficiency. The key for optimization lies in the understanding of different biotransformation mechanisms and deciphering of the immense number of enzymatic routes involved in the different biological wastewater treatments.

### **Progress in advanced oxidation processes (AOPs)**

Some oxidative wastewater treatments (i.e., ultraviolet (UV)/hydrogen peroxide (H<sub>2</sub>O<sub>2</sub>) treatment, ozonation (O<sub>3</sub>), photo-Fenton) have reached a high level of development and have been commercialized. Further improvements are focused on the optimization of operational performances, reactor designs and utilization of new technological developments to increase their efficiency. On the other hand, some AOPs are still at the

stage of laboratory research or are merely proof-of-concept. One of the most promising AOPs is based on the use of non-thermal plasma to produce H<sub>2</sub>O<sub>2</sub>, molecular oxygen and hydrogen, and hydroxyl, hydroperoxyl, atomic hydrogen and oxygen, as well as other radicals. Although shown to rapidly and efficiently degrade many organic compounds, little is known about the feasibility of plasma treatment for the removal of more recalcitrant compounds from wastewater or regarding their degradation kinetics and energy efficiency, as well as degradation by-products generated and their toxicity.

### **New materials and application of nanotechnology in WW treatment**

Novel (nano)engineered materials, such as (nano)adsorbents, composite membranes and(photo)catalysts are very promising candidates for the development of next generation treatment technologies. Generally, they exhibit various merits, such as high capacities, fast kinetics, specific affinity towards targeted contaminants, enhanced photocatalytic response for a broad light spectrum, and strong anti-bacterial activity. The field of their application is extremely wide and some examples include carbon tubes, fullerene derivatives, graphene-based materials (graphene, graphene oxide and reduced graphene oxide), functionalized zeolites, fibers with core shell structure, nano metals or metal oxides.

### **Hybrid WW treatments**

Combining biological processes with innovative physico-chemical processes employing novel (nano) engineered materials and/or next-generation integrated membrane processes establishes multiple barriers towards a wide range of different OMPs that should also be effective against microbial contaminants (i.e., viruses, antibiotic resistant bacteria or antibiotic resistance genes) as well as remove residual nutrients. Such high performing and compact hybrid systems will also offer new opportunities to establish robust concepts for decentralized wastewater treatment facilitating local water reclamation and reuse.

We would like to thank to all participants and especially to the invited speakers and sponsoring organizations for their support in this event, as well as the Inter-University Centre Dubrovnik for the excellent facilities.

Wishing you an enjoyable stay in Dubrovnik!

Sandra Babić, Dragana Mutavdžić-Pavlović, Hrvoje Kušić, Mira Petrović

*This project has received funding from the European Union's Horizon 2020 research and innovation programme under the Marie Skłodowska-Curie grant agreement No 812880*

# CONFERENCE PROGRAMME

## Wednesday, 11<sup>th</sup> May 2022

- 9:00 – 10:00 Registration  
10:00 – 10:15 Welcome  
10:15 – 11:00 **Christa McArdell**, EAWAG, Duebendorf, Switzerland  
*Advanced wastewater treatment: experience in Switzerland*

### SESSION 1. Advances in biological treatment of wastewater

- 11:00 – 11:30 **Alette Langenhoff**, Wageningen University, the Netherlands  
*Biological treatment technologies for the removal of micropollutants*
- 11:30 – 12:00 Poster session / Coffee break
- 12:00 – 12:30 **Silvana Quiton-Tapia**, University of Santiago de Compostela, Spain  
Supervisors: Francisco Omil, Andreas Schaeffer, Sonia Suarez  
*Evaluating antibiotic biotransformation during denitrification by heterotrophic and nitrite-driven anaerobic methane oxidation bacteria*
- 12:30 – 13:00 **Ana Paulina López**, RWTH Aachen University, Germany  
Supervisors: Andreas Schaeffer and Juan Lema  
*Thresholds for microbial degradation of wastewater contaminants: relationship between bioavailability and the onset of biodegradation*
- 13:00 – 13:30 **Edwin Antonio Chingate**, Technical University of Munich, Germany  
Supervisors: Jörg E. Drewes, Uwe Hübner, Maria Jose Farre  
*Transformation of sulfamethoxazole and atenolol by microbial community adapted to histidine*
- 13:30 – 15:00 Lunch

### SESSION 2: Progress in advanced oxidation processes (AOPs)

- 15:00 – 15:30 **Urška Lavrenčič Štanga**, University of Ljubljana, Slovenia  
*The effect of water matrix on photocatalytic degradation of bisphenols and pharmaceuticals*
- 15:30 – 16:00 **Amit Kumar**, Institute of Physics Belgrade, Serbia  
Supervisors: Nevena Puac, Wolfgang Gernjak  
*Wastewater treatment by using cold atmospheric plasma*

- 16:00 – 16:30 **Barbara Topolovec**, Catalan Institute for Water Research (ICRA), Girona, Spain  
Supervisors: Mira Petrovic, Paola Verlicchi, Nevena Puac  
*Degradation and of per- and polyfluorinated alkyl substances (PFAS) during plasma treatment*
- 16:30 – 17:00 Poster session / Coffee break
- 17:00 – 17:30 **Danilo Bertagna Silva**, Faculty of Chemical Engineering and Technology (FKIT), University of Zagreb, Croatia  
Supervisors: Sandra Babić, Gianluigi Buttiglieri  
*Application of UV-LEDs advanced oxidation processes for the efficient removal of organic micropollutants from water*
- 18:00 Welcome party and dinner

Thursday, 12<sup>th</sup> May 2022

**SESSION 3: New materials and application of nanotechnology in wastewater treatment**

- 10:00 – 10:30 **Adrian M. T. Silva**, University of Porto, Portugal  
*Carbon materials as catalysts in AOPs for water/wastewater treatment*
- 10:30 – 11:00 **Camilo Sánchez**, Faculty of Mechanical Engineering and Naval Architecture, University of Zagreb  
Supervisors: Lidija Ćurković, Davor Ljubas, Jelena Radjenovic  
*Microwave-assisted synthesis of N/TiO<sub>2</sub>/rGO and immobilization on alumina ceramic foam substrate for photocatalytic degradation of pharmaceuticals*
- 11:00 – 11:30 **Sabrina Rose de Boer**, University of Santiago de Compostela, Spain  
Supervisors: Maria Teresa Moreira, Andreas Schaeffer  
*Magnetic biocatalyst formulation with unspecific peroxygenase from *Agrocybe Aegerita* for antibiotic removal*
- 11:30 – 12:00 Poster session / Coffee break
- 12:00 – 12:30 **Francis dela Rosa**, Faculty of Chemical Engineering and Technology (FKIT), University of Zagreb, Croatia  
Supervisors: Hrvoje Kušić, Mira Petrovic  
*TiO<sub>2</sub>-based composite photocatalytic materials for solar driven water purification: Recent achievements, challenges and opportunities*
- 12:30 – 13:00 **Barbara Kalebić**, Faculty of Technology and Metallurgy, University of Belgrade, Serbia  
Supervisors: Nevenka Rajić, Lidija Ćurković, Nikola Skoro

*Removal of ciprofloxacin using zeolite-based adsorbents: Adsorption kinetics, mechanism, and regeneration of the spent adsorbents*

13:00 – 13:30 **Matej Kern**, Ruđer Bošković Institute, Zagreb, Croatia  
*Modeling the adsorption of emerging contaminants on carbon nanomaterials*

13:30 – 15:00 Lunch

#### **SESSION 4: Hybrid wastewater treatments**

15:00 – 15:30 **Uwe Hübner**, Technical University of Munich, Germany  
*Hybrid systems for wastewater treatment*

15:30 – 16:00 **Marina Gutierrez**, University of Ferrara, Italy  
Supervisors: Paola Verlicchi, Dragana Mutavdžić-Pavlović  
*Addition of activated carbon to an MBR: Strategies to improve micropollutants removal supported by statistical analysis and adsorption experiments*

16:00 – 16:30 **Michele Ponzelli**, Catalan Institute for Water Research (ICRA), Girona, Spain  
Supervisors: Jelena Radjenovic, Konrad Koch  
*The impact of graphene oxide on methane production kinetics*

16:30 – 17:00 Poster session / Coffee break

17:00 – 17:30 **Nebojša Ilić**, Technical University of Munich, Germany  
Supervisors: Jörg Drewes, Uwe Hübner, Gumersindo Feijoo  
*Fabrication of composite materials using MOFs to achieve super hydrophobic materials with exceptional adsorption performance towards PFAS*

17.30 – 18:00 **Nikoletta Tsiarta**, Catalan Institute for Water Research (ICRA), Girona, Spain  
Supervisors: Wolfgang Gernjak, Lidija Ćurković  
*Degradation of pharmaceuticals with heterogeneous catalytic ozonation-membrane filtration process using modified ceramic membranes*

18:00 End of conference

**18:30** **City tour**

# CONTENTS

## INVITED LECTURES

<b>Christa McArdell</b> Advanced wastewater treatment: experience in Switzerland	1
<b>Alette Langenhoff</b> Biological treatment technologies for the removal of micropollutants	4
<b>Lev Matoh, Boštjan Žener, Urška Lavrenčič Štangar</b> The effect of water matrix on photocatalytic degradation of bisphenols and pharmaceuticals	7
<b>Adrian M. T. Silva</b> Carbon materials as catalysts in AOPs for water/wastewater treatment	9
<b>Jörg E. Drewes &amp; Uwe Hübner</b> Hybrid systems for wastewater treatment	11

## ORAL PRESENTATIONS

<b>Silvana Quiton-Tapia, Balboa Sabela, Sonia Suarez, Francisco Omil</b> Evaluating antibiotic biotransformation during denitrification by heterotrophic and nitrite-driven anaerobic methane oxidation bacteria	13
<b>Ana Paulina López, Alba M. Trueba S., Juan M. Lema R., Andreas Schäffer, Kilian E. C. Smith</b> Thresholds for microbial degradation of wastewater contaminants: relationship between bioavailability and the onset of biodegradation	17
<b>Edwin Antonio Chingate, M. Ozluer, M. J. Farre, Jörg E. Drewes, C. Wurzbacher, Uwe Hübner</b> Transformation of sulfamethoxazole and atenolol by microbial community adapted to histidine	21
<b>Amit Kumar, Nikola Škoro, Wolfgang Gernjak, Nevena Puac</b> Wastewater treatment by using cold atmospheric plasma	25
<b>Barbara Topolovec, Nevena Puac, Nikola Skoro, Mira Petrovic</b> Degradation and study of transformation products of per- and polyfluorinated alkyl substances (PFAS) during plasma treatment	29



<b>Danilo Bertagna Silva, Gianluigi Buttiglieri, Sandra Babić</b> Application of UV-LEDs advanced oxidation processes for the efficient removal of organic micropollutants from water	33
<b>Camilo Sánchez, Zrinka Švagelj, Vilko Mandić, Jelena Radjenovic, Davor Ljubas, Lidija Ćurković</b> Microwave-assisted synthesis of N/TiO <sub>2</sub> /rGO and immobilization on alumina ceramic foam substrate for photocatalytic degradation of pharmaceuticals	37
<b>Sabrina Rose de Boer, Andreas Schaeffer, Maria Teresa Moreira</b> Magnetic biocatalyst formulation with unspecific peroxygenase from <i>Agrocybe Aegerita</i> for antibiotic removal	42
<b>Francis dela Rosa, Hrvoje Kušić, Mira Petrović</b> TiO <sub>2</sub> -Based Composite Photocatalytic Materials for Solar Driven Water Purification: Recent Achievements, challenges and opportunities	46
<b>Barbara Kalebić, Arijeta Bafti, Gordana Matijašić, Davor Ljubas, Lidija Ćurković</b> Removal of ciprofloxacin using zeolite-based adsorbents: Adsorption kinetics, mechanism, and regeneration of the spent adsorbents	50
<b>Matej Kern, Klaudija Ivanković, Sanja Škulj, Marko Rožman</b> Modeling the adsorption of emerging contaminants on carbon nanomaterials	54
<b>Marina Gutierrez, Andrea Ghirardini, Dragana Mutavdžić Pavlović, Paola Verlicchi</b> Addition of activated carbon to an MBR: Strategies to improve micropollutants removal supported by statistical analysis and adsorption experiments	58
<b>Michele Ponzelli, Jörg E. Drewes, Jelena Radjenovic, Konrad Koch</b> The impact of graphene oxide on methane production kinetics	62
<b>Nebojša Ilić, Soumya Mukherjee, Uwe Hübner, Oliver Knoop, Roland Fischer, Jörg E. Drewes</b> Fabrication of composite materials using MOFs to achieve super hydrophobic materials with exceptional adsorption performance towards PFAS	66
<b>Nikoletta Tsiarta, Ivana Panžić, Lidija Ćurković, Wolfgang Gernjak</b> Degradation of pharmaceuticals with heterogeneous catalytic ozonation-membrane filtration process using modified ceramic membranes	70

## POSTER PRESENTATIONS

- Lucija Radetić, Igor Jajčinović, Ivan Brnardić, Ivana Grčić, Jan Marčec, Kristina Miklec**  
Study of micropollutants photocatalytic degradation using TiO<sub>2</sub> and TiO<sub>2</sub>/CNT in optimal reactor configuration 74
- Sofía Estévez, Sara Feijoo, Mohammadreza Kamali, Raf Dewil, Maria Teresa Moreira**  
Prospecting the environmental profile of advanced electrochemical oxidation according to key performance indicators (KPIs) in wastewater treatment 75
- Kristina Tolić Čop, Dragana Mutavdžić Pavlović**  
Effect of water constituents and scavengers on the photocatalytic degradation of anticancer drugs 77
- Martina Kocijan, Lidija Čurković, Tina Radošević, Damjan Vengust, Matejka Podlogar**  
Enhanced photocatalytic degradation of methylene blue by TiO<sub>2</sub>-rGO binary nanocomposites 78
- Lidija Čurković, Debora Briševac, Vilko Mandić, Davor Ljubas, Rea Veseli**  
Photocatalytic degradation of ciprofloxacin by sol-gel derived Ce-doped TiO<sub>2</sub> films 79
- Davor Ljubas, Sandra Babić, Lidija Čurković, Alan Badrov**  
Photolytic and photocatalytic degradation of trimethoprim in aqueous solution 80
- André Torres-Pinto, Hanane Boumeriame, Cláudia G. Silva, Joaquim L. Faria, Adrián M.T. Silva**  
Production of H<sub>2</sub>O<sub>2</sub> for water treatment by photoactive functionalized carbon nitride materials 81

## INVITED LECTURES

## Advanced wastewater treatment: experience in Switzerland

Christa S. McArdell

Eawag, Swiss Federal Institute of Aquatic Science and Technology, CH-8600 Dübendorf, Switzerland

### Micropollutants in the ecosystem: Swiss strategy

Effluents from conventional wastewater treatment plants (WWTPs), in which various micropollutants (MPs) are not or not completely removed, is one major source of them. Swiss authorities have decided to implement additional wastewater treatment steps as mitigation strategy to improve water quality and to avoid potential negative ecological effects by MPs. A new water protection act entered into force as from January 2016 which requires to upgrade selected wastewater treatment facilities with advanced treatment to eliminate organic MPs by 80% from influent to effluent until 2040 (Eggen et al. 2014; FOEN law 2017; Bourgin et al. 2018).

### Treatment technologies

Treatment with powdered activated carbon (PAC) and ozonation were originally the methods of choice to comply with the demands of the new law. However, other treatment technologies were also evaluated and implemented in the last years. Treatment with granular activated carbon (GAC) in a filter or in a moving bed was tested in several pilot plants, and is now implemented each in one WWTP in Switzerland. Another WWTP is running with a combination of ozonation and GAC filtration. The VSA Platform Process Engineering Micropollutants ([www.micropoll.ch](http://www.micropoll.ch)) is collecting information on the upgrade (see Figure 1), disseminates knowledge to stakeholders and supports the exchange between stakeholders.

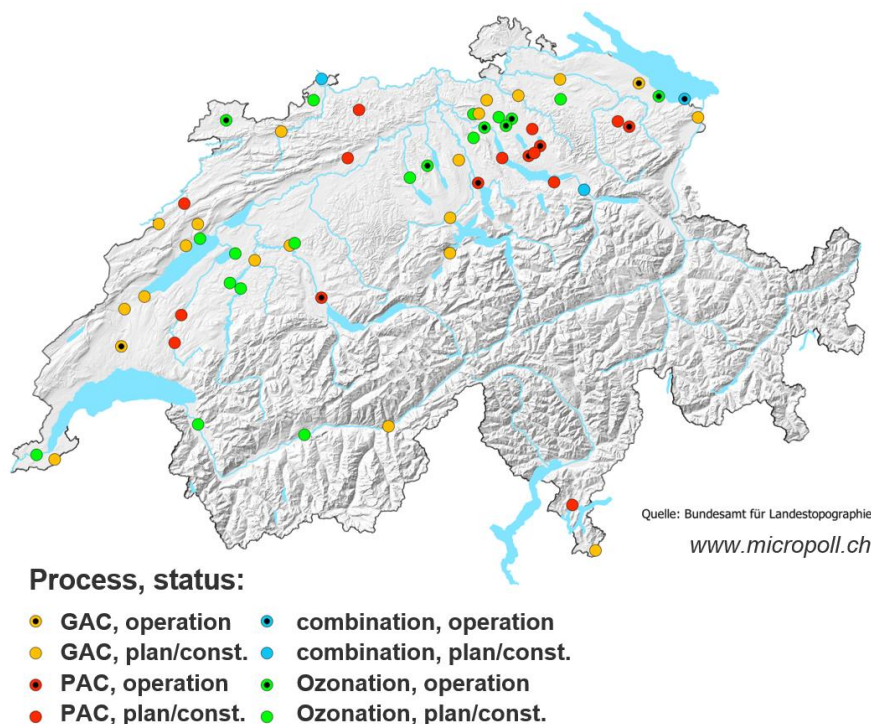


Figure 1. Advanced treatment in Swiss wastewater treatment plant, as of September 2021. Colors indicate the treatment technologies; plants with a black dot are in operation, while others are in the planning phase or under construction. Source: [www.micropoll.ch](http://www.micropoll.ch).

### *Financing*

The financing of the advanced treatment is based on the polluters pay principle. The government introduced a wastewater tax for WWTPs which asks a fee of 9 CHF (about 8 Euro) per person and year. From this stock, 75% of the investment costs for the upgrade is paid. Upgraded WWTPs do not have to pay wastewater tax anymore, but have higher operating costs. Overall, this results in an increase of costs for wastewater treatment of about 10-15%.

### *Ozonation*

Ozonation is an economic, technically feasible and robust technology with a small footprint. However, several investigations showed that toxic by-products might be formed (Schmidt and Brauch 2008; Stalter et al. 2010; Kienle et al. 2022). Therefore, the suitability of ozonation must first be tested according to a decision tool (Schindler Wildhaber et al. 2015). Ozonation must be followed by a biological post-treatment to abate potentially problematic by-products that are easily degradable, probably mostly originating from the wastewater matrix (von Gunten 2018).

The transformation products of MPs formed during ozonation (OTPs) and their fate in biological or sorptive post-treatments is largely unknown. In analogy to AOC or BDOC, it is often assumed that OTPs are well-biodegradable. This was tested in a recent study on the OTPs of 50-100 relevant MPs in wastewater as well as in surface water treatment (Gulde et al. 2021a&b). Overall, abatement of the OTPs was poor in biological sand filtration, better in GAC columns (but with decreasing efficiency with higher bed volumes), and best in PAC treatment.

### *PAC treatment*

Adsorption to PAC has proven to be a robust and efficient technology to remove MPs. Several process varieties for PAC applications are implemented. Originally, PAC dosage was mainly performed after the biological treatment with subsequent sedimentation and filtration. Recycling the loaded PAC from the post-treatment to the biological unit allows to reduce the PAC dose, and PAC is incinerated together with the sludge. Applications with smaller footprints are PAC addition onto sand filtration or directly to the conventional activated sludge, requiring a higher PAC dose (Siegrist et al. 2018).

### *GAC treatment*

The filtration with GAC is a promising alternative and is implemented already in full scale in WWTPs in Germany with good success (Benstoem et al. 2017), and also finds its application in Switzerland. GAC filtration has many benefits, as it can be filled into existing deep bed filters (sand filters), and can be reactivated and reused, therefore having a smaller CO<sub>2</sub> footprint. However, there are still uncertainties related to economic competitiveness and filter design. Pilot scale studies have shown the importance of a minimal empty bed contact time of 20 minutes (Böhler et al. 2020a&b, McArdell et al. 2020).

### *Combined treatment*

At WWTP Altenrhein, a combined treatment of a low specific ozone dose (0.15-0.3 gO<sub>3</sub>/gDOC) and GAC filters is implemented since September 2019. A low specific ozone dose as pre-treatment resulted in a lifetime of GAC more than 2x longer than a pure GAC filter (Böhler et al. 2020a, McArdell et al. 2020), and is therefore a promising alternative, but investment costs are higher.

## References

- Benstoem, F., Nahrstedt, A., Boehler, M., Knopp, G., Montag, D., Siegrist, H., Pinnekamp, J. (2017). Performance of granular activated carbon to remove micropollutants from municipal wastewater - a meta-analysis of pilot- and large-scale studies. *Chemosphere* 185, 105-118.
- Böhler, M., Hernandez, A., Baggenstos, M., McArdell, C.S., Siegrist, H., Joss, A. (2020a) Elimination von Spurenstoffen durch granulierten Aktivkohle-Filtration (GAK): Grosstechnische Untersuchungen auf der ARA Furt, Bülach. Schlussbericht Eawag, Dübendorf, Schweiz.  
<https://www.dora.lib4ri.ch/eawag/islandora/object/eawag%3A21845>
- Böhler M., Joss A., McArdell C., Meier A. (2020b). Hinweise zur Planung und Auslegung von diskontinuierlich gespülten GAK-Filtern zur Elimination organischer Spurenstoffe aus kommunalem Abwasser. Konsenspapier zum Ergebnis eines Workshops mit Fachexperten aus der Schweiz und Deutschland, Eawag und VSA, Dübendorf.  
<https://www.dora.lib4ri.ch/eawag/islandora/object/eawag%3A21003>
- Bourgin, M., Beck, B., Boehler, M., Borowska, E., Fleiner, J., Salhi, E., Teichler, R., von Gunten, U., Siegrist, H., McArdell, C.S. (2018). Evaluation of a full-scale wastewater treatment plant upgraded with ozonation and biological post-treatments: abatement of micropollutants, formation of transformation products and oxidation by-products. *Water Res.* 129, 486–498.
- Eggen, R.I.L., Hollender, J., Joss, A., Schäfer, M., Stamm, C. (2014). Reducing the discharge of micropollutants in the aquatic environment: the benefits of upgrading wastewater treatment plants. *Environ. Sci. Technol.* 48 (14), 7683–7689.
- FOEN law (2017), [www.bafu.admin.ch/bafu/de/home/themen/bildung/medienmitteilungen.msg-id-59323.html](http://www.bafu.admin.ch/bafu/de/home/themen/bildung/medienmitteilungen.msg-id-59323.html)
- Gulde, R., Rutsch, M., Clerc, B., Schollée, J.E., von Gunten, U., McArdell, C.S. (2021a) Formation of transformation products during ozonation of secondary wastewater effluent and their fate in post-treatment: From laboratory- to full-scale. *Water Res.*, 200,117200.
- Gulde, R., Clerc, B., Rutsch, M., Helbing, J., Salhi, E., McArdell, C.S. von Gunten, U. (2021b) Oxidation of 51 micropollutants during drinking water ozonation: Formation of transformation products and their fate during biological post-filtration. *Water Res.* 117812.
- Kienle, C., Werner, I., Fischer, S., Lüthi, C., Schifferli, A., Besselink, H., Langer, M., McArdell, C.S., Vermeirssen, E. (2022) Evaluation of a full-scale wastewater treatment plant with ozonation and different post-treatments using a broad range of in vitro and in vivo bioassays. *Water Res.*, 212, 118084.
- McArdell, C.S., Böhler, M., Hernandez, A., Oltramare C., Büeler A., Siegrist, H. (2020) Pilotversuche zur erweiterten Abwasserbehandlung mit granulierter Aktivkohle (GAK) und kombiniert mit Teilozonung (O3/GAK) auf der ARA Glarnerland (AVG), Ergänzende Untersuchungen zur PAK-Dosierung in die biologische Stufe mit S::Select®-Verfahren in Kombination mit nachfolgender GAK. Schlussbericht Eawag, Dübendorf, Schweiz.  
<https://www.dora.lib4ri.ch/eawag/islandora/object/eawag%3A21543>
- Schindler Wildhaber, Y., Mestankova, H., Scharer, M., Schirmer, K., Salhi, E., von Gunten, U. (2015). Novel test procedure to evaluate the treatability of wastewater with ozone. *Water Res* 75, 324–335 .
- von Gunten, U. (2018). Oxidation processes in water treatment: are we on track? *Environ. Sci. Technol.* 52 (9), 5062–5075.
- Schmidt, C.K., Brauch, H.J. (2008). N,N-dimethylsulfamide as precursor for Nnitrosodimethylamine (NDMA) formation upon ozonation and its fate during drinking water treatment. *Environ. Sci. Technol.* 42 (17), 6340–6346.
- Siegrist, H., Joss, A., Boehler, M., McArdell, C.S. Ternes, T. (2018) Organic Micro-Pollutant Control. Chapter 6 in *Advances in Wastewater Treatment*, Editors: Giorgio Mannina, George Ekama, Hallvard Ødegaard and Gustaf Olsson, IWA Publishing, ISBN 9781780409702, eISBN 9781780409719.
- Stalter, D., Magdeburg, A., Weil, M., Knacker, T., Oehlmann, J. (2010). Toxication or detoxication? In vivo toxicity assessment of ozonation as advanced wastewater treatment with the rainbow trout. *Water Res.* 44 (2), 439–448.

## Biological treatment technologies for the removal of micropollutants

Alette Langenhoff

Environmental Technology, Wageningen University

### Introduction

As most micropollutants (MPs) are poorly removed in our current wastewater treatment plants (WWTPs), our current WWTP need to be upgraded or post treatment technologies should be added. In general, micropollutants can be removed from wastewater effluent by numerous processes, that can be categorized as biological, physical or chemical technologies and combinations hereof.

In our study, we assessed the operation and biological removal of MPs in three lab scale bioreactors; a biological activated carbon filter, a sand filter, and a moving bed bioreactor. Furthermore, the removal of melamine as model compound was further tested in the biological activated carbon filter, to distinguish between biodegradation and adsorption. This helps identifying the extend of bioregeneration of the activated carbon, and thus the lifetime a biological activated carbon filter.

### Methods

Three lab scale bioreactors (1.7 L) were inoculated with a mix of biological active sludges collected at four WWTPs in the Netherlands one year prior to the experiments. Effluent of the secondary clarifier from the WWTP in Bennekom (the Netherlands) was used as feed for the three reactors. The feed was stored in a 3 m<sup>3</sup> tank at 4°C and continuously stirred. A mix of 18 MPs was spiked to the feed, to reach a MP concentration of 2 µg/L each. The reactors were operated at five flow rates (0.25, 0.5, 1, 2 and 4 L/h) in a continuous setup. Samples were taken regularly, and analysed for various parameters, including MPs.

The biodegradation and adsorption of melamine on activated carbon was studied in more detail in batch experiments.

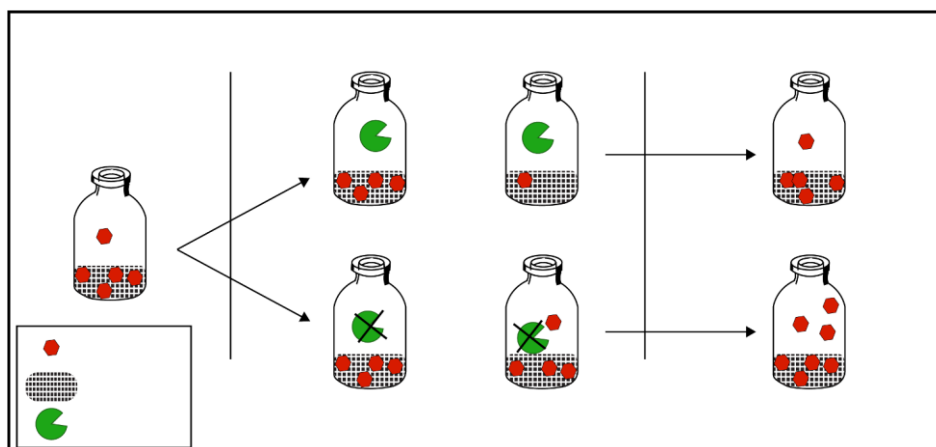


Figure 1. Schematic representation of steps in GAC bioregeneration experiment.

Melamine degrading biomass was obtained from a melamine degrading WWTP plant and used to bioregenerate activated carbon loaded with melamine in a 3-step batch experiment (Fig. 1) as follows (1) loading of activated carbon, (2) bioregeneration of activated carbon, and (3) reloading of activated carbon (assessment of bioregeneration extent).

## Results

The biological activated carbon filter showed immediate removal of the added MPs, and achieved an average removal of 85% for the 18 analysed micropollutants (Fig. 2). The sandfilter and moving bed bioreactor showed much less MP removal, varying from 0 – 60%, which slightly increased during the 12 weeks operation period.

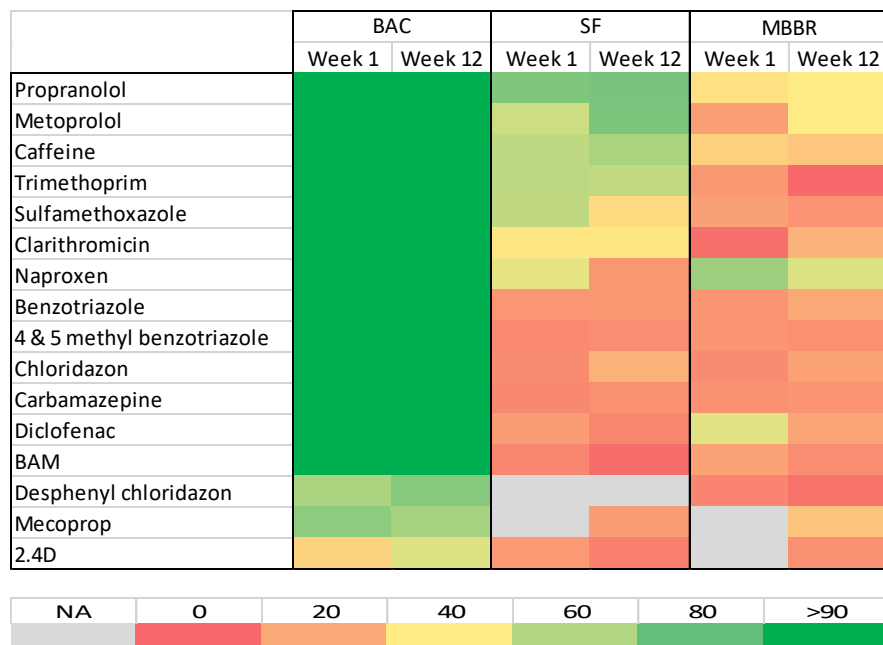


Figure 2. Micropollutant removal in the biological activated carbon (BAC) filter, sand filter (SF) and moving bed bioreactor (MBBR).

Furthermore, the biological activated carbon filter also achieved a higher organic matter removal than the sand filter and moving bed bioreactor (respectively 72%, 41%, and 21%).

The removal capacity in the biological activated carbon filter is a combination of adsorption and degradation, and the contribution of each process determines the lifetime of such a filter. Biological degradation of adsorbed compounds will release adsorbing sites of the activated carbon and will extend the lifetime of the used activated carbon.

The extend of such bioregeneration of activated carbon was tested in batch experiments with melamine as a model compound. Melamine was biodegraded under both oxic or anoxic conditions and melamine degrading biomass was found to restore at least 28% of the original GAC adsorption capacity. Furthermore, our results indicate that bioregeneration occurs mainly in the largest pore fraction of GAC, impacting adsorption kinetics.

To demonstrate these batch results also in activated carbon filters, column experiments were performed and combined with modelling.



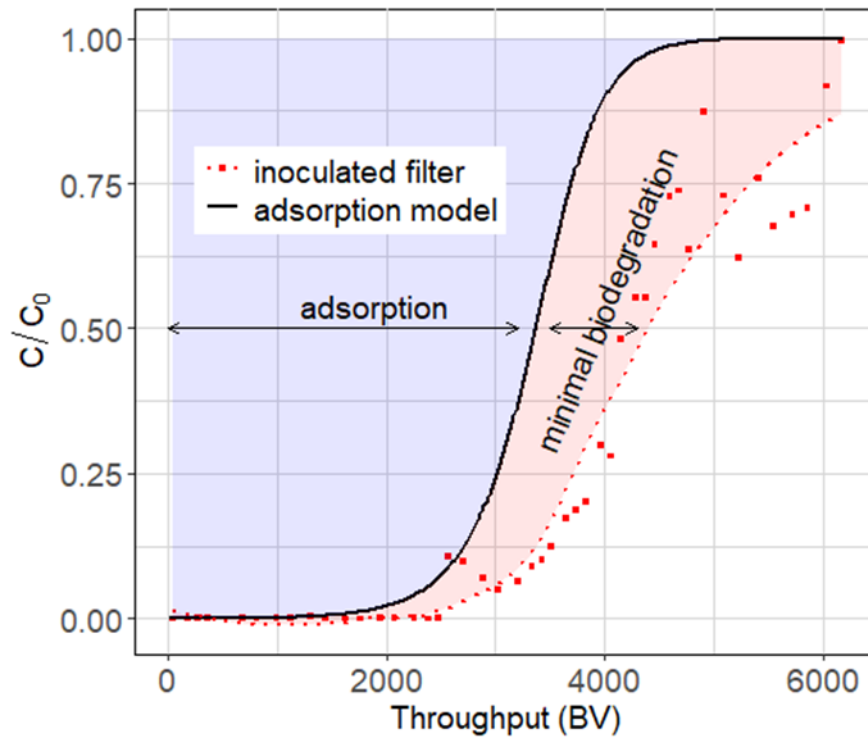


Figure 3: Relative melamine concentration in effluent of an inoculated filter (BAC 1) and modelled breakthrough curve.

Our data show that inoculation of activated carbon filters enhanced the lifetime of the filter, as pronounced biodegradation of melamine was observed (Fig. 3).

### Conclusion

A biological activated carbon filter showed the highest removal of micropollutants and organic matter, compared to a sand filter and moving bed bioreactor. The lifetime of such a filter depends on the regeneration of the activated carbon. With melamine as a model compound, we have shown that bioregeneration has a large potential for restoring and maintaining removal capacity of MPs in biological activated carbon filters. Further enhancing the biodegradation of micropollutants in these filters is a promising strategy to increase the sustainability and applicability of biological activated carbon filters.

# The effect of water matrix on photocatalytic degradation of bisphenols and pharmaceuticals

Lev Matoh, Boštjan Žener, Urška Lavrenčič Štangar\*

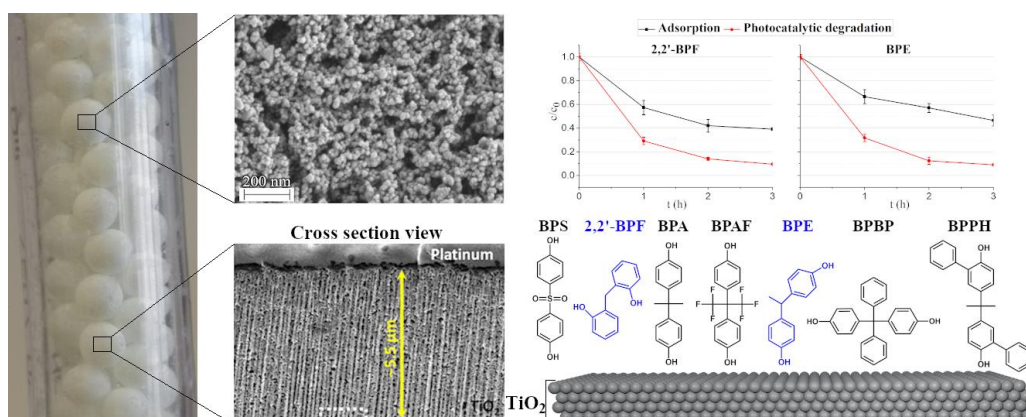
Faculty of Chemistry and Chemical Technology, University of Ljubljana, Večna pot 113, 1000 Ljubljana, Slovenia

\*Email: urska.lavrencic.stangar@fkkt.uni-lj.si

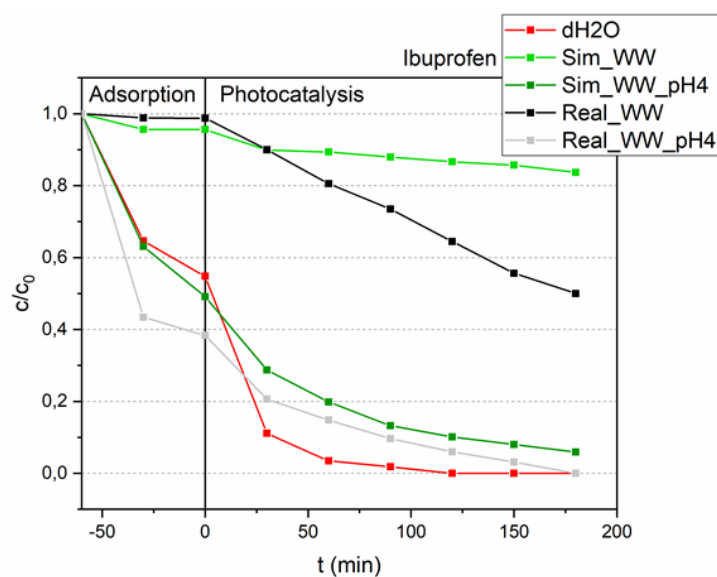
Access to clean and potable water has become increasingly important in recent years due to exponential population growth, industrialization, and irrigation. Nearly half of the world's population lives in regions where the demand for water is greater than the ability of aquifers to replenish, and because of this imbalance water reuse is crucial. Therefore, it is important to develop efficient, non-destructive, and sustainable methods for wastewater reuse [1]. Advanced oxidation processes (AOP) and especially heterogeneous photocatalysis represent a potential solution to this problem, as they are capable of degrading organic molecules to non-hazardous products – CO<sub>2</sub>, H<sub>2</sub>O and other inorganic substances [2].

Water polluting compounds are one of the biggest problems today. Among the most potent xenobiotics are pharmaceuticals and endocrine disruptors that are dissolved in wastewater and released into the environment. Powerful photocatalytic reactors are necessary to make efficient use of photocatalysis, as they allow the reuse of water in production processes, thus reducing the consumption of potable water and the release of mobile and persistent chemicals into the environment [3]. For the experiments conducted in this study, a packed bed reactor system was used in which the titanium dioxide photocatalyst was deposited on ~3 mm glass beads [4]. These beads were then packed into a tube (diameter ~10 mm) with a volume of 50 mL. We chose glass beads as substrates because it allowed us to achieve good filling and a relatively large available surface area of the photocatalyst for improved efficiency. The photocatalyst in film or powder form was characterized by thermal analysis, XRD, FIB /SEM, TEM /EDS and XPS measurements.

The photocatalytic efficiency of our system was first tested by observing the degradation rate of plasmocorinth B, an organic dye. Then, 18 bisphenols were co-dissolved in distilled water and simulated wastewater to follow their removal under UV light [4]. The simulated wastewater influent was prepared and processed according to Kovačič et al. [5] by first dissolving the nutrients in 20 L of tap water. Two suspended activated sludge reactors were fed with 2 L/day of the synthetic wastewater for five days. The reactor effluent was then collected and used for the photodegradation experiments and calibration curve generation. The developed photocatalytic reactor effectively removed organic dye and bisphenols from the aqueous medium by a combination of adsorption and photocatalysis. The degradation rates of bisphenols in simulated wastewater were, as expected, lower than in pure water, because wastewater contains other organics that the photocatalyst can degrade. Nevertheless, a removal rate of 90% can be observed for most compounds after 2 hours of illumination and almost complete removal after 3 hours, except for most polar BPS (~ 60%). The lower degradation rate of the latter can be attributed to its lower adsorption rate.



We also focused on the degradation of various pharmaceutical compounds in simulated wastewater and water effluent from a central wastewater treatment plant and compared the results with degradation in deionized H<sub>2</sub>O. Again, as expected, the reactions in wastewater were slower than in deionized H<sub>2</sub>O, yet it was shown that removal of the compounds from the water was still possible even when other organic molecules were present. The compounds tested included: metronidazole (used in our previous work with the CPC reactor [6]), oxytetracycline, marbofloxacin, ibuprofen, diclofenac, phenytoin, ciprofloxacin, sulfamethoxazole. The effect of adjusting the pH of wastewater on the degradation speeds of selected compounds was also explored and the results showed that acidic pH can increase the reaction rate and adsorption on the photocatalyst surface. The figure below shows the adsorption and photocatalytic degradation of ibuprofen in different water matrices (clean water, simulated wastewater, real water effluent from a central wastewater treatment plant) and at different pH values (natural and acidic).



**Keywords:**

**photocatalysis; TiO<sub>2</sub>; organic pollutants; wastewater treatment**

**References**

- [1] G. Crini, E. Lichtfouse, Environ. Chem. Lett. 17 (2019) 145–155.
- [2] M.R. Al-Mamun, S. Kader, M.S. Islam, M.Z.H. Khan, J. Environ. Chem. Eng. 7 (2019) 1-17.
- [3] K.P. Sundar, S. Kanmani, Chem. Eng. Res. & Des. 154 (2020) 135-150.
- [4] B. Žener, L. Matoh, P. Rodič, D. Škufca, E. Heath, U. Lavrenčič Štangar, J. Environ. Chem. Eng. 9 (2021) 106814.
- [5] A. Kovačič, M. Česen, M. Laimou-Geraniou, D. Lambropoulou, T. Kosjek, D. Heath, E. Heath, Environ. Res. 179 (2019) 108738.
- [6] S. Talwar, A. Kumar Verma, V. Kumar Sangal, U. Lavrenčič Štangar, Chem. Eng. J. 388 (2020) 124184.

**Acknowledgements**

The authors acknowledge the financial support from the Slovenian Research Agency (research core funding No. P1-0134 and project No. L7-1848).

## Carbon materials as catalysts in AOPs for water/wastewater treatment

Adrián M.T. Silva<sup>1,2</sup>

<sup>1</sup> LSRE-LCM - Laboratory of Separation and Reaction Engineering – Laboratory of Catalysis and Materials, Faculty of Engineering, University of Porto, Rua Dr. Roberto Frias, 4200-465 Porto, Portugal.

<sup>2</sup> ALiCE - Associate Laboratory in Chemical Engineering, Faculty of Engineering, University of Porto, Rua Dr. Roberto Frias, 4200-465 Porto, Portugal.

adrian@fe.up.pt

We are facing new challenges with the spread of organic chemical micropollutants in water bodies. Water is a highly sensitive natural resource and priority substances (PSs) and contaminants of emerging concern (CECs) have been found in the aquatic environment, often up to  $\mu\text{g L}^{-1}$  levels. In this context, Directive 2013/39/EU was launched to update the water framework policy in Europe, emphasizing the need to develop new water treatment technologies to deal with this problem [1]. In addition, a dynamic watch list of substances was defined to allow targeted EU-wide monitoring of specific compounds of possible concern [2], the most recent version being included in Decision 2020/1161 to collect data supporting prioritization in future revisions of the PSs list. It is thus clear that alternatives are required to minimize water contamination, aiming at enhanced environmental and life quality in Europe. However, the problem is far to be solved, more pollutants being detected in effluents of urban wastewater treatment plants, seawater and even in drinking water [1-3].

An overview of the author's experience in the monitoring of these micropollutants, and in the synthesis, characterization and application of active and stable catalysts, including catalytic membranes, will be discussed in this lecture by considering different water and wastewater treatment technologies [4-10]. Special emphasis will be placed on the use of carbon materials and their respective functionalization, since carbon materials with no added metals can be used as active catalysts in some of these processes. Three major questions will be answered: *Which is the appropriate surface chemistry? What about textural properties? What type(s) of carbon material(s) are best suited in each case?* The aim is to reveal how to perform a meticulous tailoring of the surface chemistry (surface oxidation and heteroatom doping) and texture (surface area, pore size, distance between adjacent sheets/stacks) of carbon materials with different dimensionalities. Besides the oxidation of EU-relevant chemical micropollutants by generating highly reactive radicals from  $\text{O}_3$ , persulfate activation or  $\text{H}_2\text{O}_2$  (added or photocatalytically generated in-situ), water disinfection (eliminating antibiotic resistant bacteria and their genes) will also be discussed.

### References

- [1] Ribeiro, A. R.; Nunes, O.C.; Pereira, M.F.R.; Silva, A.M.T.; *Environ. Int.*, **2015**, 75, 33.
- [2] Barbosa, M.; Moreira, F.F.N.; Ribeiro, A.R.; Pereira, M.F.R.; Silva, A.M.T.; *Water Res.*, **2016**, 94, 257.
- [3] Sousa, J.C.G.; Ribeiro, A.R.; Barbosa, M.O.; Pereira, M.F.R.; Silva, A.M.T.; *J. Hazard. Mater.*, **2018**, 344, 146.
- [4] Pedrosa, M.; Drazic, G.; Tavares, P.B.; Figueiredo, J.L.; Silva, A.M.T.; *Chem. Eng. J.*, **2019**, 369, 223.

- [5] Torres-Pinto, A.; Sampaio, M.J.; Silva, C.G.; Faria, J.L.; Silva, A.M.T.; *Appl. Catal. B: Environ.*, **2019**, 252, 128.
- [6] Moreira, N.F.F.; Sampaio, M.J.; Ribeiro, A.R.; Silva, C.G.; Faria, J.L.; Silva, A.M.T.; *Appl. Catal. B: Environ.*, **2019**, 248, 184.
- [7] Pedrosa, M.; Pastrana-Martínez, L.M.; Pereira, M.F.R.; Figueiredo, J.L.; Silva, A.M.T.; *Chem. Eng. J.*, **2019**, 348, 888.
- [8] Pedrosa, M.; Da Silva, E.; Pastrana-Martínez, L.M.; Drazic, G.; Falaras, P.; Faria, J.L.; Figueiredo, J.L.; Silva, A.M.T.; *J. Colloid Interf. Sci.*, **2020**, 567, 243.
- [9] Vieira, O.; Ribeiro, R.S.; Pedrosa, M.; Ribeiro, A.R.L.; Silva, A.M.T., *Chem. Eng. J.*, **2020**, 402, 126117.
- [10] Ribeiro, R.S.; Vieira, O.; Fernandes, R.; Roman, F.; Diaz de Tuesta, J.L.; Silva, A.M.T.; Gomes, H.T.; *J. Environ. Manage.*, **2022**, 308, 114622.

#### Acknowledgments

This work was financially supported by projects: NORTE-01-0145-FEDER-031049 (InSpeCt - PTDC/EAM-AMB/31049/2017) funded by FEDER funds through NORTE 2020 - *Programa Operacional Regional do NORTE* and by national funds (PIDDAC) through FCT/MCTES; POCI-01-0145-FEDER-031439 (PLASTIC TO FUEL&MAT) funded by FEDER funds through COMPETE2020 – *Programa Operacional Competitividade e Internacionalização* (POCI), and by national funds (PIDDAC) through FCT/MCTES; and NORTE-01-0145-FEDER-000069 (Healthy Waters) funded by NORTE 2020 under the PORTUGAL 2020 Partnership Agreement through FEDER. This work also was financially supported by LA/P/0045/2020 (ALiCE), UIDB/50020/2020 and UIDP/50020/2020 (LSRE-LCM), funded by national funds through FCT/MCTES (PIDDAC).

## **Hybrid Systems for Wastewater Treatment**

Jörg E. Drewes & Uwe Hübner

Chair of Urban Water Systems Engineering, Technical University of Munich, Germany

Increasingly more stringent regulations to mitigate the risk from constituents posing potentially adverse effects on human health and aquatic life require a holistic view where and how to minimize contributions of these constituents to the water cycle. The EU Commission has taken a lead globally by pursuing a zero pollution ambition for a toxic-free environment as a cornerstone of its new European Green Deal policy.

Constituents of emerging concern are comprised of household chemicals, pharmaceutical residues, endocrine disrupting chemicals, per- and polyfluorinated alkyl substances but also microbial contaminants including bacteria, viruses, protozoa as well as antimicrobial resistant bacteria and antimicrobial resistance genes. Water treatment could be an effective barrier against these constituents, in particular when these processes result in mineralization, destruction or inactivation. However, there is no single process that is capable of reliably removing all of these constituents. There is also increasing concern that the addition of various advanced water treatment processes to conventional treatment facilities will result in a significant increase of the associated carbon- and energy footprint.

Thus, there is a need to develop hybrid treatment systems that are designed as multi-objective treatment process combinations while taking advantage of synergies and minimizing the associated overall carbon footprint. This approach also offers the integration of novel materials, new treatment concepts, and contemporary approaches for better process understanding and control. For instance, combining biological processes with innovative physico-chemical processes employing novel (nano) engineered materials and/or next-generation integrated membrane processes can establish multiple barriers towards a wide range of different trace organic chemicals that should also be effective against microbial contaminants (i.e., viruses, antibiotic resistant bacteria or antibiotic resistance genes) as well as to remove residual nutrients. Such high performing and compact hybrid systems will also offer new opportunities to establish robust concepts for decentralized wastewater treatment facilitating local water reclamation and reuse.

This presentation will initially feature traditional approaches to multi-objective treatment systems by evaluating recent development in various EU member states to mitigate a wide range of trace organic chemicals by using ozonation or activated carbon adsorption after conventional biological wastewater treatment. Another advanced and energy-intense approach has emerged in treatment trains that facilitate direct potable reuse to augment drinking water supplies. The pros and cons of these approaches will be discussed with examples from the United States.

These developments will be contrasted by hybrid treatment systems that take advantage of the interplay of biologically-, oxidative- and adsorptive-based processes by featuring new treatment

train developments. As a point of reference this discussion will start with ozone-managed aquifer recharge (MAR) hybrid systems. In addition, novel nature-based approaches can be operated by stricter control of redox and substrate conditions offering a targeted sequential treatment that can be augmented by integrating oxidative and adsorptive processes for constituents that are not amendable to biological transformation. These systems can also take advantage of novel materials and process insights by employing state-of-the-art biomolecular and analytical methods. Nevertheless, these novel approaches also come with operational limitations and caveats that need to be acknowledged. Examples for these approaches will be highlighted from various installations of hybrid systems at pilot- and full-scale.

An important aspect of novel hybrid systems relates to scalability, transferability, and ease of operation. While hybrid systems are offering clear advantages as multi-objective treatment trains, they are also coming with a higher degree of complexity. Thus, questions like process robustness and scalability are immanent for process implementation. An additional aspect are synergies that evolve by implementing systems decentralized, which can not only offer tailored solutions to the local conditions but also facilitate water reclamation and reuse.

# ORAL PRESENTATIONS



## Evaluating antibiotic biotransformation during denitrification by heterotrophic and nitrite-driven anaerobic methane oxidation bacteria.

*Silvana Quiton-Tapia, Balboa Sabela, Sonia Suarez, Francisco Omil.*  
 CRETUS Centre. Department of Chemical Engineering, Universidade de Santiago de Compostela, Rúa Lope Gómez de Marzoa, E-15782 Santiago de Compostela, Spain

### Abstract

The removal of antibiotics was evaluated in two anoxic systems, each with a stable biomass and similar activity to gain insight towards the linkage between biotransformation and the microbial community functional structure. On one side, classical denitrification was studied in two CFSR reactors at steady operation to evaluate antibiotic biotransformation during heterotrophic denitrification. On the other side, the novel autotrophic N-Damo bacteria (nitrite- dependent anaerobic methane oxidation) was also evaluated using two analogous MBRs. A mix of seven antibiotics belonging to different classes at environmental relevant concentrations were fed to one of the reactors in each anoxic system while keeping the second reactor as a microbiological control. Most antibiotics (CFX, SMX, and TMP) were removed at a high extent in both systems, apart from CIP which was persistent in both. However, differences in the extent of removal were observed mainly in macrolides ROX, AZY and particularly CLA that showed a removal of 95% in the heterotrophic system versus only a 25% removal during the N-Damo process.

### Introduction

The denitrification is microbe-driven process that is key for biological nitrogen removal from wastewater. Denitrification can be accomplished by a wide array of heterotrophic and autotrophic microorganisms (Ni et al., 2017). Denitrifying bacteria are responsible of reducing nitrite/nitrate to nitrogen gas under anoxic conditions, being the carbon sources needed for their metabolic processes different for the heterotrophic and autotrophic bacteria (i.e., anammox, N-Damo). Furthermore, the enzymes involved in the denitrifying microbial pathway can also differ, which is supposed to have an impact on the microbial mediated transformation processes (Glass and Orphan, 2012). In figure 1, two denitrifying microbial pathways are depicted which include the presence of different enzymes, depending on the different cofactors needed for their activation. In the same manner, it is widely accepted that the biodegradation of micropollutants, including antibiotics, is mainly achieved by microorganisms through the action of a series of metabolic enzymes.

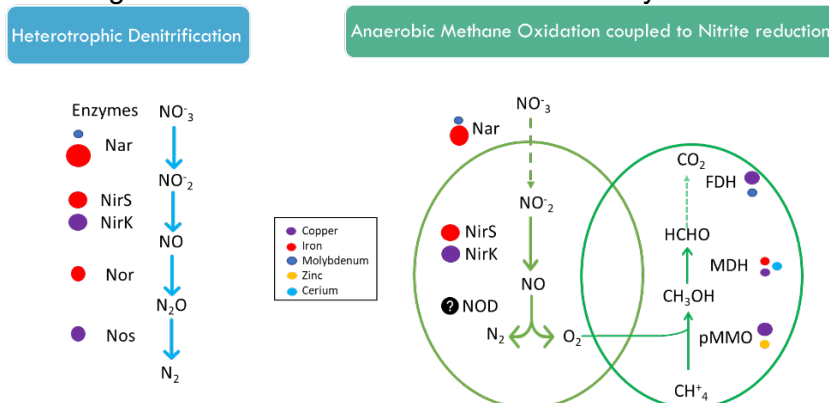


**Figure 1.** Microbial pathways involved in denitrification by heterotrophic and nitrite-driven anaerobic methane oxidation bacteria (AMO) and their associated enzymes.

Research has evidenced that micropollutants can be removed during denitrifying process (Burke et al., 2014). Some research has shown that antibiotic exposure might decrease the denitrification temporally or even permanently, due to growth inhibition of denitrifying microbes or inhibition of the expression of key genes (Bílková et al., 2019; Brandt et al., 2015; DeVries and Zhang, 2016). Understanding the metabolic pathway at environmental relevant concentrations, can help to improve denitrifying processes from a technological perspective. In this study, the novel autotrophic N-Damo process and conventional heterotrophic denitrifying process were assessed as anoxic systems to evaluate how the different microbial populations influence the removal of antibiotics, as well as to determine if the presence of antibiotics could generate specific microbial pathways represented by changes in the microbial composition. The comparison was done under similar biomass denitrifying activity determined by the nitrogen load fed to the system.

## Material and Methods

### *Reactor configuration and operation*

For each type of denitrifying bacteria (heterotrophic and N-Damo) two lab-scale anoxic reactors were operated as indicated in Table 1, one with and the other without spiking antibiotics. The reactors were feed with synthetic wastewater containing macronutrients and trace compounds to foster denitrification. All reactors were analyzed when steady-state operation was reached, in terms of antibiotics and microbial population.

**Table 1.** Operational characteristics of the two denitrifying systems.

Type of anoxic	Heterotrophic	N-Damo
Number of reactors	2	2
Reactor design	CSFR	Anaerobic MBR
Inoculum	Biological sludge WWTP	Denitrifying MBR system (Methanogenic bioreactor)
Nitrogen source	Nitrate	Nitrite
Nitrogen Load [ $\text{mgN}\cdot\text{L}^{-1}\cdot\text{d}^{-1}$ ]	108 $\pm$ 4.16	80 $\pm$ 9.9
Feed Medium	Synthetic WW	Synthetic WW and gas mix 90% $\text{CH}_4$ + 10% $\text{CO}_2$
Working Volume	5 Liters	6,5 Liters
HRT	1 day	1 day
SRT	27 days	-

### *Selected OMPs*

The reactors were spiked with a mixture of seven antibiotics corresponding to different classes: Cephalexin (CFX), Sulfamethoxazole (SMX), Trimetoprim (TMP), Ciprofloxacin (CIP), Roxythromycin (ROX), Azythromycin (AZY) and Clarythromycin (CLA) at a concentration of 5  $\mu\text{g}\cdot\text{L}^{-1}$ .

### *Analytical methods*

Nitrogen species and antibiotic concentrations were determined as described in Martínez-Quintela et al., (2021). Microbiological analysis included an a complete 16S rRNA gene amplicon sequencing targeting gene hypervariable V3 and V4 region using Novaseq 6000.

## Results and Discussion

### *Reactor operation*

Each anoxic system operated under steady-state conditions with an average Nitrogen Loading Rate (NLR) of 80 $\pm$ 9.9  $\text{mgN}\cdot\text{L}^{-1}\cdot\text{d}^{-1}$  composed mainly by nitrite for the autotrophic N-

Damo system and of  $108 \pm 4 \text{ mgN.L}^{-1} \cdot \text{d}^{-1}$  in the form of nitrate for the heterotrophic system. Nitrogen was completely removed during the whole operation.

#### *Antibiotic removal*

Overall, most antibiotics were highly biodegradable in both systems, with removal efficiencies (%RE) above 60% with the exemption of CIP, that showed a recalcitrant behavior (Fig. 2). CIP persistence during denitrification agrees with previous research that indicates that denitrifying bacteria are particularly sensitive to trace concentrations of CIP or similar fluoroquinolones (even at  $\text{ngL}^{-1}$  level) (Zou et al., 2021). Interestingly, CLA and AZY showed significant different %RE between anoxic conditions. In the case of CLA, the difference was more notorious as %RE were 95% versus only 25% in the heterotrophic and N-Damo processes, respectively.

ROX also showed some variation in the extent of removal but in both conditions, it was highly biodegradable: almost 100% in the heterotrophic and higher than 60% in the N-damo system. Similarly, Martínez-Quintela et al., (2021) evidenced a removal close to 80% of ROX during the N-Damo process. In fact, when comparing with different redox conditions, previous research found that ROX was solely removed in anoxic conditions (Burke et al., 2014), suggesting that the necessary enzymes and/or microbial population capable to degrade this type of molecule are specific of such conditions.

Both TMP and SMX were highly removed by the two systems with %RE ranging from 70-80%. The results agree with the evidenced by Bai et al., (2019), that showed that sulfonamides were more degradable under anoxic than oxic and suboxic conditions. However, this results are significantly higher to what was evidenced in Martínez-Quintela et al., (2021) for the autotrophic N-Damo, but this can be explained by the influence of the NLR, which in this case was also higher. CFX was also efficiently removed during both microbial pathways, surpassing 85% removal during N-Damo and reaching almost 100% for heterotrophic denitrification, respectively. This can also indicate favorable conditions for CFX abatement by denitrifying population and their associated enzymes.

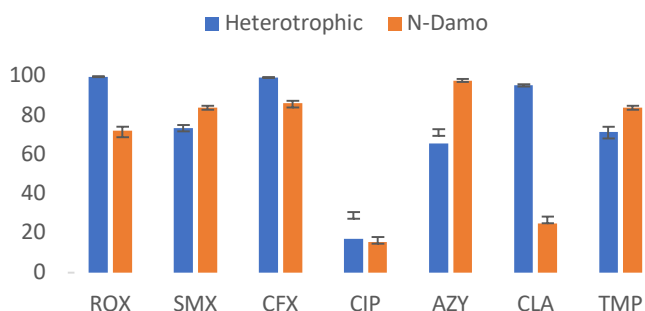


**Figure 2.** Removal efficiencies of selected antibiotics during heterotrophic and N-Damo.

#### *Influence of Antibiotics on the Microbial Community*

Heterotrophic denitrifying process was significantly affected by the presence of environmental relevant concentrations of antibiotics, which appears to provoke selection pressures on compositions of denitrifying community. In contrast, N-Damo microbial community was less affected which could indicate a higher resilience. In both systems, microorganisms represented by the order *Rhizobiales* seem to be favored in presence of antibiotics, mainly during heterotrophic denitrification. Similarly, previous research that zoomed in the microbial community functional structure, suggested that the order *Rhizobiales* were key functional taxa for the biotransformation of organic pollutants. In fact, different types of xenobiotic compound degrading genes were abundant in *Rhizobiales* (Joshi et al., 2017).

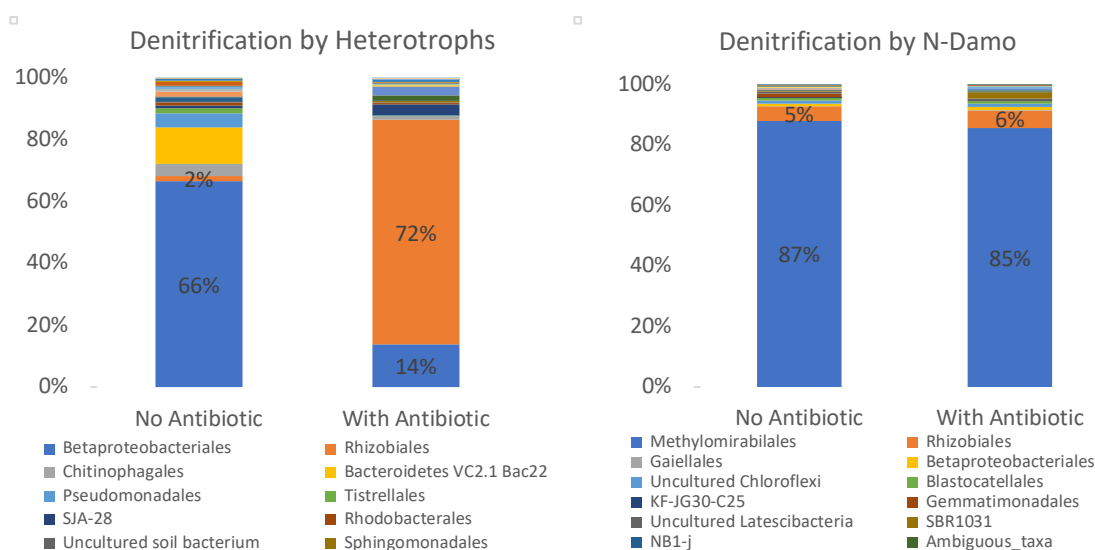


**Figure 4.** Microbial communities present in denitrification by heterotrophic (above) and anaerobic methane oxidation bacteria (below) depicted by Order level. Relative abundances over 1%. The left column represents the reactor control that was not exposed to antibiotics and the right column characterizes the reactor exposed to the antibiotic mixture (5µg.L<sup>-1</sup>).

## Conclusions

Most antibiotics were highly degraded, with the exception for CIP. The type of anoxic system, represented by the different microbial denitrifying communities seems to have some influence on the extent of removal of some compounds, especially CLA and AZY. CLA was particularly better removed during heterotrophic denitrification while AZY was better removed by nitrite-driven anaerobic methane oxidation bacteria. The presence of antibiotics seems to have an impact on the microbial community composition during denitrifying heterotrophic systems.

## Acknowledgements

This research was supported by NOWELTIES a Marie Skłodowska Curie Action European Joint Doctorate (EJD) project (programme Innovative Training Networks (ITN) of Horizon 2020). Authors belong to Galician Competitive Research Group (GRC ED431C 2021/37).

## References

- Bai, Y., Ruan, X., Wang, F., Antoine, G., van der Hoek, J.P., 2019. Sulfonamides removal under different redox conditions and microbial response to sulfonamides stress during riverbank filtration A laboratory column study.pdf. *Chemosphere* 668–677.
- Burke, V., Richter, D., Hass, U., Duennbier, U., Greskowiak, J., Massmann, G., 2014. Redox-dependent removal of 27 organic trace pollutants: Compilation of results from tank aeration experiments. *Environ. Earth Sci.* 71, 3685–3695. <https://doi.org/10.1007/s12665-013-2762-8>
- Glass, J.B., Orphan, V.J., 2012. Trace metal requirements for microbial enzymes involved in the production and consumption of methane and nitrous oxide. *Front. Microbiol.* 3, 1–20. <https://doi.org/10.3389/fmicb.2012.00061>
- Joshi, D.R., Zhang, Y., Gao, Y., Liu, Y., Yang, M., 2017. Biotransformation of nitrogen- and sulfur-containing pollutants during coking wastewater treatment: Correspondence of performance to microbial community functional structure. *Water Res.* 121, 338–348. <https://doi.org/10.1016/j.watres.2017.05.045>
- Martínez-Quintela, M., Arias, A., Alvarino, T., Suarez, S., Garrido, J.M., Omil, F., 2021. Cometabolic removal of organic micropollutants by enriched nitrite-dependent anaerobic methane oxidizing cultures. *J. Hazard. Mater.* 402, 123450. <https://doi.org/10.1016/j.jhazmat.2020.123450>
- Ni, B.J., Pan, Y., Guo, J., Viridis, B., Hu, S., Chen, X., Yuan, Z., 2017. CHAPTER 16: Denitrification Processes for Wastewater Treatment, RSC Metalobiology. The Royal Society of Chemistry. <https://doi.org/10.1039/9781782623762-00368>
- Suarez, S., Lema, J.M., Omil, F., 2010. Removal of Pharmaceutical and Personal Care Products (PPCPs) under nitrifying and denitrifying conditions. *Water Res.* 44, 3214–3224. <https://doi.org/10.1016/j.watres.2010.02.040>
- Yi, K., Wang, D., QiYang, Li, X., Chen, H., Sun, J., An, H., Wang, L., Deng, Y., Liu, J., Zeng, G., 2017. Effect of ciprofloxacin on biological nitrogen and phosphorus removal from wastewater. *Sci. Total Environ.* 605–606, 368–375. <https://doi.org/10.1016/j.scitotenv.2017.06.215>
- Zou, H., He, J., Guan, X., Zhang, Y., Deng, L., Li, Y., Liu, F., 2021. Microbial responses underlying the denitrification kinetic shifting exposed to ng/L- and µg/L-level lomefloxacin in groundwater. *J. Hazard. Mater.* 417. <https://doi.org/10.1016/j.jhazmat.2021.126093>

## Thresholds for microbial degradation of wastewater contaminants: relationship between bioavailability and the onset of biodegradation

Ana P. Lopez G.<sup>\*,°</sup>, Alba M. Trueba S.<sup>°</sup>, Juan M. Lema R.<sup>°</sup>, Andreas Schäffer\* and Kilian. E. C. Smith\*\*

\* Institute for Environmental Research, RWTH Aachen University, Worringerweg 1, 52074 Aachen, Germany

<sup>°</sup>Group of Environmental Biotechnology, School of Engineering (ETSE), USC, Rúa Lope Gómez de Marzoa s/n, 15782 Santiago de Compostela, Spain

\*\*Environmental Chemistry, Magdeburg-Stendal University of Applied Sciences, Breitscheidstraße 2, Building 6, 39114 Magdeburg, Germany

Degradation of organic pollutants in wastewater is performed by diverse microorganisms including fungi and bacteria (Kanaujiya et al., 2019). For this to occur the dissolved and bioavailable contaminants have to pass through the microbial membrane, either by passive or active transport, prior to being degraded. Biodegradation rates have been observed to vary according to the pollutant's concentration. For instance, van Bergen et al. (2021) investigated pharmaceutical degradation at environmental levels, and reported that high concentrations (30nM) resulted in higher biodegradation rates compared to lower concentrations (3nM). In addition, Ehrl et al. (2019) described a decrease in the formation of transformation products when reaching dissolved pesticide concentrations of 32µg L<sup>-1</sup>. Such low biodegradation rates and slow metabolites production may additionally hamper monitoring the degradation of environmental pollutants and lead to incorrect conclusions about non-degradation.

Monitoring metabolites in water at low concentrations can be complemented with analysis of microbial responses such as enzymatic activity, protein biosynthesis and gene expression. These subcellular responses can be used to support the detection of any threshold of pollutant biodegradation at the level of metabolic pathway. Kundu et al. (2019) observed that bacteria adapted to degrade organic pollutants had low protein expression and an increase of stress-related proteins when they were cultured at concentrations around 10µg L<sup>-1</sup> of the herbicide atrazine. Although these findings suggested a biodegradation threshold, adaptation of bacteria to the new conditions could lead to lower biodegradation thresholds.

### **Biodegradation of Sulfamethoxazole (SMX)**

Degradation of micropollutants, such as pharmaceuticals, has been addressed due to the persistence of such chemicals in water bodies. Sulfamethoxazole (SMX) is a rather polar antibiotic (log Kow of the uncharged molecule 0.89, pKa 5.7; Baumer et al. 2017), which inhibits bacterial growth. Some bacteria are capable of degrading SMX. One of these strains (*Microbacterium* sp BR1) has been isolated from a membrane bioreactor (MBR), and further enriched to elucidate SMX metabolic pathways (Bouju et al.,2012; Ricken et al.,2015). *Microbacterium* sp BR1 is capable of mineralizing SMX as a sole carbon source or under cometabolic conditions: the catabolism of SMX occurs by ipso-hydroxylation, with the Sad A, Sad B and Sad C as the main enzymes involved. The first two are Flavin dependent monooxygenases whereas the latter is a Flavin reductase (Ricken et al.,2017). However, these studies were performed over a range of concentrations of ca. 10-25 mg L<sup>-1</sup> SMX, which are well-above the concentrations found in water bodies (typically 5 ng L<sup>-1</sup> - 440 µg L<sup>-1</sup>) (Kanaujiya et al.,2019). Therefore, the first aim of this study is to explore biodegradation thresholds of SMX by *Microbacterium* sp BR1 when this is provided at environmental levels as the sole source of carbon. The second aim is to investigate correlations between SMX degradation and metabolite production to the proteomic expression of under different conditions.

### *Materials and methods*

Previous experiments included measuring mineralization rates by monitoring turnover of radiolabelled SMX (<sup>14</sup>C-SMX) into <sup>14</sup>C-CO<sub>2</sub> over a range of concentrations from 25µg L<sup>-1</sup> to

0.1 µg L<sup>-1</sup> (data not shown). These experiments are looking for biodegradation thresholds via the analysis of SMX and some of its metabolites generated during degradation tests performed in parallel to the above radiolabelled tests. In addition, proteomic analyses of the biomass used in these tests is being done to examine the regulation of Sad enzymes involved in the metabolism of SMX.

#### *SMX and metabolites*

Phosphate buffer (PBS) was used as the reaction medium for the above SMX degradation tests. For analysis of the SMX and metabolites, the reaction media containing the biomass was sampled at specific times, and then centrifuged at 3634g for 35 min at 4°C. The supernatant was stored frozen until analysis. The PBS reaction medium needs to be desalted and up-concentrated before LC-MS/MS analysis. Two methods will be tested for this: lyophilisation coupled to organic solvent extraction and filtration with centrifuge desalting filters. Standard solutions will be used to assess the recovery prior to sample processing.

#### *Proteomics*

Bacterial samples of *Microbacterium sp. BR1* from the reaction media of SMX degradation tests were washed twice with NaCl at 4°C and stored at -26°C until further processing. Whole proteome samples of the culture in different conditions are being analysed by in-solution shotgun proteomics. Briefly, bacterial cells are harvested by centrifugation and cell lysis is performed in two steps. First, cells are digested with 1% SDS at 90°C and subsequently mechanically disrupted by beating with glass beads. The supernatant containing the solubilized proteins is recovered and proteins are then precipitated in two incubation steps with cold acetone at -20°C. Protein concentrations in the samples are determined through the bicinchoninic acid (BCA) protein assay. Afterwards, a SDS-PAGE protein electrophoresis under denaturing conditions is performed to analyze the quality of the protein extract (i.e. absence of protein degradation). Electrophoresis is run for 10 µg protein aliquots and gel staining is done using a standard Coomassie protocol. Then, dissolved protein samples are trypsin-digested. The obtained peptide mix is injected in a tims-TOF Pro (Bruker) nLC-MS/MS for peptide separation, ion fragmentation and mass to charge identification. The peptides contained in the samples are identified with a software tool (Proteome discoverer) dedicated for proteomics and compared with the existing database of *Microbacterium sp. BR1* proteome (from UniProt public database). Finally, protein profiles from bacteria adapted and actively degrading SMX are compared to bacteria cultured without SMX.

#### *Preliminary tests*

The proteomics protocol was optimized according to the cell density contained in the frozen samples. For this, samples with different volumes and bacterial pellet sizes were selected and processed according to the method described above (Fig. 1). In addition, when necessary protein concentration methods were performed (eg., using centrifugation filters) prior to the electrophoresis step.

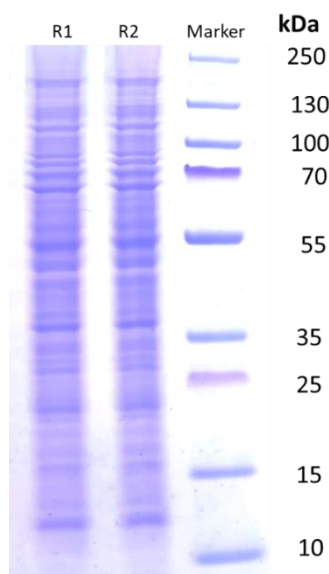


Figure 1. SDS-electrophoresis of protein extract from *Microbacterium sp. BR1* cultured in absence of SMX. Clear bands of the proteins with different molecular weight (expressed in kDa). The absence of low molecular weight bands confirms no degradation of the sample. R1 and R2 stand for replicas of the sample.

## References

- Baumer, Andreas; Bittermann, Kai; Klüver, Nils; Escher, Beate I. (2017): Baseline toxicity and ion-trapping models to describe the pH-dependence of bacterial toxicity of pharmaceuticals. In *Environmental science. Processes & impacts* 19 (7), pp. 901–916. DOI: 10.1039/c7em00099e.
- Bouju, Helene; Ricken, Benjamin; Beffa, Trello; Corvini, Philippe F-X; Kolvenbach, Boris A. (2012): Isolation of bacterial strains capable of sulfamethoxazole mineralization from an acclimated membrane bioreactor. In *Applied and environmental microbiology* 78 (1), pp. 277–279. DOI: 10.1128/AEM.05888-11.
- Ehrl, Benno N.; Kundu, Kankana; Gharasoo, Mehdi; Marozava, Sviatlana; Elsner, Martin (2019): Rate-Limiting Mass Transfer in Micropollutant Degradation Revealed by Isotope Fractionation in Chemostat. In *Environmental science & technology* 53 (3), pp. 1197–1205. DOI: 10.1021/acs.est.8b05175.
- Kanaujiya, Dipak Kumar; Paul, Tanushree; Sinharoy, Arindam; Pakshirajan, Kannan (2019): Biological Treatment Processes for the Removal of Organic Micropollutants from Wastewater: a Review. In *Curr Pollution Rep* 5 (3), pp. 112–128. DOI: 10.1007/s40726-019-00110-x.
- Kundu, Kankana; Marozava, Sviatlana; Ehrl, Benno; Merl-Pham, Juliane; Griebler, Christian; Elsner, Martin (2019): Defining lower limits of biodegradation: atrazine degradation regulated by mass transfer and maintenance demand in *Arthrobacter aurescens* TC1. In *The ISME journal* 13 (9), pp. 2236–2251. DOI: 10.1038/s41396-019-0430-z.
- Ricken, Benjamin; Fellmann, Oliver; Kohler, Hans-Peter E.; Schäffer, Andreas; Corvini, Philippe François-Xavier; Kolvenbach, Boris Alexander (2015): Degradation of sulfonamide antibiotics by *Microbacterium sp. strain BR1* - elucidating the downstream pathway. In *New biotechnology* 32 (6), pp. 710–715. DOI: 10.1016/j.nbt.2015.03.005.
- Ricken, Benjamin; Kolvenbach, Boris A.; Bergesch, Christian; Benndorf, Dirk; Kroll, Kevin; Strnad, Hynek et al. (2017): FMNH2-dependent monooxygenases initiate catabolism of sulfonamides in *Microbacterium sp. strain BR1* subsisting on sulfonamide antibiotics. In *Scientific reports* 7 (1), p. 15783. DOI: 10.1038/s41598-017-16132-8.

*van Bergen, Tamara J. H. M.; Rios-Miguel, Ana B.; Nolte, Tom M.; Ragas, Ad M. J.; van Zelm, Rosalie; Graumans, Martien et al. (2021): Do initial concentration and activated sludge seasonality affect pharmaceutical biotransformation rate constants? In Applied microbiology and biotechnology 105 (16-17), pp. 6515–6527. DOI: 10.1007/s00253-021-11475-9.*



## Transformation of Sulfamethoxazole and Atenolol by a Microbial Community Adapted to Histidine

E. A. Chingate\*, M. Ozluer\*, M. J. Farre\*\*, J.E. Drewes\*, C. Wurzbacher\* and U. Hübner\*.

\* Chair of Urban Water Systems Engineering, Technical University of Munich, Am Coulombwall 3, 85748 Garching, Germany

\*\* Catalan Institute for Water Research (ICRA), Emili Grahit 101- 17003 Girona, Spain

### Abstract

Biotransformation of trace organic chemicals is not well understood yet. Previous research showed good removal of atenolol and sulfamethoxazole in between 23 more trace organic chemicals, with environmental relevant concentration. This study aimed to get insight on the removal of these two compound by increasing their concentration. After 7 days exposure in a stable microbial community, atenolol achieve a removal of ~10 % and sulfamethoxazole, ~70%. Atenolol behavior could be related to already studied metabolic pathways, but sulfamethoxazole still requires more detailed experiments.

### Keywords

Adaptation; biotransformation; molecular similarity; trace organic chemicals

## INTRODUCTION

At metabolic level biotransformation of trace organic chemicals (TOrcs) implies multiple complex processes that are not well understood yet. Cometabolism is accepted as main mechanism for biotransformation of TOrcs, as their concentration would not be able to sustain degraders (Rittman, 2001). On the other hand, Egli (2010) proposed that within several energy sources in a concentrations lower than 1 mg/L, microorganisms express as many catabolic pathways as they can to harvest several carbon source simultaneously.

Studies already found some highlights in experiments biofiltration with sand columns. Nature and concentration of the primary carbon source seems to be directly related to the biotransformation of TOrcs (Alidina et al., 2014; Regnery et al. (2016); Müller et al. 2017; Hellauer et al. 2019). However, the correlation between the molecular structure of the main energy source and the TOrcs was not addressed, and it be a relevant factor.

A preliminary work of Chingate et al. (2022, manuscript in preparation) in a well controlled environment, found that in between a mixture of 25 TOrcs with concentrations around ~ 500 ng/L, only atenolol and sulfamethoxazole were significantly biotransformed by microbial communities adapted to aniline, histidine, or di-sodium succinate as a carbon source. This work aims to compare the biotransformation of atenolol and sulfamethoxazole with a concentration of ~100 µg/L by a histidine degrader microbial community

## MATERIALS AND METHODS

### Experimental set-up

500 mL lab-scale membrane bio-reactors were used to maintain bacteria under oligotrophic and oxic conditions in continuous operation. Peristaltic pums for influent and effluent were Leadfluid FZ10 (Fleischhacker GmbH, Germany) and Longerpump T-S107/JY15-12 (Drifton, Denmark), respectively. Puron® membranes with of 75 cm<sup>2</sup> of surface and a pore size of 20 nm were donated by KOCH Separation Systems (United states).

A scale (Kern PCB 6000-1 by Voelkner, Germany) was used as sensor to control the weight of the reactor by changing the speed of the pumps. Dissolved oxygen (DO) was monitored daily with fiber optical spots (SP-PSt3-NAU-D5-YOP by PreSens, Germany) attached to the inner wall of the reactor. Air was constantly provided to maintain DO concentrations higher than 8 mg/L. Temperature inside the reactor was monitored (Probe thermometer by TFA Dostmann, Germany) and kept between 21 °C and 23 °C.

Reactors were inoculated with activated sludge from the wastewater treatment plant Garching (Germany) and monitored for 3 weeks before a stable biomass concentration was reached

measured as adenosin triphosphate (ATP) content. Microbial media culture was adapted from Helbling et al. (2014) and dilution rate for the reactors was  $0.04 \text{ h}^{-1}$ . Histidine (9 mg/L) was used as the unique carbon source.

After biological stabilization, a mixture of carbamazepine, atenolol and sulfamethoxazole, was added to the microbial culture medium to achieve  $\sim 100 \text{ }\mu\text{g/L}$ . Samples for TOxCs quantification from the reactors were taken after 5 days of operation with the new microbial medium to avoid mixing effects.

### Chemical analyses

Full mixture of TOxCs was quantified with LC-MS/MS following a method previously described by Müller et al. (2017). Prior to quantification, samples were filtrated with  $0.2 \text{ }\mu\text{m}$  pore size polyvinylidene fluoride (PVDF) filters (BGB, Germany) and spiked with a mixture of isotope-labelled internal standards. ATP was quantified using the "BacTiter-Glo™ Microbial Cell Viability Assay" (Promega GmbH, Germany)

## RESULTS AND DISCUSSION

After stabilization of the reactors, carbamazepine achieves the same concentration as in the feeding solution; while atenolol was removed in  $\sim 10\%$ , and sulfamethoxazole  $\sim 70\%$  (figure 2). Carbamazepine is reported to be a recalcitrant compound in oxic environments, and it can be used as a tracer and quality control in our experiments. Atenolol is reported to be highly removed in other studies within environmental relevant concentrations with another energy sources available (Alidinda, Muller, Chingate), and as unique energy source (), apart from this study where concentration was higher than in the environment, and histidine was the main energy source. Sulfamethoxazole is showing removal higher than  $70\%$  in most studies, apart from its concentration.

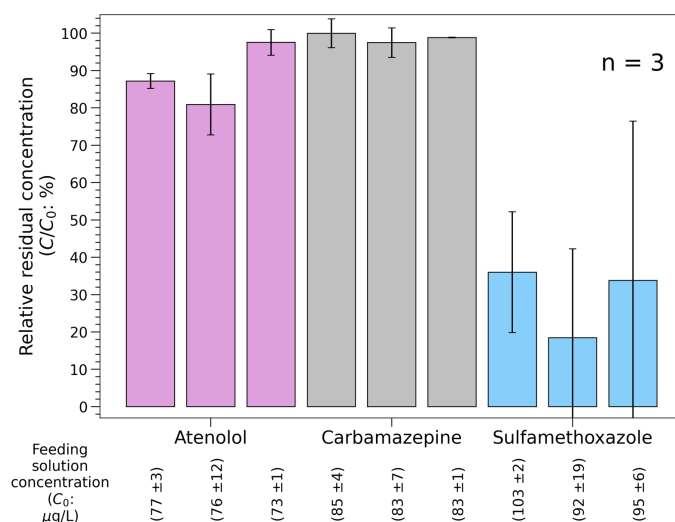


Figure 1. Relative residual concentration ( $C/C_0$ ) of atenolol, carbamazepine and sulfamethoxazole in a retentostat running with a histidine degrader microbial community at a dilution rate or  $0.04 \text{ h}^{-1}$

A metabolic pathway like the one described by Yi et al. (2022) would explain the difference in removal observed in between figures 1 and 2. Yi et al. (2022) describes two hydrolysis reactions as first steps, first one forms atenolol acid, and second one 4-hydroxyphenylacetic acid. Second steps depends on  $\alpha$ -ketoglutarate, one of the members of Krebs cycle. Within the same histidine concentration in feeding solution and biomass in both experiments, proportion in between atenolol and histidine, as well as, atenolol and  $\alpha$ -ketoglutarate, increases almost 200 times. Absolute removal of atenolol increased only by 70 times with a concentration 200 times higher, so the

relative value decreased. More studies with intermediate concentration would clarify the behavior of this process.

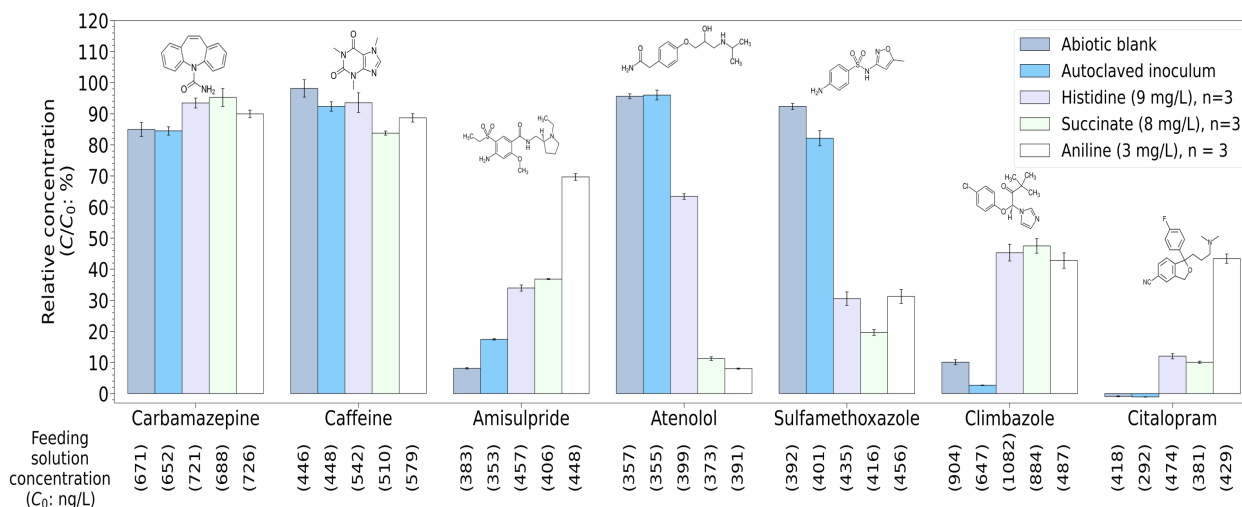


Figure 2. Relative residual concentration ( $C/C_0$ ) of selected TOxTs upon different operational conditions in the retentostat system. Initial concentration for each substance in each experiment is reported under the bar lines, and final concentration is the average value for the values measured along 3 days. While histidine, Succinate and Aniline refer to experiments with a microbial community adapted to these substances as the unique carbon source, Abiotic blank and Autoclaved inoculum refer to experiments in reactors without any inoculation and inoculation with dead bacteria, respectively. (Chingate et al. 2022, manuscript in preparation)

Sulfamethoxazole removal seems to be stable, suggesting that only one enzyme controls the process and that its saturation concentration is still higher. On the other hand, sulfamethoxazole is an antibiotic as well, so higher concentrations trigger adaptation and selection as well. Removal behavior is not giving any clue on metabolism of sulfamethoxazole, further analytical efforts are necessary to clarify the process, as the number of possibilities are higher than for atenolol (Larcher et al., 2012). Identification of dependence of metabolism with concentration could be useful to improve its understanding since an analytical point of view. Higher concentration of parent compounds drives to higher concentration on the metabolites, and reduces the analytical effort.

Current research on identification of transformation products is still ongoing. We aim to combine it with the microbiological characterization to propose the metabolic pathways related to the biotransformation of atenolol and sulfamethoxazole.

## REFERENCES

- Alidina, M., Li, D., & Drewes, J. E. 2014. Investigating the role for adaptation of the microbial community to transform trace organic chemicals during managed aquifer recharge. *Water Research*. **56**, 172 - 180.
- Egli, T. 2010. How to live at very low substrate concentration. *Water Research*. **44** (17), 4826-4837.
- Helbling, D. E., Hammes, F., Egli, T., & Kohler, H. P. E. 2014. Kinetics and yields of pesticide biodegradation at low substrate concentrations and under conditions restricting assimilable organic carbon. *Applied and Environmental Microbiology*, **80**(4), 1306–1313.
- Hellauer, K., Martínez Mayerlen, S., Drewes, J. E., & Hübner, U. 2019. Biotransformation of trace organic chemicals in the presence of highly refractory dissolved organic carbon. *Chemosphere*. **215**, 33-39
- Larcher, S., & Yargeau, V. 2012. Biodegradation of sulfamethoxazole: current knowledge and perspectives. *Applied Microbiology and Biotechnology* 2012 96:2, **96**(2), 309–318.

Müller, J., Drewes, J. E., & Hübner, U. 2017. Sequential biofiltration – A novel approach for enhanced biological removal of trace organic chemicals from wastewater treatment plant effluent. *Water Research*, **127**, 127–138.

Regnery, J., Wing, A. D., Kautz, J., & Drewes, J. E. 2016. Introducing sequential managed aquifer recharge technology (SMART) - From laboratory to full-scale application. *Chemosphere*. **154**, 8 - 16

Rittmann, B. E., & McCarty, P. L. 2001. *Environmental biotechnology : principles and applications*. McGraw-Hill.

## Wastewater treatment by using cold atmospheric plasma

*Amit Kumar<sup>1,2</sup>, Nikola Škoro<sup>1</sup>, Wolfgang Gernjak<sup>3,4</sup>, and Nevena Puač<sup>1</sup>*

<sup>1</sup> *Institute of Physics, University of Belgrade, Pregrevica 118, 11080 Belgrade, Serbia*

<sup>2</sup> *Universitat de Girona, 17003 Girona, Spain*

<sup>3</sup> *Catalan Institute for Water Research (ICRA), 17003 Girona, Spain*

<sup>4</sup> *Catalan Institution for Research and Advanced Studies (ICREA), 08010, Barcelona, Spain*

### Abstract

In this study, we addressed the treatment of anthraquinone dye (Acid Blue 25) containing aqueous solutions by using cold atmospheric plasma. Atmospheric pressure plasma jet (APPJ) with multi-electrode configuration was used as a plasma source. Plasma was driven by RF power source, with argon as a working gas. In the configuration, argon plasma was formed at liquid surface in contact with ambient air. The experiments were conducted with two different initial volumes and five different treatment times at a fixed dye concentration. Optical emission spectroscopy (OES) was performed to identify the presence of reactive species in the gas phase during plasma-liquid interaction. OES diagnostics confirmed the evidence of reactive oxygen and nitrogen species (RONS) in the gas phase. A spectrophotometer device was used to monitor the final dye concentration after plasma treatment. The treatment results revealed that plasma-generated reactive species degraded the AB25 molecules in water.

### Introduction

Dye wastewater pollution is one of the major environmental problems due to its influence on water bodies [1, 2]. The main origin of dye in groundwater and surface water is due to the direct discharge of textile waste effluents. In this study, AB25 was selected as the target compound as it has wide range of applications (wool, silk, polyamide, leather and mixed fabric, cosmetic) [4]. AB25 dye consists of an anthraquinone chromophore group (containing three fused aromatic rings). Anthraquinone dyes are the second-highest consumable dyes after azo dyes by textile industries. Anthraquinone dyes are regularly detected in various concentrations in industrial wastewater. However, conventional wastewater treatment plants are not always effective to treat various dye effluents due to their low biodegradability [5]. Therefore, advanced oxidation processes (AOPs) are demonstrated as alternative methods [2, 5].

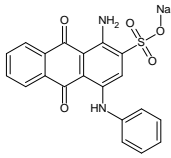
In this work, we have used cold atmospheric plasma as an AOP to remove AB25 from water. Plasma is an ionized gas consisting of energetic electrons, ions, metastables, photons, electric fields, UV lights [3]. Plasma can be generated by supplying electrical energy to a working gas (e.g. argon, helium, air, nitrogen, etc.) in form of an electric field [3, 5]. If the applied electric field is high enough to initiate the electrical breakdown of gas plasma can be formed. The discharge operates due to the collision of fast electrons generated in the plasma with gas molecules or atoms [3, 5].

Contact of plasma with a liquid surface can generate a rich mixture of RONS (e.g. HO·, O·, O<sub>3</sub>, H<sub>2</sub>O<sub>2</sub>, ·NO, ONOOH, NO<sub>3</sub><sup>-</sup>, NO<sub>2</sub><sup>-</sup>...), which are capable to degrade a wide range of pollutants [1, 2, 6]. Cold plasma-based treatments processes are eco-friendly since it operates without any additional chemicals at atmospheric conditions. Cold plasma sources with different reactor configurations have been used by many authors to decompose a range of dyes in water [2].

## Materials and Methods

AB25 (product number: 210684; purity: 45 %) was purchased from Sigma Aldrich. The characteristics of AB25 are shown in Table 1. Dye-containing solution with a concentration of 50 mg/L was prepared by dissolving an adequate amount of analytical grade of AB25 in distilled water.

**Table 1.** Chemical data of AB25.

Chemical formula	Chemical structure	MW (g/mol)	$\lambda_{\max}$ (nm)	Appearance	Classification
$C_{20}H_{13}N_2NaO_5S$		416.38	602	Purple blue	Anionic

\*  $\lambda_{\max}$ : maximum absorbance

The schematic diagram of the experimental setup with multi-needle electrode APPJ is shown in Figure 2. Three syringe needles type electrodes were used as a high voltage source. The inner and outer diameter of each needle was about 1 mm and 1.8 mm, respectively. The needles were inserted inside the glass tubes, whereas the inner diameter, outer diameter, and length of each tube were about 3.7 mm, 5 mm, and 45 mm, respectively. The distance between the tip of each needle and the ending of each tube was 7 mm. The distance between the two adjacent needle electrodes was 20 mm. Each needle tip to solution distance was set at 14 mm. When the treatment was underway distance was not constant due to partial evaporation of liquid, and change in length of gap was ~1-2 mm. The copper tape was wrapped over the bottom of the sample vessel, and it served as a ground electrode. The plasma was driven by RF power supply with a frequency of 350 kHz. Argon gas with a total flow rate of 2 slm was used as a feed gas in all experiments. Argon flow was injected through needles.

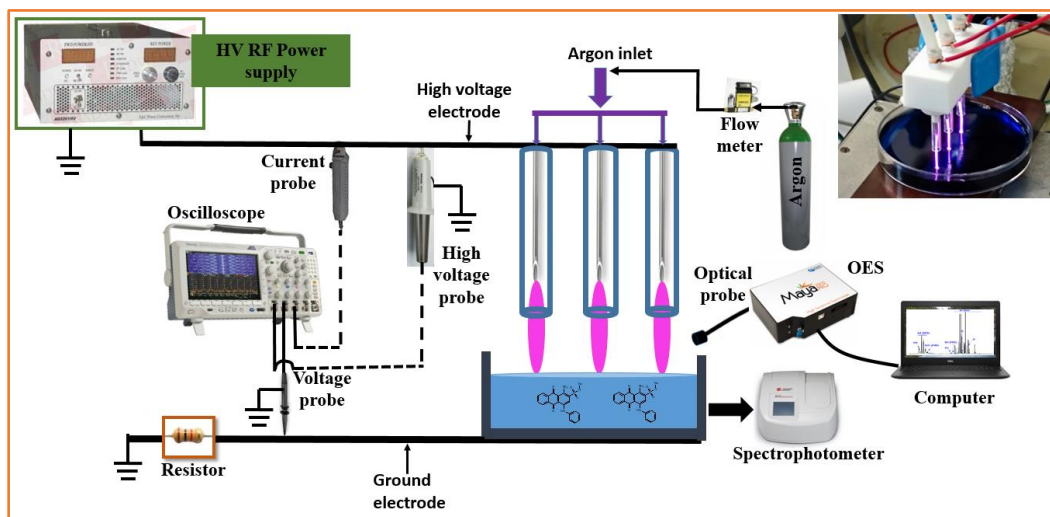


**Figure 2.** Experimental setup for dye treatment, APPJ over liquid surface (inset right).

AB25 removal efficiency was described by equation (1).  $C_o$  (mg/L) is the initial dye concentration,  $C$  (mg/L) is the final dye concentration after the plasma treatment, and  $d$  is the evaporation coefficient.

$$Removal (\%) = \frac{C_o - C \times d}{C_o} \times 100 \quad (1)$$

The energy yield was calculated, defined by the removal of AB25 per unit mean power deposition to the dye sample, determined by equation (2)

$$\text{energy yield} \left( \frac{mg}{kWh} \right) = \frac{C_o \left( \frac{mg}{L} \right) \times V_o(L) \times \frac{1}{100} \times Removal(\%)}{P_{mean \text{ at the sample}} (kW) \times t(h)} \quad (2)$$

## Results and discussion

The dye treatment experiments were conducted by direct exposure of the APPJ over AB25 containing aqueous solution. In Figure 2 (a), the degradation of AB25 in the solution is shown as a function of the plasma treatment time. The concentration of AB25 was decreased with the increase of plasma treatment. For both volumes, the faster degradation was achieved in the first 3 min and 5 min. The lower initial volume favored high removal. The removal efficiency values were about 55 % for 15 ml and 48 % for 30 ml in 5 min. After 20 min, the removal was about 83 % in 15 ml, whereas for the two times greater initial volume the obtained removal efficiency was around 76 %. Higher removal in case of lower sample volume can be attributed to enhanced interaction of the plasma-generated reactive species with pollutants due to smaller liquid volume.

The energy yield for two different dye solution volumes was compared. Energy yield as a function of removal %, shown in Figure 2 (b). In the best-case scenario, the higher energy yield was about 408 mg/kWh for 38 % removal in 15 ml and 690 mg/kWh for 32 % removal in 30 ml. The higher removal had a negative influence on energy yield due to a longer treatment time. In the case of higher removal, energy yield was about 133 mg/kWh for 83 % removal in 15 ml and 244 mg/kWh for 76 % removal in 30 ml. It can be concluded that the higher initial volume promoted higher energy yield for all removal efficiencies.

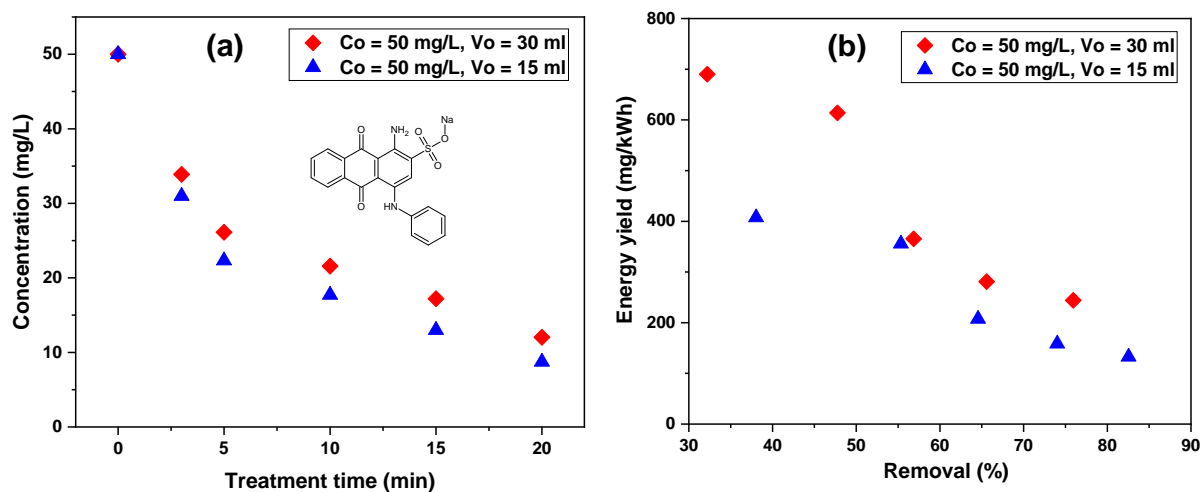


**Figure 2.** Change in dye concentration with treatment time (a) and the energy yield vs dye removal % (b). Experimental conditions: AB25 concentration 50 mg/L, dye solution volume 15 ml and 30 ml, argon flow 2 slm, mean power deposition to the sample 14 watts, discharge gap 14 mm.

The plasma emission was recorded by OES. It was found that various excited species including  $\text{HO}^\cdot$ ,  $\text{O}^\cdot$ ,  $\text{N}_2^*$ ,  $\text{N}_2^+$ ,  $\cdot\text{NO}$ ,  $\text{Ar}^*$  were present in the plasma environment during APPJ-liquid interaction.  $\text{HO}^\cdot$  and  $\text{O}^\cdot$  are considered the major reactive oxygen species (having high oxidation potential) in AOPs, and they can rapidly degrade most of the organic contaminants.

## Conclusions

We have used a multi-electrode-APPJ to eliminate the AB25 dye from aqueous solution. Argon-APPJ formed streamers in surrounding air and touching the liquid surface. Interaction of APPJ with liquid can provide a diverse reactive environment containing RONS, which can react and oxidize the dye molecules in water. OES was carried out to capture emission of the reactive species - the most pronounced was recorded from  $\text{N}_2$ ,  $\text{O}$  and  $\text{OH}$  species. When comes to dye removal, almost 50 % dye degraded in the first 5 min and more than 70 % after 20 min of plasma treatment with both volumes. In all the cases, the highest energy yield was obtained at higher solution volume. The experimental results showed that this type of plasma source can be used for efficient degradation of AB25. Overall, cold plasma technology can provide an attractive and new method for wastewater treatment.

## Acknowledgement

This work was carried out under NOWELTIES project. NOWELTIES received funding from the European Union's Horizon 2020 research and innovation programme under the Marie Skłodowska-Curie grant agreement No. 812880. N.S. and N.P. are funded by Ministry of Education, Science and Technological Development, grant number 451-03-68/2022-14/200024.

## References

1. Foster, J. E., Mujovic, S., Groele, J., & Blankson, I. M. (2018). Towards high throughput plasma based water purifiers: design considerations and the pathway towards practical application. *Journal of Physics D: Applied Physics*, 51(29), 293001.
2. Kumar, A., Škoro, N., Gernjak, W., & Puač, N. (2021). Cold atmospheric plasma technology for removal of organic micropollutants from wastewater—a review. *The European Physical Journal D*, 75(11), 1-26.
3. Fridman, A. (2008). *Plasma chemistry*. Cambridge university press.
4. Ghodbane, H., & Hamdaoui, O. (2009). Degradation of Acid Blue 25 in aqueous media using 1700 kHz ultrasonic irradiation: ultrasound/Fe (II) and ultrasound/H<sub>2</sub>O<sub>2</sub> combinations. *Ultrasonics Sonochemistry*, 16(5), 593-598.
5. Magureanu, M., Bradu, C., & Parvulescu, V. I. (2018). Plasma processes for the treatment of water contaminated with harmful organic compounds. *Journal of Physics D: Applied Physics*, 51(31), 313002.
6. Bradu, C., Kutasi, K., Magureanu, M., Puač, N., & Živković, S. (2020). Reactive nitrogen species in plasma-activated water: generation, chemistry and application in agriculture. *Journal of Physics D: Applied Physics*, 53(22), 223001.



## Degradation and of per- and polyfluorinated alkyl substances (PFAS) during plasma treatment

*Barbara Topolovec*<sup>a</sup>, *Nevena Puac*<sup>c</sup>, *Nikola Skoro*<sup>c</sup>, *Mira Petrovic*<sup>a,b</sup>,

<sup>a</sup> *Catalan Institute for Water Research (ICRA), 17003 Girona, Spain (Email: btopolovec@icra.cat)*

<sup>b</sup> *Catalan Institution for Research and Advanced Studies (ICREA), 08010, Barcelona, Spain (Email: mpetrovic@icra.cat)*

<sup>c</sup> *Institute of Physics, University of Belgrade, Pregrevica 118, 11080 Belgrade, Serbia (Email: nevena@ipb.ac.rs, nskoro@ipb.ac.rs)*

### Abstract

Non-thermal plasma (NTP) in liquid and gas-liquid environments generates in situ nitrogen-containing species, hydroxyl radical, hydroperoxyl radical, atomic hydrogen and oxygen, as well as other radicals and active chemical species. These active species are capable of degrading the organic micropollutants (OMPs) from the solution relatively quickly, using a low power discharge. The aim of this study was to investigate degradation of per- and polyfluorinated alkyl substances (PFAS) in different water matrices using the NTP in gas-liquid environment with pin-type electrode configuration. It was found that in 10 minutes treatment time most of the selected compounds can be degraded up to 90% in pure water, while the degradation in "real" water samples - tap water and WWTP secondary effluent was around 50% and 17%, respectively.

### Introduction

Increasing presence of so-called organic micropollutants (OMPs) detected in the aquatic environment has raised the awareness and concern about their adverse impact on aquatic species and human health. Among them, group of man-made chemicals called per- and polyfluoroalkyl substances (PFAS) have become a hot topic in the last few decades because of growing number of reports related to PFAS found in drinking water [1,2], human blood serum samples and animals from both areas with direct impact from the industry facilities and remote areas [3]. Taken into account the studies and the fact that PFAS structure is based on strong carbon-fluorine bond, they are considered as one of the most persistent compounds in the environment. Other studies had shown that their bioaccumulation in drinking water sources and potential to accumulate in the dietary products and human body could cause a serious health effects such as immune suppression, thyroid disease, cancer, and significant (chronic) toxicity [4]. In 2009, perfluorooctane sulfonate (PFOS) was listed as a Persistent Organic Pollutant (POP) in Stockholm Convention [5] as well as by the United States Environmental Protection Agency (USEPA). Other equally known, perfluorooctanoic acid (PFOA) was listed as possible carcinogenic compound under the EU Water Framework Directive [6]. PFOS and its derivatives are included as a priority hazardous substance with Environmental Quality Standard (AA-EQS) limit value of 0.65 ng/L in inland surface waters and 0.13 ng/L in seawater. With recent document, EU POPs regulation [7] lead to complete banish of PFOA and PFOS from the production. In terms of wastewater treatment processes, many studies and practice had shown that most PFAS are highly recalcitrant to conventional wastewater treatment processes, but also to many advanced oxidation processes (AOP).

One of the novel highly promising AOPs, non-thermal plasma (NTP) has been recently recognized as a promising technique for application in (waste)water treatment. Producing radicals that are generally required for water treatment, it can effectively degrade substances in water. In recent studies there is growing focus on using plasma treatment for compounds highly recalcitrant to known water treatment processes such as PFAS [8].

In this study, NTP in gas-liquid environment with pin-type electrode configuration has been evaluated for the removal of PFAS. Experiments have been done at laboratory scale aimed to evaluate removal efficiency of selected long/short chain/novel PFAS in aqueous solution in 3 different matrices as well as to evaluate possible transformation products.

### Experimental procedure

Atmospheric pressure plasma jet (APPJ) was used for the degradation of six PFAS: PFOS, nonfluorobutane-1-sulfonic acid (PFBS), perfluorobutyric acid (PFBA), undecafluorohexanoic acid (PFHxA), 2,3,3,3-tetrafluoro-2-(heptafluoropropoxy) propanoic acid (GenX), dodecafluoro-3H-4,8,-dioxanoate (ADONA). The plasma source consisted of stainless-steel electrode as a high voltage electrode inserted inside the ceramic tube. Both are inserted in the center of a glass tube. Copper tape was used as a ground electrode placed at the bottom of sample vessel. Argon (working gas) was generated at a liquid surface, powered by a high voltage radio frequency (332 kHz). 3 different types of matrices, ultrapure water, tap water and secondary effluent as an aqueous solutions (10 mL) were spiked with compounds, separately, with initial concentration ( $C_0$ ) of 100 ppb. Treatment time was 10 min in each experiment. Figure 1. shows schematic diagram of used plasma configuration.

□

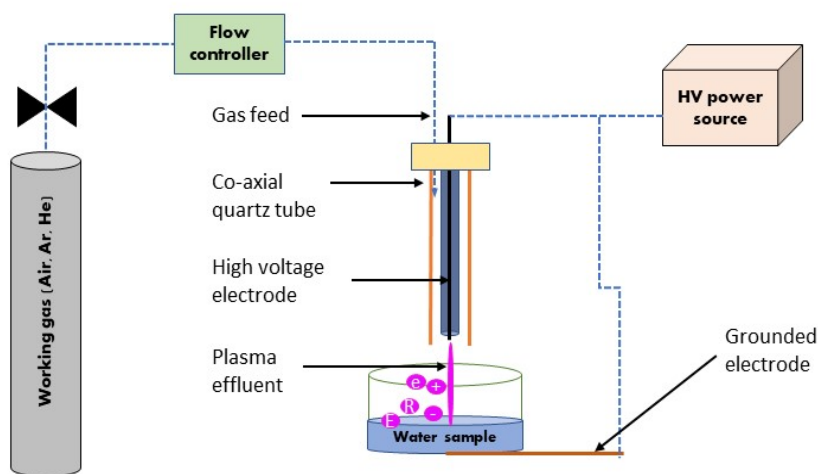


Figure 1. Schematic diagram of atmospheric pressure plasma jet (APPJ).

## Results and discussion

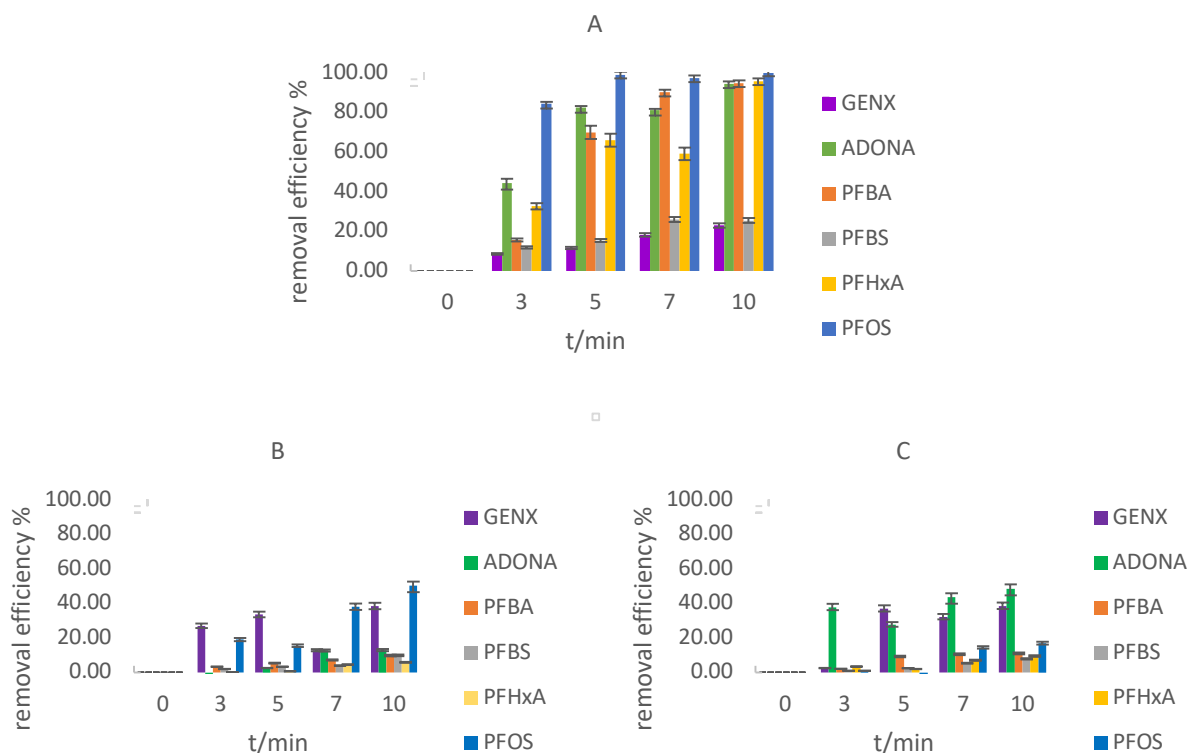


Figure 2. Removal efficiency of PFAS in pure water (A), tap water (B) and WWTP secondary effluent (C)

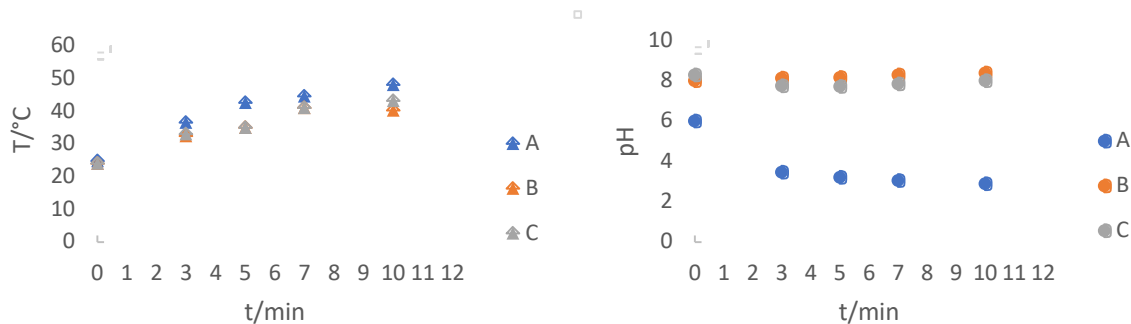


Figure 3. Temperature and pH of A (pure water), B (tap water) and C (WWTP effluent) sample during treatment time

Figure 2 shows that after 10 minutes of treatment, removal efficiency was more than 90% for most of the compounds. PFBS and Genx had shown less degradation since they are short-chained PFAS with stronger C-F bonds. For all the compounds, rapid degradation is observed in the first 5 min followed by further slower increase in removal efficiency. In the case of “real” water samples, it can be observed that when PFAS are in complex matrices, the degradation occurs but less in comparison to pure water samples. Since there are other substances in water, radicals needed

for the effective removal can react with other compounds which results in slower degradation for the same treatment time. Under plasma exposure, all liquid samples were gradually heated, starting from ambient temperature (24°C) up to max 45 °C in some cases. As it can be seen from figure 3, the rise in the temperature is not linear and the heating slows down, which means that non thermal degradation was performed in all types of matrices. As for the pH, it was observed that it decreased drastically in case of distilled water which means there is possible formation of nitrogen species in solution, but in case of “real” water samples there is no significant plasma influence on pH value. Overall, experimental results showed promising performance of APPJ configuration and high degradation of PFAS in short treatment time. It can also be observed that long chained PFAS, such as PFOS showed better degradation than short chained ones in the same matrix type. Degradation of PFOS in tap water and WWTP secondary effluent was 50% and 17%, respectively, achieved in 10 minutes treatment time.

## References

1. W. A. Gebbink, L. van Asseldonk, S.P.J. van Leeuwen, Presence of Emerging Per- and Polyfluoroalkyl Substances (PFASs) in River and Drinking Water near a Fluorochemical Production Plant in the Netherlands, *Environmental Science & Technology* 2017 51 (19), 11057-11065, DOI: 10.1021/acs.est.7b02488
2. J. Campo, M. Lorenzo, F. Pérez, Y. Picó, M. la Farré, D. Barceló, Analysis of the presence of perfluoroalkyl substances in water, sediment and biota of the Júcar River (E Spain). Sources, partitioning and relationships with water physical characteristics, *Environmental Research*, Volume 147, 2016, Pages 503-512, <https://doi.org/10.1016/j.envres.2016.03.010>
3. D. Muir, R. Bossi, P. Carlsson, M. Evans, A. De Silva, C. Halsall, C. Rauert, D. Herzke, H. Hung, R. Letcher, F. Rigét, A. Roos, Levels and trends of poly- and perfluoroalkyl substances in the Arctic environment – An update, *Emerging Contaminants*, Volume 5, 2019, Pages 240-271, <https://doi.org/10.1016/j.emcon.2019.06.002>.
4. Y. Xu, Y. Li, K. Scott, C. H. Lindh, K. Jakobsson, T. Fletcher, B. Ohlsson, E. M. Andersson, Inflammatory bowel disease and biomarkers of gut inflammation and permeability in a community with high exposure to perfluoroalkyl substances through drinking water, *Environmental Research*, Volume 181, 2020, 108923, <https://doi.org/10.1016/j.envres.2019.108923>.
5. Council, O. F. T. H. E. (2020). Directive 2013/11/EU of the European Parliament and of the Council. In *Fundamental Texts On European Private Law* (Vol. 2013, Issue July, pp. 1–17). <https://doi.org/10.5040/9781782258674.0032>
6. European Commission. (2000). European Commission. EU Water Framework Directive - Integrated River Basin Management in Europe. Directive 2000/60/EC. European Commission October 23, 2000. [https://ec.europa.eu/environment/water/water-framework/index\\_en.html](https://ec.europa.eu/environment/water/water-framework/index_en.html)
7. EU Commission, 2019. Regulation (EU) 2019/1021 of the European Parliament and of the Council of 20 June 2019 on persistent organic pollutants (Text with EEA relevance.). Official J. Eur. Union.
8. Nzeribe, N., Crimi, M., Thagard, S., M. & Holsen, M., T., Physico-Chemical processes for the treatment of per- and polyfluoroalkyl substances (PFAS): A review blossom, *Critical Reviews in Environmental Science and Technology*, 1064-3389(Print) 1547-6537.

## Acknowledgements

This research has received funding from the European Union's Horizon 2020 research and innovation program under Marie Skłodowska-Curie grant agreement No. 812880 (EJD NOWELTIES).

## Application of UV-LEDs Advanced Oxidation Processes for the efficient removal of Organic Micropollutants from water

*Danilo Bertagna Silva<sup>1</sup>, Gianluigi Buttiglieri<sup>2,3</sup>, Sandra Babić<sup>1</sup>*

<sup>1</sup>*Faculty of Chemical Engineering and Technology, University of Zagreb. Trg Marka Marulića 19, 10000, Zagreb, Croatia*

<sup>2</sup>*ICRA – Catalan Institute of Water Research. Emili Grahit 101, 17003, Girona, Spain*

<sup>3</sup>*University of Girona. Girona, Spain*

### Introduction

In the current scenario of water scarcity<sup>1</sup> and raising awareness about the harm caused by contaminants of emerging concern<sup>2</sup>, it is fundamental to develop new and sustainable water treatment technologies that are capable of degrading these anthropogenic substances to avoid their bio accumulation and persistence in the environment<sup>3</sup>. Advanced oxidation processes (AOPs) have shown a great capacity to degrade organic micropollutants (OMPs), but even technologies that attract a large amount of scientific attention in the past decades, such as photocatalysis, are still far away from real large-scale applications due to their high energy demands<sup>4,5</sup>. Nevertheless, the fast development of ultra-violet light-emitting diodes (UV-LEDs) has a potential to open new horizons for water treatment technologies. The point-source character of UV-LEDs and other unique features, like controlled periodic illumination (CPI), allow more flexible photoreactor designs<sup>6</sup>.

There is a lack of data evaluating the impact of different reactor designs and other variables related to the matrix composition on the degradation rates of OMPs during photocatalysis<sup>6</sup>, as well as the impact of novel technologies on total organic carbon (TOC) abatement and effluent's toxicity. The EU Watch List of Contaminants of Emerging Concern<sup>7</sup> serves as a guideline for scientists, highlighting substances which are ubiquitously found in European surface waters so that their fate and degradation pathways – as well as degradation possibilities – can be investigated further.

### Materials and methods

The photolytic and photocatalytic degradation of 5 contaminants of emerging concern (ciprofloxacin, sulfamethoxazole, trimethoprim, venlafaxine and desvenlafaxine – all currently in the EU watch list) was investigated. Trace concentrations of the compounds were analyzed by High Performance Liquid Chromatography. Initially, the simulation of light profiles for a photoreactor using different UV-LED arrays was performed using an optical software. Two identical lab scale (150 mL) cylindrical quartz reactors were used. In one of them a titanium dioxide (TiO<sub>2</sub>) nanofilm was embedded on its inner walls for photocatalytic experiments. **Figure 1** shows the experimental set up. To find the best design, a full-factorial design of experiments (DoE) was performed investigating the impact of 4 independent variables and their combined effects on ciprofloxacin's degradation rate and electrical energy per order ( $E_{EO}$ ) consumption. Following that, two other DoE were performed to evaluate the simultaneous degradation of the 5

target pollutants ( $C_0$  of each: 2 mg/L) under a wide range of scenarios using this optimal design. Variables investigated in DoE #2 were LEDs' wavelength, CPI, presence of catalyst nanofilm and water matrix (ultra-pure vs tap water). Evaluated outcomes were each pollutant's degradation rates, as well as the effluent's TOC's abatement and toxicity reduction, represented by the difference between post and pre-treatment bioluminescence of *Vibrio fischeri*. In DoE #3, the impact of inorganic ions and humic acids commonly found in real water bodies on the degradation rates of the 5 target pollutants were investigated during UV-A photocatalysis. Additionally, experiments were performed investigating the influence of the initial pH of reaction; the effect of adding  $H_2O_2$ ; combination of UV-LEDs of different wavelengths (UV-A and UV-C); the presence of scavengers of different reactive species generated during photocatalysis to elucidate reaction pathways for each compound; and, finally, the *Vibrio fischeri*'s bioluminescence of individual solutions of the 5 pollutants was monitored during UV-A photocatalysis to verify the influence of degradation by-products in the overall toxicity of each effluent.

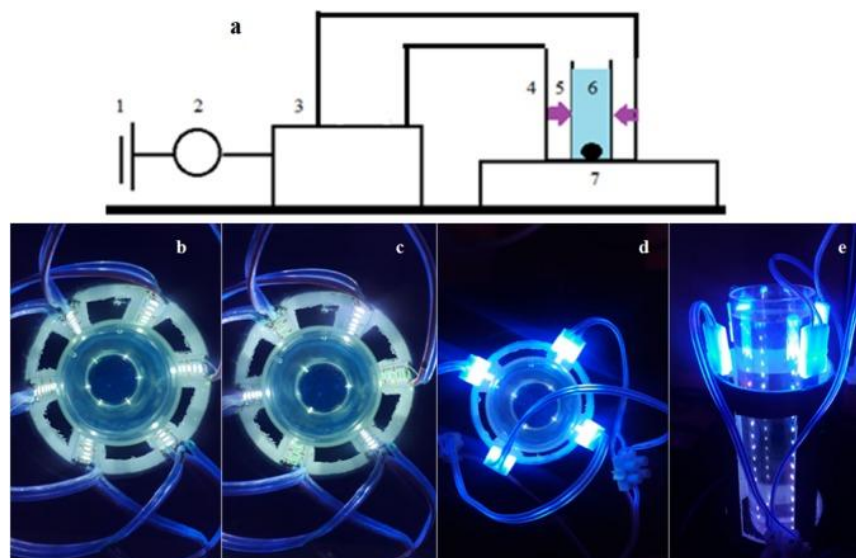


Figure 1. Experimental setup. (a) 1 - energy source, 2 - power meter, 3 - LED control board, 4 - LED columns, 5 - UV rays reaching the reactor, 6 – reactor, and 7 - magnetic stirrer. Below, upviews (b-d) and side view (e) of different arrays

## Results and discussion

The software's simulation of light for different UV-LED arrays showed that a more homogenous illumination profile was not obtained when additional light sources were used. Given the chosen cylindrical geometry, additional LEDs concentrate light in the reactor's central axis, causing light intensity peaks that decrease photocatalysis' efficiency<sup>8</sup>. The most homogenous design was the one containing 3 UV-LED strips, since it was the only one in which none of the light sources were directly facing each other.

The DoE #1 provided an accurate model to predict degradation rates and  $E_{EO}$  values for degradation of ciprofloxacin in ultra-pure water. Results indicated that while the adoption of more LEDs and CPI increased the degradation rates, the energetic trade-off was not statistically

sufficient to turn this gain into lower  $E_{EO}$  values. Only the presence of a  $TiO_2$  nanofilm and a reduction of the distance between the LEDs and the reactor walls were capable of reducing  $E_{EO}$  values. It was demonstrated that CPI can only be effective in the presence of a catalyst, not contributing during photolysis alone. The optimal photoreactor design chosen matched the one that combined the highest light homogeneity and lowest  $E_{EO}$  value.

DoE #2 also successfully provided accurate models to predict degradation rates of 5 target pollutant simultaneously, as well as TOC decrease and difference in toxicity levels. It was observed that best degradation results were obtained by UV-A photocatalysis and/or UV-C photolysis, depending on the pollutant. This is due to the fact that: 1) four out of five tested compounds are impervious to UV-A photolysis; and 2) UV-C rays, although more capable of breaking pollutants' chemical bonds, are easily absorbed by substances on the way than rays of longer wavelengths. Because of that, the presence of the  $TiO_2$  nanofilm caused a screening effect that hindered degradation. Moreover, the impact of matrix was significant for every pollutant, and especially for TOC decrease. This highlights the importance of pre-treatments for an optimal performance of photo-based processes. Toxicity analysis suggests that experiments performed with UV-C reduced the effluent's overall toxicity, while experiments performed with UV-A increased it.

DoE #3 provided accurate models for degradation for some of the target compounds, but not all. Possible explanations for that can be the influence of other variables which were not considered during the analysis, such as the influence of initial pH and the presence of multiple degradation products. However, surface-response graphs were obtained showing how the degradation constant rate of each compound responds differently to changes in the matrix.

Experiments investigating the impact of initial pH and the presence of scavengers during UV-A photocatalysis reinforced the fact that each compound will respond differently to each situation. The use of combined wavelengths did not cause any improvement in reaction rates or  $E_{EO}$  values. The addition of  $H_2O_2$  substantially improved reaction rates for all scenarios – particularly for cases without the catalyst nanofilm due to the previously discussed screening effect. Monitoring of *Vibrio fischeri* bioluminescence of individual solutions of all target pollutants during UV-A photocatalysis showed a toxicity increase for all cases, even after the parent compound is completely degraded.

## Conclusions

Different photoreactor designs and other unique features provided by UV-LEDs were able to increase photolytic and photocatalytic degradation rates of pharmaceuticals which are currently in the EU watch list of contaminants of emerging concern. However, the energy demands of these treatments still rank very high, even among other AOPs, remaining unfeasible for practical purposes. DoE is a powerful tool to further understand and obtain empirical models to describe systems containing multiple significant variables such as photocatalysis. The results show that each compound had different responses to each treatment/scenario, meaning that the optimized design will depend on matrix composition, target pollutant reactivity and required effluent standards of each case. When performing photocatalysis, UV-C sources should be avoided due to their screening effect – although they can be highly effective on photolysis-based systems (e.g. disinfection). Pre-treatments are fundamental for an efficient performance of photo-based processes, and attention should be paid to the more toxic degradation by-products which may be formed from the multiple photocatalytic degradation routes.

Although photocatalysis' energy demands are still very high, the quick development of UV-LEDs in the past decade suggests that their wall-plug efficiencies will keep decreasing exponentially, which can lead to a substantial decrease on the process' costs.  $E_{EO}$  values of UV-LED photocatalysis have already reached the same levels of traditional UV mercury lamps, and even shorter wavelengths (e.g. UV-C) are now approaching levels of UV-A or visible light.

## References

1. van Vliet, M.; Jones, E.; Florke, M.; Franssen, W.; Hanasaki, N.; Wada, Y.; Yearsley, J. Global water scarcity including surface water quality and expansions of clean water technologies. *Environ. Res. Letters*, **2021**, *16*, 024020.
2. Wilkinson, J.; Hooda, P.; Barker, J.; Barton, S.; Swinden, J. Occurrence, fate and transformation of emerging contaminants in water: An overarching review of the field. *Environ. Pollut.* **2017**, *231*, 954–970.
3. Chávez-Mejía, A.; Navarro-Gonzalez, I.; Magana-Lopez, R.; Uscanga-Rodan, D.; Zaragoza-Sanchez, P.; Jimenez-Cisneros, B. Presence and natural treatment of organic micropollutants and their risks after 100 years of incidental water reuse in agricultural irrigation. *Water (Switzerland)*, **2019**, *11*, 2148.
4. Loeb, S.; Alvarez, P.; Brame, J.; Cates, E.; Choi, W.; Sedlak, D.; Waite, T.; Westerhoff, P.; Kim, J.; Crittenden, J.; Dyonysius, D.; Li, Q.; Li-Puma, G.; Quan, X.; Sedlak, D.; Waite, T.; Westerhoff, P.; Kim, J. The technology horizon for photocatalytic water treatment: Sunrise or sunset? *Environ. Sci. Technol.* **2019**, *53*, 2937–2947.
5. Miklos, D.; Remy, C.; Jekel, M.; Linden, K.; Drewes, J.; Hübner, U. Evaluation of advanced oxidation processes for water and wastewater treatment - A critical review. *Water Res.* **2018**, *139*, 118–131.
6. Bertagna Silva, D.; Buttiglieri, G.; Babić, S. State-of-the-art and current challenges for TiO<sub>2</sub>/UV-LED photocatalytic degradation of emerging organic micropollutants. *Environ. Sci. Pollut. Res.* **2020**, *28*, 103–120.
7. European Commission. EUR-Lex—2020/1161 of 4 August 2020 establishing a watch list of substances for Union-wide monitoring in the field of water policy pursuant to Directive 2008/105/EC of the European Parliament and of the Council. *Off. J. Eur. Union* **2020**, *257*, 32–35.
8. Boyjoo, Y.; Ang, M.; Pareek, V. Light intensity distribution in multi-lamp photocatalytic reactors. *Chem. Eng. Sci.* **2013**, *93*, 11–21.

## Acknowledgments

This research was funded by the European Union's Horizon 2020 research and innovation program under the Marie Skłodowska-Curie grant agreement No 812880 (NOWELTIES), Joint PhD Laboratory for New Materials and Inventive Water Treatment Technologies, Harnessing resources effectively through innovation. The authors thank Generalitat de Catalunya through the Consolidated Research Group 2017-SGR-1318. ICRA researchers give thanks for funding from the CERCA program/Generalitat de Catalunya.



## Microwave-assisted synthesis of N/TiO<sub>2</sub>/rGO and immobilization on alumina ceramic foam substrate for photocatalytic degradation of pharmaceuticals

*C. Sanchez\**, *Z. Švagelj\**, *V. Mandić\*\**, *J. Radjenović<sup>†,§</sup>*, *D. Ljubas\** and *L. Čurković\**

*\* Faculty of Mechanical Engineering and Naval Architecture, University of Zagreb, Ivana Lučića 5, 10002 Zagreb, Croatia*

*\*\*Faculty of Chemical Engineering and Technology, University of Zagreb, Marulićev trg 20, 10000 Zagreb, Croatia*

*†Catalan Institute for Water Research (ICRA), Emili Grahit 101, 17003 Girona, Spain*

*§Catalan Institution for Research and Advanced Studies (ICREA), Passeig Lluís Companys 23, 08010 Barcelona, Spain*

### Abstract

Nitrogen-doped TiO<sub>2</sub>/reduced graphene oxide (N/TiO<sub>2</sub>/rGO) photocatalyst was synthesized by the microwave-assisted process and subsequently immobilized on Al<sub>2</sub>O<sub>3</sub> ceramic foam. The obtained photocatalyst was characterized by XRD, FTIR, Raman, SEM-EDS, XPS, and N<sub>2</sub> adsorption isotherms. N/TiO<sub>2</sub>/rGO photocatalytic activity was evaluated for ciprofloxacin (CIP) and diclofenac (DCF) degradation under UVA, solar and visible light irradiation sources. The crystalline phase of TiO<sub>2</sub> present in the N/TiO<sub>2</sub>/rGO nanocomposite was anatase. In removing CIP and DCF under different irradiation sources, N/TiO<sub>2</sub>/rGO immobilized on Al<sub>2</sub>O<sub>3</sub> ceramic foam surface (Al<sub>2</sub>O<sub>3</sub>@N/TiO<sub>2</sub>/rGO) showed a competitive degradation rate compared to the photocatalyst in suspension. Al<sub>2</sub>O<sub>3</sub>@N/TiO<sub>2</sub>/rGO showed good stability and reusability, which are critical parameters in photocatalytic processes.

### Keywords

Microwave-assisted method, N/TiO<sub>2</sub>/rGO, Al<sub>2</sub>O<sub>3</sub> support, UVA, visible light, simulated solar light.

## INTRODUCTION

In the last 20 years, organic micropollutants (OMPs) have gained significant attention because of their impact on the environment. Apart from the fact that some of these OMPs, especially pharmaceuticals, cannot be efficiently removed by the conventional wastewater treatment plants (WWTPs), they could bioaccumulate, prove harmful to the aquatic system and represent a threat to public health [1,2]. Therefore, to ensure the complete removal of OMPs from the wastewater, additional treatment technologies should be coupled to the existing WWTPs.

Advanced oxidation processes (AOPs) such as Fenton, photocatalysis, ozonation, etc., have been considered as a great alternative for the removal of OMPs from the wastewater. Among different AOPs, TiO<sub>2</sub> heterogeneous photocatalysis is actively studied because of TiO<sub>2</sub>'s outstanding photocatalytic activity, low cost, excellent chemical stability, and non-toxicity. However, TiO<sub>2</sub> is only photoactive under UV light irradiation due to its high bandgap (3.2 eV), hindering its applicability under solar irradiation (4% UV, 48% visible). Moreover, the photogenerated electron-hole pair can quickly recombine, decreasing the photocatalytic activity [3]. Therefore, modification of TiO<sub>2</sub> by metals or non-metals doping can be a strategy to reduce the recombination rate and/or to redshift its optical response to the visible range.

Apart from the drawbacks related to energy bandgap and recombination effect, photocatalyst recovery is another challenge that hampers its large-scale application from an economical point of view. The immobilization of TiO<sub>2</sub> on different substrate surfaces is considered one of the most feasible approaches to avoid photocatalyst recovery and simplify its usage [4]. Therefore, this study focuses on the synthesis of N/TiO<sub>2</sub>/rGO photocatalyst using the microwave-assisted method and subsequent immobilization on Al<sub>2</sub>O<sub>3</sub> ceramic foam surface to remove pharmaceuticals ciprofloxacin (CIP) and diclofenac (DCF) in aqueous solutions using different irradiation sources.

## EXPERIMENTAL SECTION

### **Used materials**

Titanium (IV) isopropoxide (TIP, 97%, Sigma-Aldrich), acetylacetone ( $\geq 99\%$ , Honeywell), ethanol absolute (p.a., Grammol), urea (99.5%, Sigma-Aldrich), graphene oxide water dispersion (0.4 wt% concentration, Graphenea), ascorbic acid (p.a., Sigma-Aldrich), tetraethyl orthosilicate (TEOS, 98%, Merck), hydrochloric acid (37%, Merck), commercial  $\text{Al}_2\text{O}_3$  powder CT 3000 SG (Almatis), carbonic acid-based polyelectrolyte Dolapix CE 64 (Zschimmer & Schwarz Chemie), polyvinyl alcohol (PVA, 99+ % hydrolyzed, Sigma-Aldrich), antifoaming agent Contraspum K 1012 (Zschimmer & Schwarz Chemie) Polyurethane foam (Rekord-tim) with the pore density of 17 pores per inch (ppi), ciprofloxacin (CIP, 98%, Acros Organics) and diclofenac sodium salt (DCF, Sigma-Aldrich) were used as received without further purification. Ultrapure quality water was used throughout the experiments (electrical conductivity of  $0.055 \mu\text{S}/\text{cm}$  at  $25^\circ\text{C}$ ).

### ***N/TiO<sub>2</sub>/rGO microwave-assisted synthesis***

Previously to photocatalyst synthesis, graphene oxide (GO) was reduced using a similar procedure reported by Baptista-Pires et al. [5]. N/TiO<sub>2</sub>/rGO containing 0.25 wt% of rGO was synthesized by the sol-gel method combined with the microwave-assisted approach. Briefly, rGO was dispersed in ethanol and sonicated for 45 minutes at 35 Hz in an ultrasound bath. Meanwhile, TIP was mixed with acetylacetone, then ethanol/rGO solution was added while stirring at room temperature; these reagents were mixed at a molar ratio of TIP:AcAc:EtOH = 0.014:0.039:1.37 and labelled as solution A. On the other hand, urea (N/Ti molar ratio equal 12) was dissolved in 20 mL of deionized water and labelled as solution B. Solutions A and B were added dropwise to 80 mL of deionized water while stirring at room temperature. This final solution was stirred for 1 hour at room temperature. After one hour, the solution was transferred to four Teflon vessels in the microwave (MW) oven for thermal treatment at  $200^\circ\text{C}$  and 10 minutes. The synthesized photocatalyst was washed several times with ethanol and water, centrifuged, and dried at  $65^\circ\text{C}$  overnight.

### ***Preparation of Al<sub>2</sub>O<sub>3</sub> ceramic foam substrate***

Open-cell alumina ( $\text{Al}_2\text{O}_3$ ) ceramic foam was prepared following the Schwarzwald and Somers replica method. The alumina foam was designed in the form of a ring with outer and inner diameters of approximately 90 and 40 mm, respectively, and a thickness of 15 mm. For that purpose, a polyurethane (PU) sponge with a pore density of 17 pores per inch (ppi) was impregnated with the aqueous ceramic suspension containing alumina powder ( $\alpha\text{-Al}_2\text{O}_3$ , CT 3000 SG), dispersant (Dolapix CE 64), binder (poly (vinyl alcohol)) and antifoaming agent (Contraspum K 1012). The following amounts were used: 75, 0.4, 1.5, and 0.1 wt.%, respectively. After impregnation and overnight drying, the foam was thermally treated. First applying a slow heating rate of  $1^\circ\text{C}/\text{min}$  to  $600^\circ\text{C}$  with 1 h holding period at  $300^\circ\text{C}$  and at  $600^\circ\text{C}$  to prevent the structure from collapsing during the burnout of the PU foam and other organic matter. After that, the temperature was increased to  $1600^\circ\text{C}$  with a rate of  $5^\circ\text{C}/\text{min}$ . The foam was kept at the final sintering temperature for 2 hours before furnace cooling. Švagelj et al. published a manuscript with more details about this procedure [6].

### ***Deposition of N/TiO<sub>2</sub>/rGO nanocomposite on Al<sub>2</sub>O<sub>3</sub> foam substrate***

In order to promote good adhesion between N/TiO<sub>2</sub>/rGO containing 0.25 wt% of rGO and  $\text{Al}_2\text{O}_3$  foam surface, a binder solution was prepared. 2 mol of deionized water was acidified with 0.01 mol of HCl, followed by the addition of 0.02 mol of TEOS, and the solution was kept under stirring conditions for 5 hours at room temperature to form a binder solution. Then, a coating solution containing binder:ethanol:N/TiO<sub>2</sub>/rGO in a weight ratio of 7.5:85:7.5 was sonicated for 30 minutes at 35 Hz. Meanwhile,  $\text{Al}_2\text{O}_3$  ceramic foam was placed in a vacuum chamber (CitoVac, Struers) at 0.16 bar for 20 minutes; then, the coating solution was injected slowly into the vacuum chamber until the ceramic foam was completely covered, keeping the vacuum for another 20 minutes. After the coating time, the ceramic foam was removed from the vacuum chamber and was left to dry at room temperature for 30 minutes. Afterward, it was thermally treated at  $65^\circ\text{C}$  for 3 h, followed by another 3 h at  $90^\circ\text{C}$ , and finally at  $120^\circ\text{C}$  overnight.

### Characterization of photocatalyst

Structural, morphological and optical properties of N/TiO<sub>2</sub>/rGO were determined by X-Ray Diffraction (XRD), Fourier-transform infrared (FTIR) spectroscopy, Scanning electron microscopy (SEM-EDS), specific surface area (BET) analysis, Raman spectroscopy, Diffuse reflectance spectroscopy (DRS) and X-Ray Photoelectron Spectroscopy (XPS).

### Photolysis and photocatalytic activity evaluation

The photocatalytic activity of N/TiO<sub>2</sub>/rGO nanocomposite with 0.25 wt.% rGO deposited on Al<sub>2</sub>O<sub>3</sub> foam surface (Al<sub>2</sub>O<sub>3</sub>@N/TiO<sub>2</sub>/rGO) was evaluated through the degradation of ciprofloxacin (CIP) and diclofenac (DCF), using different irradiation sources: UVA (365 nm, 70 W), solar light simulator (SLS), cold visible light (CVL) (450 nm and 600 nm, 100 W), and blue visible light (BVL) (405 nm, 70 W). In each experiment, the Al<sub>2</sub>O<sub>3</sub>@N/TiO<sub>2</sub>/rGO was placed in 100 mL of pollutant solution (CIP or DCF, 10 mg·L<sup>-1</sup>) and irradiated from above with lamps 20 cm away from the reactor. The Al<sub>2</sub>O<sub>3</sub>@N/TiO<sub>2</sub>/rGO was left in contact with the pollutant for 30 minutes in the dark to ensure adsorption-desorption equilibrium, followed by 2 hours of irradiation. Samples were taken from the reactor at intervals of 0, 10, 20, 30, 45, 60, 90, and 120 min, filtered using a 0.45 μm mixed cellulose ester membrane filter and analysed with a UV-Vis spectrophotometer (HEWLETT PACKARD, Model HP 8430) at 273 nm (maximum absorption peak of CIP) and 276 nm (maximum absorption peak of DCF). During the whole experiment, the temperature was kept at 25 °C by a thermostatic bath. For comparative purposes, the photocatalytic activity of N/TiO<sub>2</sub>/rGO nanocomposite was evaluated in suspension, using the same pollutants and irradiation sources described above. In this case, 25 mg of the photocatalyst was dispersed in 100 mL of pollutant solution (10 mg·L<sup>-1</sup>), left in dark adsorption for 30 minutes, and irradiated for 2 hours. The sampling and analysis were the same as previously described. For the photolysis process, 100 mL of pollutant solution (10 mg·L<sup>-1</sup>) was irradiated for 2 hours, applying the same sampling and analysis described before.

## RESULTS

The structural, morphological, and optical properties of N/TiO<sub>2</sub>/rGO are determined by different analytical techniques summarized in Table 1. The specific surface area of N/TiO<sub>2</sub>/rGO is larger than commercial TiO<sub>2</sub>, which could be attributed to the rGO incorporation. The XRD and Raman analysis showed that the obtained material presented only the anatase phase, the most photoactive crystalline phase. The energy bandgap of N/TiO<sub>2</sub>/rGO was calculated based on the DRS analysis through the Tauc plot. The energy bandgap was observed to be reduced compared to the commercial TiO<sub>2</sub>, probably due to the interstitial nitrogen doping, confirmed by the XPS analysis.

**Table 1.** Morphological and optical properties of N/TiO<sub>2</sub>/rGO containing 0.25 wt% rGO.

	S <sub>BET</sub> , m <sup>2</sup> g <sup>-1</sup>	V <sub>Pore</sub> , cm <sup>3</sup> g <sup>-1</sup>	Average pore size	Crystal phase	Energy bandgap
N/TiO <sub>2</sub> /rGO 0.25 wt%	176.45	0.309	6.67 nm	Anatase	3.11 eV
TiO <sub>2</sub> Degussa P25*	50	-	-	Anatase/Rutile (80/20)	3.20 eV

\*Data from the literature

The photocatalytic activity of N/TiO<sub>2</sub>/rGO and Al<sub>2</sub>O<sub>3</sub>@N/TiO<sub>2</sub>/rGO was evaluated in the degradation of CIP and DCF aqueous solution (10 mg·L<sup>-1</sup>) under UVA light, solar light, blue light and visible light, as it is shown in **Figure 1**. The photocatalytic experiments under UVA light and solar light showed that N/TiO<sub>2</sub>/rGO and Al<sub>2</sub>O<sub>3</sub>@N/TiO<sub>2</sub>/rGO removed both pollutants completely after 120 minutes of irradiation. However, under solar light (**Figure 1b**), a faster degradation is observed than under UVA light (**Figure 1a**). This faster degradation could be attributed to the co-doping effect, where nitrogen shifts the light absorption to the visible range, while the rGO acts as an electron trap, avoiding the charges recombination ( $h^+/e^-$ ). Although the suspended photocatalyst showed a better degradation rate, the immobilized photocatalyst presented a competitive degradation rate. Under visible lights

(Cold and Blue, **Figure 1c, d**), the immobilized photocatalyst displays better removal efficiencies of CIP and DCF than the photocatalyst in suspension. Complete removal was observed under blue visible light for CIP, while partial removal was achieved under cold visible light. In the case of DCF, it was partially removed under blue visible light, while under cold visible light, no removal was observed. Degradation of DCF by photolysis was observed only under solar light, while CIP showed degradation by photolysis under UVA light and solar light.

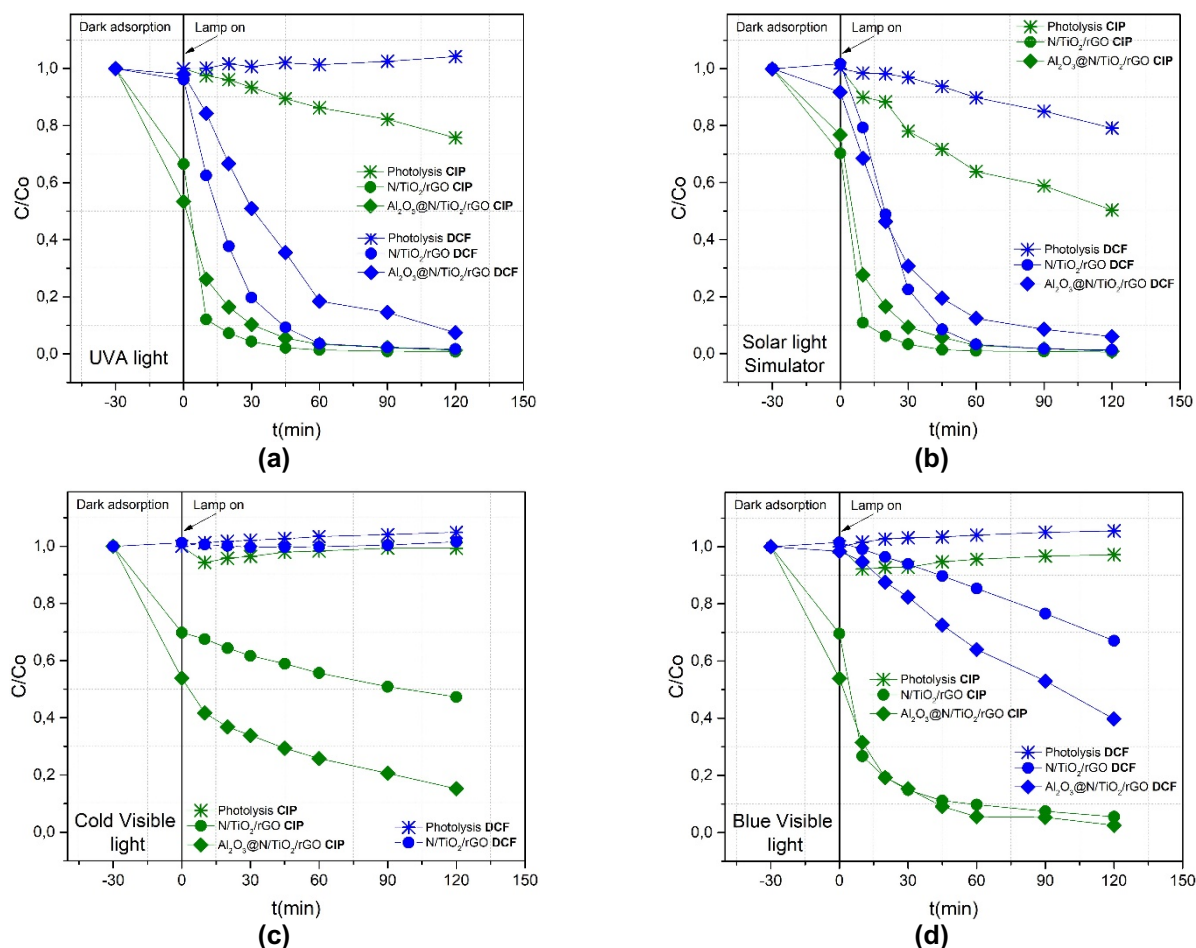


**Figure 1.** Photolysis and photocatalytic degradation of CIP and DCF by N/TiO<sub>2</sub>/rGO and Al<sub>2</sub>O<sub>3</sub>@N/TiO<sub>2</sub>/rGO under (a) UVA light, (b) solar light, (c) cold visible light, and (d) blue visible light.

## CONCLUSIONS

Synthesis of N/TiO<sub>2</sub>/rGO photocatalyst was successfully achieved under mild conditions (200 °C, 10 min) by microwave-assisted synthesis, where anatase phase was obtained without further calcination procedure that usually is required on the conventional synthesis methods. The Al<sub>2</sub>O<sub>3</sub>@N/TiO<sub>2</sub>/rGO photocatalyst showed good photoactivity compared to the material in suspension, having good stability and reusability. These results indicate that the immobilization method and the selected Al<sub>2</sub>O<sub>3</sub> ceramic foam substrate are good strategies for photocatalyst reusability without need for a recovery step.

## ACKNOWLEDGEMENT

This research is part of the NOWELTIES project and has received funding from the European Union's Horizon 2020 research and innovation program under the Marie Skłodowska Curie grant agreement No. 812880.

## REFERENCES

1. Ebele, A.J.; Abou-Elwafa Abdallah, M.; Harrad, S. Pharmaceuticals and personal care products (PPCPs) in the freshwater aquatic environment. *Emerg. Contam.* **2017**, *3*, 1–16,

doi:10.1016/j.emcon.2016.12.004.

2. Khurana, P.; Pulicharla, R.; Kaur Brar, S. Antibiotic-metal complexes in wastewaters: fate and treatment trajectory. *Environ. Int.* **2021**, *157*, 106863, doi:10.1016/j.envint.2021.106863.
3. Fagan, R.; McCormack, D.E.; Dionysiou, D.D.; Pillai, S.C. A review of solar and visible light active TiO<sub>2</sub> photocatalysis for treating bacteria, cyanotoxins and contaminants of emerging concern. *Mater. Sci. Semicond. Process.* **2016**, *42*, 2–14, doi:10.1016/j.mssp.2015.07.052.
4. Magnone, E.; Kim, M.K.; Lee, H.J.; Park, J.H. Facile synthesis of TiO<sub>2</sub>-supported Al<sub>2</sub>O<sub>3</sub> ceramic hollow fiber substrates with extremely high photocatalytic activity and reusability. *Ceram. Int.* **2021**, *47*, 7764–7775, doi:10.1016/j.ceramint.2020.11.121.
5. Baptista-Pires, L.; de la Escosura-Muñiz, A.; Balsells, M.; Zuaznabar-Gardona, J.C.; Merkoçi, A. Production and printing of graphene oxide foam ink for electrocatalytic applications. *Electrochem. Commun.* **2019**, *98*, 6–9, doi:10.1016/j.elecom.2018.11.001.
6. Švagelj, Z.; Mandić, V.; Čurković, L.; Biošić, M.; Žmak, I.; Gaborardi, M. Titania-Coated alumina foam photocatalyst for memantine degradation derived by replica method and sol-gel reaction. *Materials (Basel)*. **2020**, *13*, doi:10.3390/ma13010227.

## Magnetic biocatalyst formulation with unspecific peroxygenase from *Agrocybe Aegerita* for antibiotic removal

Sabrina Rose de Boer<sup>1</sup>, Andreas Schaeffer<sup>2</sup>, Maria Teresa Moreira<sup>1</sup>

<sup>1</sup> CRETUS, Department of Chemical Engineering, Universidade de Santiago de Compostela, 15782-Santiago de Compostela, Galicia, Spain; <sup>2</sup>RWTH Aachen University, Institute for Environmental Research, Worringerweg 1, 52074 Aachen, Germany

### Abstract

Laccase-based wastewater treatment is limited by their narrow substrate scope and low pH optimum. To efficiently degrade non-phenolic pollutants as antibiotics, other oxidoreductases are needed. 500 U/L unspecific peroxygenase from *Agrocybe Aegerita* (AaeUPO) transforms 5 mg/L sulfamethoxazole (SMX) within 10 minutes at pH=7, however, it is less stable compared to laccases in wastewater conditions. We aimed to improve AaeUPO stability by immobilization onto magnetic nanoparticles via glutaraldehyde crosslinking and subsequent organosilica shielding. Even though stability could be improved by the shielding, the reusability is not yet satisfactory, dropping to 70% of SMX removal after the third cycle.

### Introduction

Despite the numerous publications on oxidoreductases in wastewater treatment, only few examples exist for pilot scale application.[1] This can be explained by three main issues still present at lab scale level: limited substrate scope, slow reaction kinetics and instability in wastewater conditions. The intrinsic selectivity of enzymes impedes the simultaneous transformation of a broad range of compounds present in wastewaters. While laccases could be successfully applied for phenolic substances, pharmaceuticals without those functional groups were not satisfactorily removed. This limitation was sought to be overcome by the addition of mediator compounds, however these compounds add high costs and can increase toxicity of the effluents.[2] Other oxidoreductases with a broader substrate scope such as peroxidases and peroxygenases can overcome this limitation. While peroxidases showed already an improved removal performance compared with laccases, peroxygenases remain underrepresented in the field of bioremediation. [3,4] Nevertheless, AaeUPO proved to be applicable to transform a wide range of pollutants which are recalcitrant to laccase treatment, showing transformation of several pharmaceuticals in less than 10 minutes.[5] The mayor limitation for its scale-up is the limited stability, particularly in excess presence of its cofactor hydrogen peroxide (H<sub>2</sub>O<sub>2</sub>). We therefore aim to stabilize this enzyme onto magnetic nanoparticles for its repeated reuse.

### Materials and methods

*Magnetic nanoparticle synthesis:* 1988.3 mg (10 mmol) iron(II)chloride (FeCl<sub>2</sub>\*4H<sub>2</sub>O) and 3244.0 mg (20 mmol) iron(III)chloride (FeCl<sub>3</sub>\*6H<sub>2</sub>O) and 424.95 g (5 mmol) sodium nitrate (NaNO<sub>3</sub>) were dissolved in 10 mL water. The solution was purged with nitrogen for 30 minutes and subsequently, 32.9 mL of a 2 M NaOH solution, which was accordingly degassed, was added in one pulse to the reaction mixture under continuous stirring at 200 rpm. The mixture was left stirring for 15 min, and the black precipitate was washed six times with water. *APTES functionalization:* To 30 mL of a 12.25 mg mL<sup>-1</sup> solution of MNP in sodium phosphate buffer (0,1 M pH=7.5) 1.98 mL of APTES (18 mmol/g MNP) were added and the reaction mixture was kept at 80°C for 20h. Resulting particles were washed four times with deionized water. *Ninhydrin assay:* 200 mg Ninhydrin and 30 mg Hydrindantin were dissolved in 7.5 mL degassed DMSO. 2.5 mL 4 M sodium acetate buffer (pH=5.6) were added. Calibration standards contained APTES in a 50:50 EtOH/water solution. Nanoparticles were dispersed in

a 50:50 EtOH/water solution in exactly determined concentrations in the range of 1-5 mg/mL. 250  $\mu\text{L}$  of the standards or samples were thoroughly mixed with 250  $\mu\text{L}$  staining solution and incubated at 95°C for 15 min in sealed Eppendorf tubes. The tubes were immediately cooled in an ice bath and 500  $\mu\text{L}$  EtOH were added. The samples containing particles were centrifuged at 22140 x g or 5 min. 200 $\mu\text{L}$  of the supernatant were placed in a 96-well plate and the absorbance was read at 570 nm. *Zeta potential* was measured in disposable capillary cells (DTS1070) in a Malvern Zetasizer Nano ZS equipped with the Zetasizer software version 4.17. Suspensions were diluted to 0.5  $\text{g L}^{-1}$  and pH was adjusted with few drops of NaOH or HCl solutions. *Glutaraldehyde functionalization*: 3.2  $\text{g L}^{-1}$  aminofunctionalized magnetite nanoparticles were immersed for 1 h in a 1 % glutaraldehyde solution in sodium carbonate buffer, pH=9. *Enzyme immobilization*: A defined amount of enzyme was added to glutaraldehyde functionalized particles at different pH values at 20°C. Further immobilizations were performed with optimized parameters. *Enzyme shielding*: 6 mL of a 3.2  $\text{g L}^{-1}$  of the enzyme functionalized magnetite nanoparticles were incubated with 29  $\mu\text{L}$  TEOS in potassium phosphate buffer (pH=7). After one hour, 7 $\mu\text{L}$  APTES were added, and the reaction proceeded for 15 h, then, the particles were washed and cured in potassium phosphate buffer for 24h at 20°C.[6] *Enzyme activity* was determined via ABTS oxidation (0.5 mM ABTS, 1 mM  $\text{H}_2\text{O}_2$ , pH=4.4) in a microplate reader. One unit of activity corresponds to 1 $\mu\text{mol}$  ABTS<sup>+</sup>/min formed in the assay mixture. *SMX degradation* was monitored in 4 mL vials,  $\text{H}_2\text{O}_2$  was dosed manually in one pulse at the beginning of the experiment or in consecutive pulses. Initial SMX concentrations were set at 5 mg/L, and enzyme activity at 500U/L. SMX was quantified using an Agilent Zorbax eclipse XDB-C18 column, mobile phase A:water, 0.1% formic acid; mobile phase B: acetonitrile, 0.1% formic acid (ACN), using a linear gradient of 20% -100% B(1-11 min) followed by 2 min 100% B, after which the column was re-equilibrated to initial conditions until 16 min. SMX was detected via DAD detector at 275nm.

## Results

Figure 1 shows the characterization results obtained during the steps of biocatalyst synthesis.

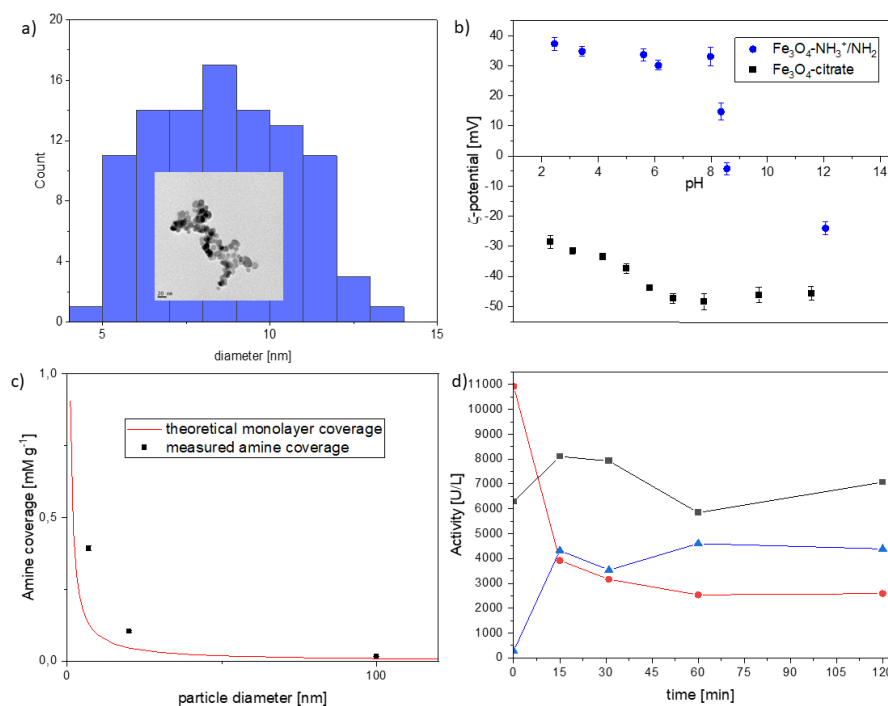


Figure 1:a) Size distribution histogram of synthesized magnetic nanoparticles (insert: TEM Image); b) zeta potential of citrate stabilized magnetic nanoparticles (black rectangles) and aminofunctionalized magnetic nanoparticles (blue dots) in dependence of the pH. c) red line: theoretical monolayer coverage of amino groups in dependence of the particle diameter; black rectangles: measured amino group coverage. d) Attained laccase activity onto the catalyst, which had been submerged

to different glutaraldehyde incubation times. black: initial activity, red: supernatant activity; blue: immobilized enzyme after wash.

Magnetite particles were prepared by oxidative coprecipitation, yielding a mean particle diameter of  $9\pm 3$  nm, determined via TEM image processing (Figure 1a). The subsequent aminofunctionalization was monitored qualitatively by zeta potential measurement, showing a shift towards positive values in the range of pH=2-8.25. Accessible amino groups were quantified by the ninhydrin assay (Figure 1b). Figure 1c shows the measured amine coverage in mM/g and the theoretical monolayer coverage based on the estimations by Sun et al. [7] The obtained amine coverages are above the theoretical monolayer coverages, possibly by the formation of organosilane aggregates due to condensation of several APTES molecules under aqueous conditions.[8] Figure 1d shows the immobilized activity of laccase as test enzyme in dependence of glutaraldehyde reaction time. After 60 minutes of incubation there is no further increase in immobilized activity indicating that all available amino groups reacted with glutaraldehyde. During immobilization, the recovered activity of AaeUPO showed highest values at pH=9 and reached a plateau after 1h of incubation (data not shown).

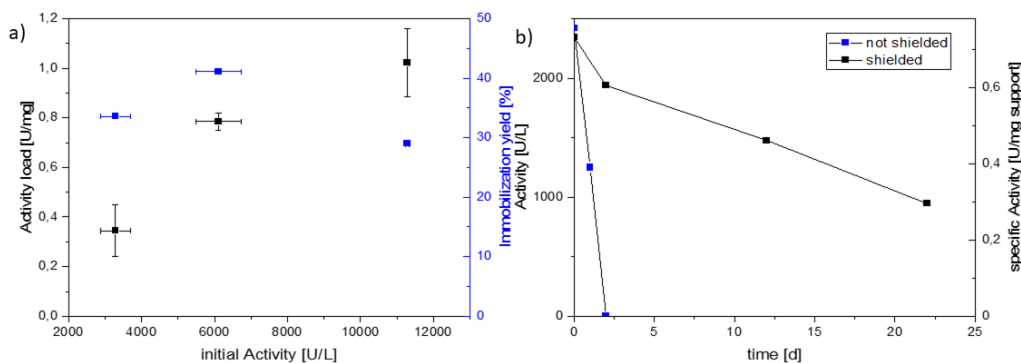


Figure 2: a) Immobilization yield and activity load in dependence of initially applied AaeUPO activity; b) Activity retention of the unshielded (blue rectangles) and the shielded nanocatalyst (black rectangles).

The optimization of initial AaeUPO amount during immobilization indicates that a considerable share of enzyme activity is deactivated during the process, allowing a maximal immobilization yield of  $40\pm 8\%$  (Figure 2a). Even though this value is lower compared to other more complex covalent immobilization strategies, the obtained maximal activity load of  $1.04\pm 0.14$  U/mg is one of the highest reached so far.[3,9] When the immobilized catalyst is not further treated, the activity drops to zero within two days of storage (Figure 2b). Conversely, when the catalyst is shielded by an organosilica layer according to Corroero et al. the activity maintains 40% of its original value after three weeks of storage.[6]

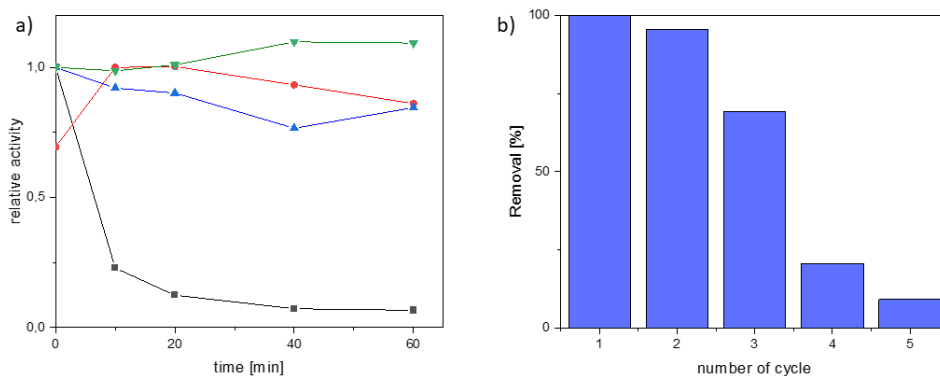


Figure 3: a) Stability over time of the immobilized and free enzyme at 1mM H<sub>2</sub>O<sub>2</sub> (red and black graph, respectively) and at 0.01mM H<sub>2</sub>O<sub>2</sub> (green and blue graph, respectively); b) Removal percentage of SMX in consecutive 10-min cycles, enzyme



activity: 500U/L;  $c_0(\text{SMX})=5 \text{ mg/L}$ ;  $\text{pH}=7$ ;  $T=20^\circ\text{C}$ . Initial  $\text{H}_2\text{O}_2$  concentration was 0.1 mM, every minute, an additional amount of 0.05mM was added.

Figure 3a shows the stability of the immobilized and free enzyme at different hydrogen peroxide concentrations in potassium phosphate buffer in the presence of SMX. Especially at high hydrogen peroxide concentrations, the positive effect of enzyme immobilization is visible. Figure 3b shows the reusability of 500U/L immobilized catalyst for SMX removal. While in the third cycle, 70% SMX removal could still be reached, the achieved removal drops to 20% in the fourth cycle.

## Conclusions

We could successfully immobilize AaeUPO for the first time onto magnetic nanoparticles, obtaining a high activity load and a considerable retention of stability under storage conditions. The immobilized catalyst achieves complete removal of SMX within 10 min. Even though the stability of the immobilized enzyme is competitive with reported literature results, the application at larger scale is not feasible yet regarding the low reusability performance. We are currently aiming to optimize the shielding procedure to increase the reusability of the catalyst and to identify the SMX transformation products.

## Acknowledgements

This project was funded by the European Union's Horizon 2020 research and innovation program under Marie Skłodowska-Curie grant agreement No. 81288 We gratefully acknowledge Prof. Frank Hollmann (TU Delft) for providing samples of AaeUPO.

## References

- [1] C.A. Gasser, L. Yu, J. Svojitka, T. Wintgens, E.M. Ammann, P. Shahgaldian, P.F.-X. Corvini, G. Hommes, Advanced enzymatic elimination of phenolic contaminants in wastewater: a nano approach at field scale, *Appl. Microbiol. Biotechnol.* 98 (2014) 3305–3316. <https://doi.org/10.1007/s00253-013-5414-8>.
- [2] D. Becker, S. Varela Della Giustina, S. Rodriguez-Mozaz, R. Schoevaart, D. Barceló, M. de Cazes, M.P. Belleville, J. Sanchez-Marcano, J. de Gunzburg, O. Couillerot, J. Völker, J. Oehlmann, M. Wagner, Removal of antibiotics in wastewater by enzymatic treatment with fungal laccase – Degradation of compounds does not always eliminate toxicity, *Bioresour. Technol.* 219 (2016) 500–509. <https://doi.org/10.1016/j.biortech.2016.08.004>.
- [3] M. Hobisch, D. Holtmann, P. Gomez de Santos, M. Alcalde, F. Hollmann, S. Kara, Recent developments in the use of peroxygenases – Exploring their high potential in selective oxyfunctionalisations, *Biotechnol. Adv.* 51 (2021) 107615. <https://doi.org/10.1016/j.biotechadv.2020.107615>.
- [4] A. Karich, R. Ullrich, K. Scheibner, M. Hofrichter, Fungal Unspecific Peroxygenases Oxidize the Majority of Organic EPA Priority Pollutants, *Front. Microbiol.* 8 (2017). <https://doi.org/10.3389/fmicb.2017.01463>.
- [5] M. Poraj-Kobielska, M. Kinne, R. Ullrich, K. Scheibner, G. Kayser, K.E. Hammel, M. Hofrichter, Preparation of human drug metabolites using fungal peroxygenases, *Biochem. Pharmacol.* 82 (2011) 789–796. <https://doi.org/10.1016/j.bcp.2011.06.020>.
- [6] M.R. Correro, N. Moridi, H.H. Schützinger, S. Sykora, E.M. Ammann, E.H. Peters, Y. Dudal, P.F.-X. Corvini, P. Shahgaldian, Enzyme Shielding in an Enzyme-thin and Soft Organosilica Layer, *Angew. Chemie Int. Ed.* 55 (2016) 6285–6289. <https://doi.org/10.1002/anie.201600590>.
- [7] Y. Sun, F. Kunc, V. Balhara, B. Coleman, O. Kodra, M. Raza, M. Chen, A. Brinkmann, G.P. Lopinski, L.J. Johnston, Quantification of amine functional groups on silica nanoparticles: a multi-method approach, *Nanoscale Adv.* 1 (2019) 1598–1607. <https://doi.org/10.1039/C9NA00016J>.
- [8] A. Simon, T. Cohen-Bouhacina, M.C. Porté, J.P. Aimé, C. Baquey, Study of Two Grafting Methods for Obtaining a 3-Aminopropyltriethoxysilane Monolayer on Silica Surface, *J. Colloid Interface Sci.* 251 (2002) 278–283. <https://doi.org/10.1006/jcis.2002.8385>.
- [9] P. Molina-Espeja, P. Santos-Moriano, E. García-Ruiz, A. Ballesteros, F. Plou, M. Alcalde, Structure-Guided Immobilization of an Evolved Unspecific Peroxygenase, *Int. J. Mol. Sci.* 20 (2019) 1627. <https://doi.org/10.3390/ijms20071627>.

## TiO<sub>2</sub> –Based Composite Photocatalytic Materials for Solar Driven Water Purification: Recent Achievements, challenges and opportunities

Francis M. dela Rosa<sup>a, b, c</sup>, Hrvoje Kušić<sup>a</sup>, Mira Petrović<sup>c, d</sup>

<sup>a</sup> Faculty of Chemical Engineering and Technology, University of Zagreb, Maruličev trg 19, Zagreb 10000, Croatia

<sup>b</sup> University of Girona, Girona 17071, Spain

<sup>c</sup> Catalan Institute for Water Research (ICRA), C/Emili Grahit, 101, Girona 17003, Spain

<sup>d</sup> Catalan Institution for Research and Advanced Studies (ICREA), Passeig Lluís Companys 23, 08010, Barcelona, Spain

Email: [frosa@fkit.hr](mailto:frosa@fkit.hr), [hkusic@fkit.hr](mailto:hkusic@fkit.hr), [mpetrovic@icra.cat](mailto:mpetrovic@icra.cat),

### Abstract

Clean water is considered to be one of the main goals in the effort to achieve a sustainable living environment. The fulfillment of this goal may include the use of solar-driven photocatalytic processes that are found to be quite effective in water purification. Photocatalytic degradation of organic pollutants in water rely on the formation of electron/hole ( $e^-/h^+$ ) pairs at a semiconducting material upon its excitation by the light with sufficient photon energy. Titanium dioxide remains a benchmark photocatalyst with a high stability, low cost and toxicity. However, the wider application of this technology requires the harvesting of a broader spectrum of solar irradiation and the suppression of the recombination of photogenerated charge carriers. These limitations can be overcome by the use of different strategies, among which the focus is put on the creation of heterojunctions with another narrow bandgap semiconductor, thus providing a high response in the visible light region. Despite all the recent advances in improvement of TiO<sub>2</sub> photocatalytic technology, major challenges still arise for its large scale applicability, life-cycle assessment and production of more toxic organic byproducts. To this prospect, an opportunity to solve challenges for larger scale applications has also been implemented, including the new design of photocatalytic membranes and reactors.

**Keywords:** TiO<sub>2</sub>, photocatalytic degradation, water treatment, large scale applicability

### Introduction

Accessible clean water is one of the major priorities for sustainable economic growth and societal wellbeing. Water supports life and is a crucial resource for humanity; it is also at the core of natural ecosystems and climate regulation. Water stress is primarily a water quantity issue, but it also occurs as a consequence of a deterioration of water quality and a lack of appropriate water management [1]. Environmental problems that are associated with water pollution have been a persistently important issue over recent decades, correlated negatively with the health and ecosystem. Activities of the Water JPI's Strategic Research and Innovation Agenda focus on, among others, new materials and processes, energy efficiency, thus supporting key enabling technologies for clean water and wastewater treatment [2]. In 1972, pioneering work of Fujishima and Honda for photoelectrochemical H<sub>2</sub> production from water using TiO<sub>2</sub> gave birth for the field of semiconductor photocatalysis[3]. Works by Ollis et.al. [4], involving mechanistic study of hydroxyl radicals formed on the surface of TiO<sub>2</sub> which leads to photocatalytic degradation of organic contaminants in water, practically opened a new research field within new water purification technologies. TiO<sub>2</sub> wide application has been promoted due to: (i) high photocatalytic activity under the incident photon wavelength of  $300 < \lambda < 390$  nm and (ii) multi-faceted functional properties, such as chemical and thermal stability, resistance to chemical breakdown, and attractive mechanical

properties [5,6]. However, harvesting a broader spectrum of solar irradiation involves the lowering of the band gap of semiconducting material, whilst inhibiting the recombination of photogenerated charges. Strategies, including doping with non-metals, incorporation or deposition of noble metals (ions), and material engineering solutions that are based on composites formation using transition metals, carbon nanotubes, dye sensitizers, conductive polymers, graphene (oxide), and semiconducting materials, present viable solutions for set tasks [5-9]. It is of great importance to combine TiO<sub>2</sub> with narrow band gap semiconductors with visible light response to obtain an effective composite for photocatalytic applications. The obtained synergistic effect between two or more semiconductors will then promote efficient charge separation, sufficient visible light response, and high photocatalytic performance.

## Recent Achievements

### Photocatalytic Water Treatment

The general mechanism for TiO<sub>2</sub> semiconductor photocatalysis (**Figure 1**) is composed of three main steps: 1.  $e^-/h^+$  pairs are generated on the surface of the semiconductor under illumination with the required wavelength or energy; then, 2.) photogenerated charges (i.e.,  $e^-/h^+$ ) migrate to the surface of the semiconductor; and lastly, 3.)  $e^-$  and  $h^+$  induce redox reactions on the surface that facilitate destruction of organic pollutants [10,11]. As stressed above, TiO<sub>2</sub> is still the most studied and widely used material for photocatalytic degradation reactions.

### Junction Architectures

Three main types of heterojunction architectures are reported for TiO<sub>2</sub>/semiconductor composites [12]. In Type I heterojunction, the conduction band (CB) of TiO<sub>2</sub> is higher in energy (more negative potential) when compared to the CB of semiconductor 2 and the valence band (VB) of TiO<sub>2</sub> is lower in energy (more positive potential) as compared to the VB of semiconductor 2 [13,14]. This leads to the accumulation of photogenerated  $h^+$  and  $e^-$  in semiconductor 2. In Type II heterojunction (where TiO<sub>2</sub> can be semiconductor 1 or 2), the CB of semiconductor 2 is higher than the CB position of semiconductor 1 leading to facile transfer of photogenerated  $e^-$  from CB of semiconductor 2 to CB of semiconductor 1 [15]. Meanwhile, photogenerated  $h^+$  in VB of semiconductor 1 can be transferred to the VB of semiconductor 2, which facilitates efficient charge separation. Type III heterojunction (also known as broken gap situations) [16] shares the same charge transfer mechanism like Type II heterojunction. In this case, the CB and VB of semiconductor 2 are higher than CB and VB of TiO<sub>2</sub> [17].

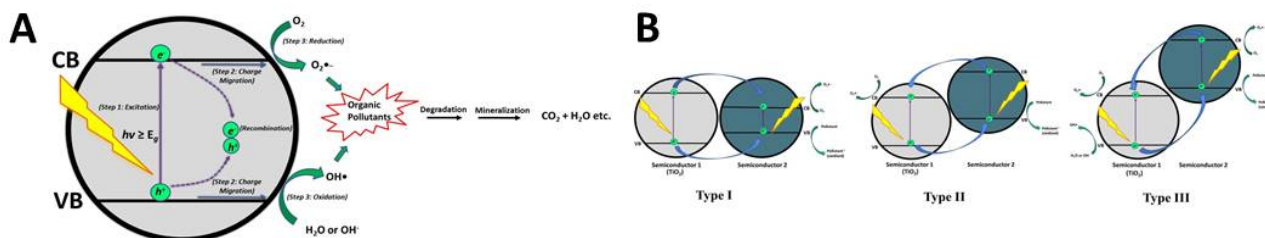


**Figure 1.** A) Photocatalytic reaction mechanism over semiconductor material. B) Band alignment in Type I, II, and III TiO<sub>2</sub>-semiconductor coupled heterojunctions

## Challenges

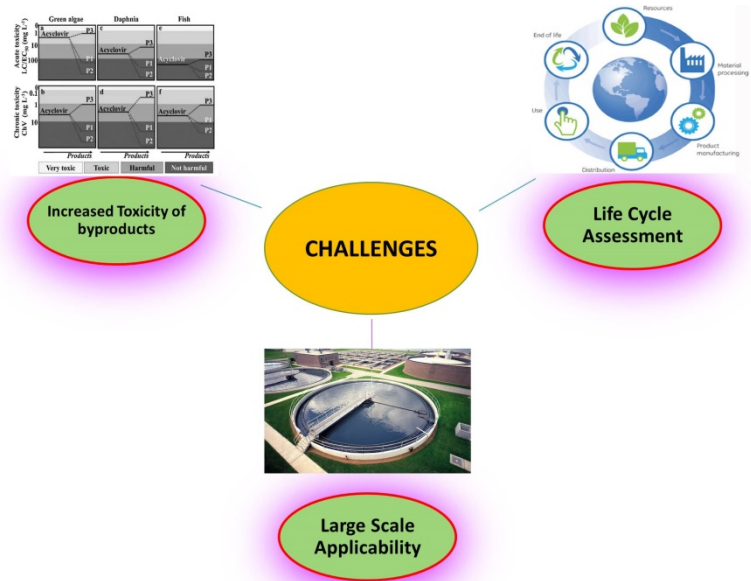


Figure 2. Scheme for TiO<sub>2</sub> Photocatalysis - Challenges[18-20]

## Opportunities

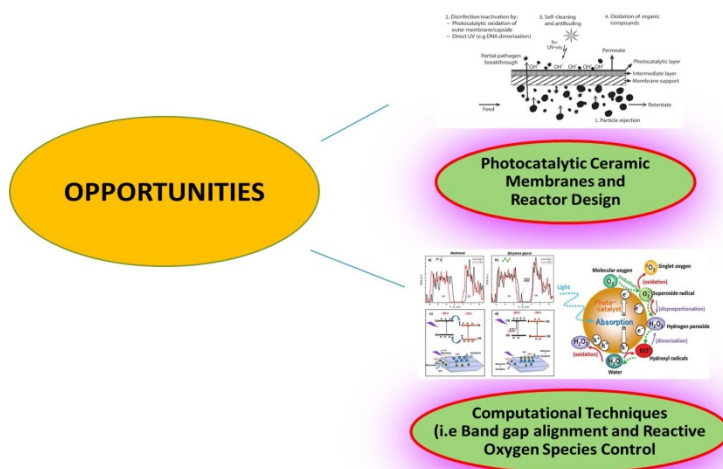


Figure 3. Scheme for TiO<sub>2</sub> Photocatalysis – Opportunities[21,22]

## References

1. European Commission. Directive 2000/60/EC of the European Parliament and of the Council, of 23 October 2000. Off. J. Eur. Communities 2000, 327, 1–72.
2. Water JPI. Available online: <http://www.waterjpi.eu/mapping-agenda/strategic-re> (accessed on 12 December 2019).
3. Fujishima, A.; Honda, K. Electrochemical Photolysis of Water at a Semiconductor Electrode. *Nature* 1972, 238, 37–38.
4. Turchi, C.S.; Ollis, D.F. Photocatalytic degradation of organic water contaminants: Mechanisms involving hydroxyl radical attack. *J. Catal.* 1990, 122, 178–192.
5. Schneider, J.; Matsuoka, M.; Takeuchi, M.; Zhang, J.; Horiuchi, Y.; Anpo, M.; Bahnemann, D.W. Understanding TiO<sub>2</sub> photocatalysis: Mechanisms and materials. *Chem. Rev.* 2014, 114, 9919–9986.
6. Pichat, P. *Photocatalysis and Water Purification: From Fundamentals to Recent Applications*; Wiley: Weinheim, Germany, 2013.
7. Chong, M.N.; Jin, B.; Chow, C.W.K.; Saint, C. Recent developments in photocatalytic water treatment technology: A review. *Water Res.* 2010, 44, 2997–3027
8. Pelaez, M.; Nolan, N.T.; Pillai, S.C.; Seery, M.K.; Falaras, P.; Kontos, A.G.; Dunlop, P.S.M.; Hamilton, J.W.J.; Byrne, J.A.; O'Shea, K.; et al. A review on the visible light active titanium dioxide photocatalysts for environmental applications. *Appl. Catal. B Environ.* 2012, 125, 331–349.
9. Fagan, R.; McCormack, D.E.; Dionysiou, D.D.; Pillai, S.C. A review of solar and visible light active TiO<sub>2</sub> photocatalysis for treating bacteria, cyanotoxins and contaminants of emerging concern. *Mater. Sci. Semicond. Process.* 2016, 42, 2–14.
10. Tong, H.; Ouyang, S.; Bi, Y.; Umezawa, N.; Oshikiri, M.; Ye, J. Nano-photocatalytic materials: Possibilities and challenges. *Adv. Mater.* 2012, 24, 229–251.
11. Pasternak, S.; Paz, Y. On the similarity and dissimilarity between photocatalytic water splitting and photocatalytic degradation of pollutants. *ChemPhysChem* 2013, 14, 2059–2070
12. Moniz, S.J.A.; Shevlin, S.A.; Martin, D.J.; Guo, Z.X.; Tang, J. Visible-light driven heterojunction photocatalysts for water splitting—a critical review. *Energy Environ. Sci.* 2015, 8, 731–759
13. Moniz, S.J.A.; Shevlin, S.A.; An, X.; Guo, Z.X.; Tang, J. Fe<sub>2</sub>O<sub>3</sub>–TiO<sub>2</sub> nanocomposites for enhanced charge separation and photocatalytic activity. *Chem. A Eur. J.* 2014, 20, 15571–15579.
14. Macías-Tamez, R.; Villanueva-Rodríguez, M.; Ramos-Delgado, N.A.; Maya-Treviño, L.; Hernández-Ramírez, A. Comparative Study of the Photocatalytic Degradation of the Herbicide 2,4-D Using WO<sub>3</sub>/TiO<sub>2</sub> and Fe<sub>2</sub>O<sub>3</sub>/TiO<sub>2</sub> as Catalysts. *Water Air Soil Pollut.* 2017, 228, 379. [
15. Luo, L.; Long, J.; Zhao, S.; Dai, J.; Ma, L.; Wang, H.; Xia, L.; Shu, L.; Jiang, F. Effective visible-light-driven photocatalytic degradation of 17 $\alpha$ -ethynylestradiol by crosslinked CdS nano-rod/TiO<sub>2</sub> (B) nano-belt composite. *Process Saf. Environ. Prot.* 2019, 130, 77–85.
16. Marschall, R. Semiconductor composites: Strategies for enhancing charge carrier separation to improve photocatalytic activity. *Adv. Funct. Mater.* 2014, 24, 2421–2440.
17. Kaur, A.; Salunke, D.B.; Umar, A.; Mehta, S.K.; Sinha, A.S.K.; Kansal, S.K. Visible light driven photocatalytic degradation of fluoroquinolone levofloxacin drug using Ag<sub>2</sub>O/TiO<sub>2</sub> quantum dots: A mechanistic study and degradation pathway. *New J. Chem.* 2017, 41, 12079–12090.
18. Flanagan, W.; Dhaliwal, H; Glass or Plastic: An Environmental Life Cycle Assessment (LCA) and Related Economic Impact of Contrast Media Packaging. *Medicine.* 2015
19. <https://www.warsiwatersolutions.com/wastewater-treatment-plants/>
20. Li, G.; Nie, X.; Gao, Y.; An, T. Can environmental pharmaceuticals be photocatalytically degraded and completely mineralized in water using g-C<sub>3</sub>N<sub>4</sub>/TiO<sub>2</sub> under visible light irradiation?—Implications of persistent toxic intermediates. *Appl. Catal. B Environ.* 2016, 180, 726–732.
21. Horovitz, I.; Horovitz, I.; Gitis, V.; Avisar, D.; Mamane, H. Ceramic-based photocatalytic membrane reactors for water treatment Where to next? *Rev. Chem. Eng.* 2020, 36, 593–622.
22. Nosaka, Y.; Nosaka, A.Y. Generation and Detection of Reactive Oxygen Species in Photocatalysis. *Chem. Rev.* 2017, 117, 11302–11336.

## Acknowledgements

This paper is part of a project that has received funding from the European Union's Horizon 2020 – Research and Innovation Framework Programme under the H2020 Marie Skłodowska-Curie Actions grant agreement No. 812880. The paper reflects only the authors' view and the Agency is not responsible for any use that may be made of the information it contains.

## Removal of ciprofloxacin using zeolite-based adsorbents: Adsorption kinetics, mechanism, and regeneration of the spent adsorbents

*Barbara Kalebić<sup>1,3</sup>, Arijeta Baftić<sup>2</sup>, Gordana Matijašić<sup>2</sup>, Davor Ljubas<sup>3</sup>, Lidija Ćurković<sup>3</sup>*

<sup>1</sup>*Faculty of Technology and Metallurgy, University of Belgrade, Serbia*

<sup>2</sup>*Faculty of Chemical Engineering and Technology, University of Zagreb, Croatia*

<sup>3</sup>*Faculty of Mechanical Engineering and Naval Architecture, University of Zagreb, Croatia*

### Abstract

The adsorption of antibiotic ciprofloxacin (CIP) from an aqueous solution by natural and modified zeolite – clinoptilolite (CLI) from Serbian deposit Slanci was investigated. CLI was modified with magnetite (M-CLI) and magnetite and graphene oxide (GO-M-CLI) by microwave-assisted and ultrasound method, respectively, to improve CLI adsorption capacity and separation ability. All the studied adsorbents showed a high adsorption affinity towards CIP at 10, 15 and 20 °C at a pH of 5, and the adsorption kinetics were studied for the initial concentrations of 15-50 mg CIP dm<sup>-3</sup>. Response surface methodology (RSM) will be employed to achieve the best conditions for the CIP adsorption. Strong electrostatic interactions between the cationic form of CIP and aluminosilicate lattice could explain the adsorption mechanism. For the regeneration of spent adsorbents, microwave-assisted method will be investigated.

*Keywords:* clinoptilolite, adsorption, ciprofloxacin, magnetite, graphene oxide, microwave-assisted method.

### 1. Introduction

Nowadays, the use of antibiotics (that can be, from environmental point of view, assumed as organic micropollutants – OMPs) in both human and veterinary medicine is constantly increasing and their presence in natural waters could have adverse effects on aqueous environments and human health. Furthermore, conventional wastewater treatment processes cannot remove OMPs efficiently, thus it is important to develop alternative technologies for their removal [1]. As a model pollutant in this research, a frequently used fluoroquinolone antibiotic ciprofloxacin (CIP) was used.

Adsorption has generally proved to be a promising method for inorganic and organic compound removal from aqueous media due to its simplicity, environmental and economic feasibility as well as a wide range of available adsorbent materials [2]. Among different adsorbents, natural zeolite – clinoptilolite (CLI) has been extensively studied due to its unique structural features, adsorption properties, non-toxic nature, and availability. This good adsorption efficiency of CLI can also be ascribed to its propensity to be modified without structural changes. Thus, the impregnation of CLI lattice with metal oxide nanoparticles, magnetite (M) in this case, and graphene oxide (GO) increases its specific surface area and adsorption ability. Microwave-assisted synthesis proved to be a simple and efficient method for the synthesis of nanoparticles. The main advantages of microwave-assisted synthesis are rapid and homogeneous heating of the precursor's materials. Rapid heating of the precursor's materials by microwave irradiation significantly reduces the overall synthesis time [3].

This research presents a novel method for natural clinoptilolite modification and formation of CLI-based composite which showed excellent adsorption efficiency for CIP removal from aqueous solution. To study the prepared adsorbents reusability, a microwave irradiation was investigated for their regeneration.

## 2. Experimental part

*Starting material:* Clinoptilolite-rich zeolitic tuff (Z) obtained from the Serbian deposit Slanci, near Belgrade, was used as starting material in the experiments. According to Rietveld refinements [4], Z contains CLI as the major mineral phase (>80 wt.%) and quartz (<7.5 wt.%) and feldspar (<13 wt.%) as major satellite phases. The cation exchange capacity (CEC) of the CLI determined by a standard procedure [5] was 162 mmol M<sup>+</sup>/100 g. The particle size used in the experiments was in the range of 0.063-0.125 mm for which previous studies showed the best adsorptive performance [6,7].

The microwave-assisted method was used for synthesis of magnetic zeolite (M-CLI) [3]. The GO-M-CLI was obtained by slightly modified procedure described by Yu et al. [8].

*Characterization:* Analysis of the mineral phases present in the samples was done via the powder X-ray diffraction method (PXRD). A simultaneous thermogravimetric (TGA) and differential thermal analysis (DTA) was performed to study the thermal behavior of the prepared adsorbents. The specific surface area and porosity characteristics were determined by the N<sub>2</sub> adsorption at -196 °C using the Brunauer-Emmett-Teller (BET) and Barrett-Joyner-Halenda (BJH) method, respectively. Raman spectroscopy was carried out to determine the quality and properties of GO layer in GO-M-CLI. The zeta potential and magnetic properties measurements of the prepared adsorbents were also performed.

*CIP adsorption tests:* The adsorption tests were performed by a batch method. The adsorption capacity of CLI, M-CLI and GO-M-CLI towards CIP was studied for different initial CIP concentrations (15-50 mg dm<sup>-3</sup>), temperatures (10-20 °C) and pH (5-9). 0.2 g of adsorbent was suspended in 50 cm<sup>3</sup> of the particular concentrations of CIP solution and left in thermostated incubator-shaker from 5 to 60 min. The solid was recovered by vacuum filtration and the CIP concentration in the filtrate was measured by an UV-VIS spectrophotometer at  $\lambda = 278$  nm.

*Experimental design:* Response surface methodology (RMS) will be used to optimize the number of experiments to reduce operational costs. The central composite factorial (CCF) design function of the Design-Expert® software will be used to quantify the impact of the relations between five independent factors (initial CIP concentration, pH, temperature, reaction time, and adsorbent type) on adsorption ability.

*Regeneration of spent adsorbents:* The regeneration possibility of spent CLI, M-CLI and GO-M-CLI will be investigated by microwave irradiation of the spent adsorbents in the microwave oven.

## 3. Results and discussion

The PXRD patterns (Figure 1) showed that CLI was the main mineral phase with quartz and feldspar as satellite phases. The impregnation of M and GO separately did not significantly affect the CLI crystallinity, but the modification with both M and GO leads to a decrease in GO-M-CLI crystallinity.

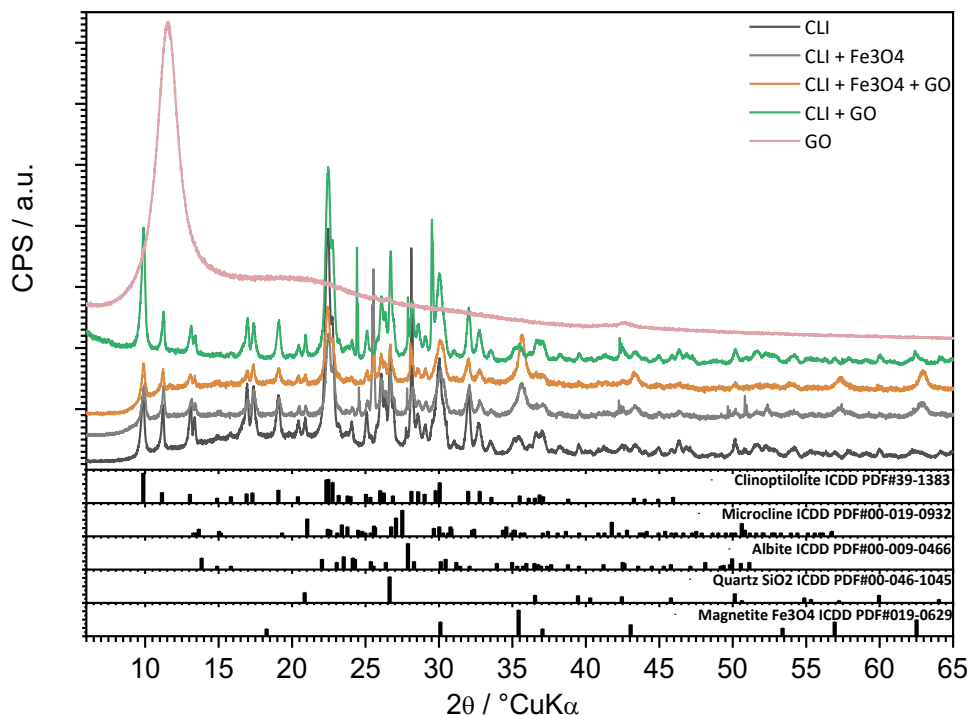


**Figure 1.** PXRD patterns of the various CLI modifications.

The textural properties of CLI changed during its conversions (Table 1). The CLI specific surface area ( $S_{\text{BET}}$ ) was doubled after the M and GO impregnation, while the synergic effect of M and GO led to its further increase. This could be attributed to large specific surface area of both M ( $\sim 100 \text{ m}^2 \text{ g}^{-1}$ ) and GO ( $\sim 400 \text{ m}^2 \text{ g}^{-1}$ ). The same effect was observed for the total pore volume ( $V_{\text{tot}}$ ).

**Table 1.** Textural properties of CLI, GO-CLI, M-CLI and GO-M-CLI.

Sample	$S_{\text{BET}} (\text{m}^2 \text{ g}^{-1})$	$V_{\text{tot}} (\text{cm}^3 \text{ g}^{-1})$
CLI	24.48	0.09904
GO-CLI	37.44	0.1202
M-CLI	52.10	0.17963
GO-M-CLI	64.80	0.21936

$S_{\text{BET}}$  – specific surface area;  $V_{\text{tot}}$  – total pore volume.

Due to the zwitterionic nature of CIP molecule, its adsorption performances strongly depend on the pH of the solution [9]. Study of the adsorption capacity dependence on pH showed that the best results can be obtained at pH of 5 (not shown). According to the adsorption experimental data obtained at  $25 \text{ }^\circ\text{C}$  and  $\text{pH} = 5$  (Figure 2), GO-M-CLI showed the highest adsorption capacity for CIP. It can be attributed to the increase in CLI specific surface area after M and GO impregnation. For all studied adsorbents, the CIP uptake increased rather sharply in the first 10 min for the lowest and highest studied CIP initial concentration. More than 85% of the maximum adsorption capacity was achieved in 10 min, indicating fast adsorption kinetics.



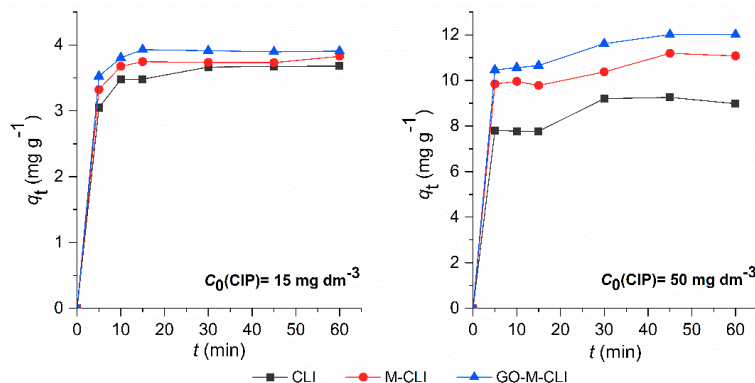


**Figure 2.** Adsorption kinetics for CIP on CLI, M-CLI and GO-M-CLI for two different initial CIP concentrations at 25 °C and pH of 5;  $q_t$  is the amount of the adsorbed CIP after time  $t$ .

#### 4. Conclusion

The study shows that impregnation of magnetite nanoparticles and graphene oxide layers on natural clinoptilolite can enhance its adsorption capacity for antibiotic ciprofloxacin removal from aqueous solution, as well as facilitate its separation from the aqueous phase. As it was expected, GO-M-CLI showed the highest adsorption capacity for CIP at all studied temperatures, pH and for all studied CIP initial concentrations. The regeneration of spent adsorbents by microwave irradiation will be performed to investigate the reusability of prepared adsorbents.

#### Acknowledgements

This study has received funding from the European Union's Horizon 2020 research and innovation program under Marie Skłodowska-Curie grant agreement No. 812880.

#### References

- [1] Kraemer, S.A.; Ramachandran, A.; Perron, G.G. Antibiotic pollution in the environment: From microbial ecology to public policy. *Microorganisms* 2019, 7, 180.
- [2] Lin, C.-C.; Lee, C.-Y. Adsorption of ciprofloxacin in water using  $\text{Fe}_3\text{O}_4$  nanoparticles formed at low temperature and high reactant concentrations in a rotating packed bed with co-precipitation. *Mater. Chem. Phys.* 2020, 240, 122049.
- [3] Pati, S.S.; Kalyani, S.; Mahendran, V.; Philip, J. Microwave assisted synthesis of magnetite nanoparticles. *J. Nanosci. Nanotechnol.* 2014, 14, 5790–5797.
- [4] Coelho, A.; TOPAS Academic 4.1, Coelho Software, Brisbane, Australia, 2007.
- [5] Ming, D.W.; Dixon, J. B. Quantitative determination of clinoptilolite in soils by a cationexchange capacity method, *Clays Clay Miner.* 1987, 35, 463-468.
- [6] Stojaković, D.; Milenković, J.; Daneu, N.; Rajić, N. A study of the removal of copper ions from aqueous solution using clinoptilolite from Serbia, *Clays Clay Miner.* 2011, 59, 277-285.
- [7] Rajić, N.; Stojanović, D.; Jovanović, M.; Zabukovec Logar, N.; Mazaj, M.; Kaučič, V. Removal of nickel(II) ions from aqueous solutions using the natural clinoptilolite and preparation of nano-NiO on the exhausted clinoptilolite, *App. Surf. Sci.* 2010, 257, 1524-1532.
- [8] Yu, Y.; Murthy, B.N.; Shapter, J.G.; Constantopoulos, K.T.; Voelcker, N.H.; Ellis, A.V. Benzene carboxylic acid derivatized graphene oxide nanosheets on natural zeolites as effective adsorbents for cation dye removal. *J. Hazard. Mater.* 2013, 260, 330–338.
- [9] Genç, N.; Dogan, E.C. Adsorption kinetics of the antibiotic ciprofloxacin on bentonite, activated carbon, zeolite, and pumice. *Desalin. Water Treat.* 2013, 53, 1–9.

## Modeling the adsorption of emerging contaminants on carbon nanomaterials

Matej Kern,<sup>1</sup> *Klaudija Ivanković*,<sup>2</sup> *Sanja Škulj*,<sup>1</sup> *Marko Rožman*<sup>1</sup>

<sup>1</sup> *Ruđer Bošković Institute, Bijenička cesta 54, Zagreb, Croatia*

<sup>2</sup> *Faculty of Chemical Engineering and Technology, University of Zagreb, Trg Marka Marulića 19, Zagreb, Croatia*

By now, the presence of trace amounts of a wide range of contaminants introduced through wastewaters and their adverse effects on the environment have received considerable attention.<sup>1,2</sup> Many advanced wastewater treatments have been considered in the search for an effective yet economical method for their removal of which adsorption has shown promise both as a direct method of contaminant removal<sup>3</sup> and as means to increase the efficiency of other, oxidation based, methods.<sup>4,5</sup> Due to the specific requirements of experimental studies on the adsorption of contaminants to carbon nanomaterials information on the thermodynamics of adsorption and more in-depth investigations of mechanisms which contribute to adsorption is available sparingly. Computational approaches enable this information to be obtained at, relatively, low cost in terms of the time required and for contaminants that may not otherwise be easily acquirable. In this study we model the adsorption of 69 pharmaceutically active compounds (PhACs) on the carbon nanomaterials (CNMs) graphene and graphene oxide, in water and n-octanol, in three pH ranges. We examine the relationship of non-covalent interactions (van der Waals,  $\pi$ -interactions, hydrogen bonding and hydrophobic interactions) and find differences in optimal removal conditions for the different classes of PhACs. The effect of temperature on the subsequent adsorbent regeneration is also discussed. Finally, as the data obtained is not influenced by the differences in nanomaterial composition introduced by variations in the protocol of its synthesis,<sup>6,7</sup> it may further contribute to towards the development of predictive adsorption models.

### Introduction

The widespread presence of antibiotics and other PhACs has been a cause of great concern due to their effects on the composition of bacterial communities, the ever-growing threat of widespread antibiotic resistance and other possible effects that may stem from their bioaccumulation and transport through both aquatic and terrestrial food webs.<sup>8-11</sup> The use of graphene and graphene oxide has previously been reported on in literature including thermodynamic data on the adsorption of several PhACs,<sup>12,13</sup> however use of different modifications of the nanomaterials in question hinders comparisons between the results of these studies. Computational studies enable the use of consistent nanomaterial models thus circumventing the difficulties associated with variations in the nanomaterial and have already contributed to the understanding of the fundamental mechanism regarding the adsorption of aromatic and pharmaceutically active compounds on carbon nanomaterials.<sup>14,15</sup> In this work we aim to fill the current knowledge gap on the thermodynamics of adsorption of antibiotics and other PhACs as well as examine interactions that contribute to the overall adsorption mechanism, their contributions and how environmental variables such as pH, solvent polarity and temperature influence them. Additionally we examine the differences in adsorption behavior between the different classes of PhACs considered and how these differences influence optimal conditions both for the removal of contaminants and the regeneration of the nanomaterial adsorbents used.

## Methods

Both PhAC and nanomaterial models were built using GausView 6.0 software and optimized at the B3LYP-D3BJ / 6-31G(d) level of theory using the SMD implicit solvation model. Several sizes of nanomaterial flake were modeled and matched to PhACs individually to minimize the computational cost, the effects of flake size on adsorption energy were studied earlier and found to be almost negligible.<sup>16</sup> Following this the optimized PhAC models were placed in six possible orientations above the nanomaterial models and preliminary evaluations (optimizations and calculation of the Gibbs free energy of adsorption) of these were done using the PM6-D3H4 semiempirical method with COSMO implicit solvation. For each combination of PhAC and nanomaterial the most energetically favorable adsorption complex was then chosen and reoptimized at the B3LYP-D3BJ / 6-31G(d) level with SMD solvation. Vibrational analysis was done to confirm that all structures were true minima. All semi-empirical calculations were performed using Mopac2016 software while DFT calculations were performed using Gaussian 16. Solution pH was simulated by addition or removal of H<sup>+</sup> from antibiotic molecules when applicable. Adsorption enthalpies (and analogously adsorption Gibbs free energies) were calculated according to the following equation:

$$\Delta H = H_{\text{complex}} - H_{\text{antibiotic}} - H_{\text{CNM}} + BSSE$$

Basis set superposition error (BSSE) was calculated by the counterpoise method.<sup>17</sup> logansen's relationship<sup>18</sup> was used to estimate hydrogen bond formation enthalpy.

## Results

### *Adsorption mechanism*

Van der Waals dispersion interactions,  $\pi$ -interactions, hydrogen bonding and hydrophobic interactions were examined as contributing factors to the overall adsorption mechanism. Van der Waals interactions were examined through the use of isotropic molecular polarizability as a proxy and found to correlate significantly vs.  $\Delta H$  in all combinations of solvent, and nanomaterial. The correlations were found to be slightly lower yet still significant in n-octanol. The influence of  $\pi$ -interactions on the enthalpy of adsorption was, at first, attempted by correlation with the LOLIPOP values.<sup>19</sup> When no significant correlations were found Welch's t-test was performed between groups of PhACs containing different numbers of aromatic rings. This approach indicated that while the average  $\Delta H$  of these groups did decrease (the adsorption was energetically more favorable) with an increase in the number of aromatic rings in the PhAC models the difference was only statistically significant for non-antibiotic PhACs as the larger antibiotics were generally not able to achieve close stacking of the aromatic rings with the nanomaterial, figure 1. This remained true irrespective of the solvent polarity. Hydrogen bonding was examined both by correlating the number of PhAC-CNM hydrogen bonds with the mean adsorption enthalpy and by correlating the sum of enthalpies of formation of PhAC-CNM hydrogen bonds with the change in adsorption enthalpy of a PhAC from graphene to graphene oxide. Both correlations were significant with the correlation vs. number of hydrogen bonds being very strong while the correlation vs. the sum of enthalpies of hydrogen bond formation was moderate. Complexes in a lower polarity solvent formed on average more stable hydrogen bonds, consistent with prior examinations of this change.<sup>20</sup> Hydrophobic interactions were examined by the correlation of the change in total van der Waals surface area of the PhAC and CNM versus the change in enthalpy of adsorption from water to n-octanol. For graphene the correlation was significant and of moderate strength which, given the negative change in adsorption enthalpy from octanol to water, would signify that the hydrophobic effect is nonclassical (enthalpic). For adsorption of antibiotics to graphene oxide the opposite trend emerges: complexes adsorb more stably in n-octanol than they do in water and the effect is again enthalpic.

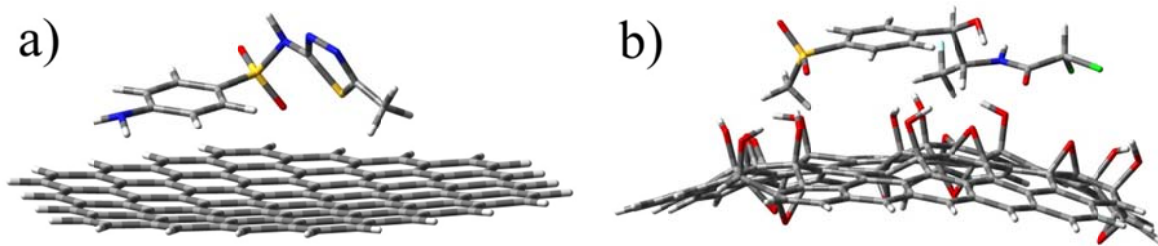


Figure 1. Both a) sulfamethizole and b) florfenicol are unable to achieve close parallel stacking of the aromatic ring with the nanomaterial.

### *Environmental variables*

Solution pH (in the 4.5 – 9.5 range), solvent polarity and temperature were considered. In agreement with previous studies,<sup>21</sup> it was found that, on average, an increase in solution pH led to the decrease of adsorption complex stability on both CNMs and in both solvents. However closer inspection of the data revealed that some combinations of nanomaterial / solvent and antibiotic group (phenicoles on graphene, quinolones on graphene oxide etc. ) do not follow this trend or even behave in the opposite manner. Nitroimidazoles, as they remain neutral in the examined pH range, adsorb only to graphene in water. The effect of changing solvent polarity was only generalizable on graphene where it led to less stable adsorption of PhACs. The effect of temperature on the adsorption of PhACs on CNMs was uniform in that all PhAC-CNMs complexes were less stable at higher temperatures. Examination of desorption temperatures points towards graphene as the adsorbent for which it is simpler to achieve regeneration as all antibiotic classes except macrolides desorb from it in n-octanol, at  $8 < \text{pH} < 10$  and  $100\text{ }^{\circ}\text{C}$ . Graphene oxide may require more elaborate regeneration protocols.

### **Conclusions**

The adsorption Gibbs free energies of 69 PhACs on graphene and graphene oxide will likely provide the most comprehensive, comparable, data on adsorption thermodynamics of PhACs on CNMs. The interactions examined as part of the adsorption mechanism operate simultaneously yet are differently modulated by changes in environmental variables and the degree of oxidation of the nanomaterial. At environmental pH, the use of graphene rather than graphene oxide may result in both more efficient removal of the studied pollutants from aquatic environments and simpler adsorbent regeneration.

### References:

1. Petrie, B., Barden, R. & Kasprzyk-Hordern, B. A review on emerging contaminants in wastewaters and the environment: Current knowledge, understudied areas and recommendations for future monitoring. *Water Res.* **72**, 3–27 (2015).
2. Kovalakova, P. *et al.* Occurrence and toxicity of antibiotics in the aquatic environment: A review. *Chemosphere* **251**, 126351 (2020).
3. Carmalin Sophia, A., Lima, E. C., Allaudeen, N. & Rajan, S. Application of graphene based materials for adsorption of pharmaceutical traces from water and wastewater- a review. *Desalin. Water Treat.* **57**, 27573–27586 (2016).
4. Zhou, X. *et al.* Persulfate activation by swine bone char-derived hierarchical porous carbon: Multiple mechanism system for organic pollutant degradation in aqueous media. *Chem. Eng. J.* **383**, 123091 (2020).

5. Thakur, K. & Kandasubramanian, B. Graphene and Graphene Oxide-Based Composites for Removal of Organic Pollutants: A Review. *J. Chem. Eng. Data* **64**, 833–867 (2019).
6. Kang, J. H. *et al.* Hidden Second Oxidation Step of Hummers Method. *Chem. Mater.* **28**, 756–764 (2016).
7. Yadav, N. & Lochab, B. A comparative study of graphene oxide: Hummers, intermediate and improved method. *FlatChem* **13**, 40–49 (2019).
8. Previšić, A. *et al.* Aquatic macroinvertebrates under stress: Bioaccumulation of emerging contaminants and metabolomics implications. *Sci. Total Environ.* **704**, 135333 (2019).
9. Previšić, A., Vilenica, M., Vučković, N., Petrović, M. & Rožman, M. Aquatic Insects Transfer Pharmaceuticals and Endocrine Disruptors from Aquatic to Terrestrial Ecosystems. *Environ. Sci. Technol.* **55**, 3736–3746 (2021).
10. Rizzo, L. *et al.* Urban wastewater treatment plants as hotspots for antibiotic resistant bacteria and genes spread into the environment: A review. *Sci. Total Environ.* **447**, 345–360 (2013).
11. van der Grinten, E., Pikkemaat, M. G., van den Brandhof, E. J., Stroomberg, G. J. & Kraak, M. H. S. Comparing the sensitivity of algal, cyanobacterial and bacterial bioassays to different groups of antibiotics. *Chemosphere* **80**, 1–6 (2010).
12. Ersan, G., Apul, O. G., Perreault, F. & Karanfil, T. Adsorption of organic contaminants by graphene nanosheets: A review. *Water Research* vol. 126 385–398 (2017).
13. Awad, A. M. *et al.* Adsorption of organic pollutants by nanomaterial-based adsorbents: An overview. *Journal of Molecular Liquids* vol. 301 (2020).
14. Tang, H., Zhang, S., Huang, T., Cui, F. & Xing, B. pH-Dependent adsorption of aromatic compounds on graphene oxide: An experimental, molecular dynamics simulation and density functional theory investigation. *J. Hazard. Mater.* **395**, (2020).
15. Ai, Y. *et al.* Insights into the adsorption mechanism and dynamic behavior of tetracycline antibiotics on reduced graphene oxide (RGO) and graphene oxide (GO) materials. *Environ. Sci. Nano* **6**, 3336–3348 (2019).
16. Daggag, D., Lazare, J. & Dinadayalane, T. Conformation dependence of tyrosine binding on the surface of graphene: Bent prefers over parallel orientation. *Appl. Surf. Sci.* **483**, 178–186 (2019).
17. Boys, S. F. & Bernardi, F. The calculation of small molecular interactions by the differences of separate total energies. Some procedures with reduced errors. *Mol. Phys.* **19**, 553–566 (1970).
18. logansen, A. V. *Direct proportionality of the hydrogen bonding energy and the intensification of the stretching  $\nu(XH)$  vibration in infrared spectra.* *Spectrochimica Acta - Part A: Molecular and Biomolecular Spectroscopy* vol. 55 (1999).
19. Gonthier, J. F. *et al.*  $\pi$ -Depletion as a criterion to predict  $\pi$ -stacking ability. *Chem. Commun.* **48**, 9239–9241 (2012).
20. Aquino, A. J. A., Tunega, D., Haberhauer, G., Gerzabek, M. H. & Lischka, H. Solvent effects on hydrogen bonds - A theoretical study. *J. Phys. Chem. A* **106**, 1862–1871 (2002).
21. Al-Khateeb, L. A., Almotiry, S. & Salam, M. A. Adsorption of pharmaceutical pollutants onto graphene nanoplatelets. *Chem. Eng. J.* **248**, 191–199 (2014).

#### Acknowledgments:

The authors gratefully acknowledge the computing resources and support provided by The University Computing Centre (SRCE) in Zagreb. Proofreading by Katarina Cetinić (Ruđer Bošković Institute, Zagreb) is gratefully acknowledged. This work was supported by the Croatian Science Foundation project no. IP-2018-01-2298.

## **Addition of activated carbon to an MBR: Strategies to improve micropollutants removal supported by statistical analysis and adsorption experiments.**

*Marina Gutiérrez<sup>1</sup>, Andrea Ghirardini<sup>1</sup>, Dragana Mutavdžić Pavlović<sup>2</sup>, Paola Verlicchi<sup>1</sup>*

<sup>1</sup>*Department of Engineering, University of Ferrara, Via Saragat 1, 44122 Ferrara, Italy*

<sup>2</sup>*Department of Analytical Chemistry, Faculty of Chemical Engineering, University of Zagreb, Trg Marka Marulića 19, 10000 Zagreb, Croatia*

### **Introduction**

Continuous release of organic micropollutants (MPs) from wastewater treatment plants entails a potential damage in aquatic and soil environments due to their toxicity and recalcitrant nature. To deal with this issue, scientists around the globe are making efforts searching for innovative advanced wastewater treatments and, when possible, decentralized solutions. Combination of biological and innovative physicochemical processes may enhance the removal of a wide range of MPs, by promoting different removal mechanisms in the so-called hybrid systems, while improving the effluent overall quality.

Advanced biological treatments (namely membrane bioreactor, MBR) have become widely used in the recent years, as integrated membrane processes provide a better-quality effluent for a wide range of contaminants. However, these systems were not initially intended for the removal of MPs. To overcome this issue, sorption on powdered activated carbon (PAC) has been proposed as a promising solution due to its high adsorption capacity, which has already been subjected to several studies related to the mitigation of membrane fouling (Ng et al., 2013).

When it comes to removal mechanisms, the removal of MPs in MBRs is mainly governed by biodegradation and sorption within the sludge. Once the PAC is added inside the bioreactor, the removal is then driven by different mechanisms. The PAC interacts with the dissolved organic matter (DOM) and the sludge flocs to create PAC-sludge complexes: PAC particles are integrated inside the flocs and at the same time the organic matter is adsorbed onto PAC surface. Thus, sorption processes (i.e. adsorption and absorption) increase their relevance in these hybrid systems. MPs are then not only subjected to the removal mechanisms associated to the MBR, but to sorption processes related to the PAC-sludge complex. In the same way, PAC addition modifies sludge properties, which may imply an enhancement of the biodegradation processes (Asif et al., 2020). In this context, wastewater treatment plants are characterized by a high content of organic matter. The nature of the influent and, in particular, the DOM play a relevant role in these hybrid systems by determining the extent of the removal of several MPs, in particular when removal relies on the adsorption onto the activated carbon.

To date, several studies have investigated the optimization of the operational conditions to improve the performance of the MBR coupled with PAC (Ng et al., 2013; Remy et al., 2009; Streicher et al., 2016), while trying to determine which are the key MP's properties that explains the extent of their removal and the influence of the water matrix (Alvarino et al., 2018; Mailler et al., 2016). This approach is crucial to determine the strategies following the operation of hybrid systems to ensure the reduction of MPs levels and therefore the impact on the receiving waters.

The current study aims to clarify the influence of the operational conditions and MPs properties, as well as the role of the DOM in the removal of MPs from wastewater in MBR coupled with PAC. To study the implication of operational conditions and MP properties, statistical analyses are performed on results regarding the removal efficiencies for a collection of MPs retrieved from relevant peer-reviewed papers. In addition, in order to

study the influence of the DOM, adsorption batch experiments are conducted for a selection of 3 MPs under different water matrixes.

## Materials and methods

### *Statistical analysis*

Exploratory data analyses (principal component analysis, cluster analysis, and regression analysis) were adopted to analyze the results obtained from 7 studies (namely Alvarino et al., 2016, 2017; Asif et al., 2020; Li et al., 2011; Nguyen et al., 2013; Serrano et al., 2011; Yu et al., 2014). Dataset was retrieved by Gutiérrez et al. (2021) and it refers to 10 investigations studying the removal of MPs in a MBR coupled with PAC. Collected investigations refer to laboratory and pilot scale reactors in which PAC was added inside the bioreactor. Studies were selected based on the availability of parameters under the study. Selected operational parameters were PAC dose, PAC retention time (that is, time PAC is inside the reactor before its disposal) and SRT. Regarding MPs properties, considered parameters are  $\text{LogD}_{\text{ow}}$ , charge and molecular weight (MW). The dataset includes 146 observations referring to 37 compounds. Statistical analyses were performed in R software. Significance level of  $p < 0.05$  was set for regression analysis.

### *Adsorption experiments*

Adsorption experiments were performed in ultra-pure water and humic acid solution testing three MPs separately (namely diclofenac, sulfamethoxazole and trimethoprim). PAC was added in amounts ranging from 2 to 20 mg (0.1, 0.25, 0.5, 1 g L<sup>-1</sup>) in glass beakers containing 20 mL solution of each MP. Six initial MP concentrations were tested (i.e. 5, 7.5, 10, 15, 20, 25 mg L<sup>-1</sup>). Humic acid solution used was 50 mg L<sup>-1</sup>. Test solutions were incubated for 24h at 25°C under continuous stirring (200 rpm). To avoid photodegradation experiments were conducted in the darkness. To determine adsorption kinetics, experiments were performed under different time periods (i.e. 10, 20, 30, 40 and 50 min; 1, 2, 4, 6, 18 and 24h). MP concentrations were analyzed by HPLC with diode-array detection.

## Results and discussion

### *Statistical analysis*

The results of this study suggest that the different operational conditions adopted in the selected studies did not imply better MPs removal efficiencies in the selected studies. No significant correlations were found among any of the selected operational parameters (PAC dosage, PAC retention time and SRT) with removal efficiencies. Cluster analysis (Table 1) grouped all the results corresponding to (Asif et al., 2020) in Cluster C, suggesting its particularly high PAC dosage (20g L<sup>-1</sup>) entails a better average removal (97.4%). However, the high removal observed does not significantly differ from the other clusters (A, B, D), ranging between 84-98% for all the remaining PAC concentrations (0.03 – 1 g L<sup>-1</sup>). Due to its exceptional PAC dosage, (Asif et al., 2020) is then defined as an outlier and not considered for further statistical analysis and interpretations. PAC retention time seems to be a parameter from which effect is strongly dependent of the mechanisms that determine the MP removal (Gutiérrez et al., 2021). For these reasons, further research is needed to clarify the role of PAC dosage and retention time in order to improve its usage in the reactor. SRT data were not considered heterogenous enough in this dataset and, as many authors did not purge sludge during the experiments to evaluate the level of saturation of PAC, range of SRT was higher than usually expected in MBR reactors (20-50 days, Metcalf & Eddy, 2014).

Regarding physico-chemical properties of MPs, results of regression analysis confirmed the charge has an important role on MP removal ( $p = 0.037$ ). Indeed, cluster A and B present the highest and lower average removals and charges, respectively (Table 1). It is well known that positively charged compounds tend to be attracted to overall negatively charged PAC-DOM complex. Electrostatic interactions favor sorption processes which increase the removal of MPs within the reactor. Low $D_{ow}$  was positively correlated with the removal of anionic and neutral compounds (clusters B and D, respectively) ( $p < 0.001$ ), suggesting that Log $D_{ow}$  is an important parameter to take into account in absence of positive electrostatic interactions. Results are confirmed in cluster analysis, from which cluster D grouped mainly neutral compounds (Table 1) with a high average removal (91%).

Table 1. Characteristics of the clusters, in terms of number of observations (n) included, average removal efficiency, and centroids of each of the six selected variables.

Cluster ID	n	Av. removal (%)	SRT (d)	PAC dosage ( $g L^{-1}$ )	PAC ret time (d)	Log $D_{ow}$	Charge	MW
A	16	97.9	200.7	0.6	78.0	1.39	0.95	785.5
B	65	84.4	139.7	0.4	73.9	0.69	-0.90	261.5
C	7	97.4	30.0	20.0	65.0	-0.56	-0.07	286.3
D	58	91.0	156.1	0.5	67.8	3.35	0.12	261.8

### Adsorption experiments

Kinetics experiments showed that 24h were the time necessary to achieve the sorption equilibrium for all the tested MPs. Results in ultra-pure water indicate that kinetics followed a pseudo-second order model ( $R^2 > 0.985$ ), suggesting that in absence of organic matter the sorption is governed by the number of available PAC active sites (Mutavdžić Pavlović et al., 2018). Adsorption of sulfamethoxazole and diclofenac followed a Freundlich isotherm ( $R^2 > 0.967$ ), meaning it was governed by a heterogenous surface sorption where active sites present different sorption energies. Instead, TMP sorption showed slightly better fitting results for Langmuir isotherm ( $R^2 > 0.957$ ), assuming a model of monolayer adsorption with a finite number of energetically equivalent active sites (Delgado et al., 2019). On the other side, MPs adsorption in humic acid solution follows a logarithmic isotherm in all tested concentrations ( $R^2 > 0.95$ ), following the saturation of the PAC active sites. However, in case of sulfamethoxazole, which was the compound with lower rates of adsorption in ultra-pure water (results not shown), the humic acid solution seemed to increase the adsorption capacity, reflecting the complexity of the interactions between MPs and DOM.

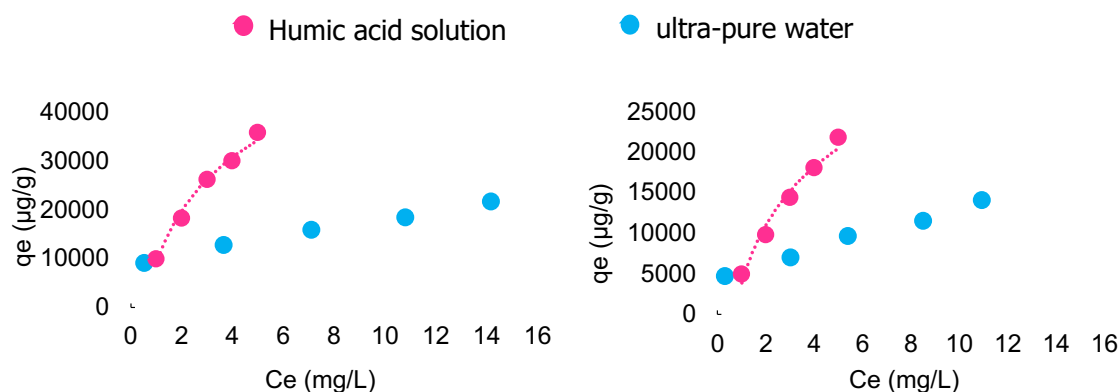


Figure 1. Adsorbed sulfamethoxazole at 0.5 gPAC L<sup>-1</sup> (left) and 1gPAC L<sup>-1</sup> (right) in ultra-pure water and humic acid solution (50 mg L<sup>-1</sup>).



## Acknowledgments

This work is supported by the European Union's Horizon 2020 research and innovation program under Marie Skłodowska-Curie grant agreement No 81288 – Nowelties ITN-EJD project.

## Bibliography

- Alvarino, T., Komesli, O., Suarez, S., Lema, J. M., & Omil, F. (2016). The potential of the innovative SeMPAC process for enhancing the removal of recalcitrant organic micropollutants. *Journal of Hazardous Materials*, 308, 29–36.
- Alvarino, T., Suarez, S., Lema, J., & Omil, F. (2018). Understanding the sorption and biotransformation of organic micropollutants in innovative biological wastewater treatment technologies. *Science of the Total Environment*, 615, 297–306.
- Alvarino, T., Torregrosa, N., Omil, F., Lema, J. M., & Suarez, S. (2017). Assessing the feasibility of two hybrid MBR systems using PAC for removing macro and micropollutants. *Journal of Environmental Management*, 203, 831–837.
- Asif, M. B., Ren, B., Li, C., Maqbool, T., Zhang, X., & Zhang, Z. (2020). Powdered activated carbon – Membrane bioreactor (PAC-MBR): Impacts of high PAC concentration on micropollutant removal and microbial communities. *Science of The Total Environment*, 745, 141090.
- Delgado, N., Capparelli, A., Navarro, A., & Marino, D. (2019). Pharmaceutical emerging pollutants removal from water using powdered activated carbon: Study of kinetics and adsorption equilibrium. *Journal of Environmental Management*, 236(February), 301–308.
- Gutiérrez, M., Grillini, V., Mutavdžić Pavlović, D., & Verlicchi, P. (2021). Activated carbon coupled with advanced biological wastewater treatment: A review of the enhancement in micropollutant removal. *Science of the Total Environment*, 790.
- Li, X., Hai, F. I., & Nghiem, L. D. (2011). Simultaneous activated carbon adsorption within a membrane bioreactor for an enhanced micropollutant removal. *Bioresource Technology*, 102(9), 5319–5324.
- Mailler, R., Gasperi, J., Coquet, Y., Derome, C., Buleté, A., Vulliet, E., Bressy, A., Varrault, G., Chebbo, G., & Rocher, V. (2016). Removal of emerging micropollutants from wastewater by activated carbon adsorption: Experimental study of different activated carbons and factors influencing the adsorption of micropollutants in wastewater. *Journal of Environmental Chemical Engineering*, 4(1), 1102–1109.
- Metcalf & Eddy. (2014). *Wastewater Engineering: Treatment and Resource Recovery* (5th ed.). McGraw-Hill Education.
- Mutavdžić Pavlović, D., Glavač, A., Gluhak, M., & Runje, M. (2018). Sorption of albendazole in sediments and soils: Isotherms and kinetics. *Chemosphere*, 193, 635–644.
- Ng, C., Sun, D., Bashir, M. J. K., Han, S., Yong, L., Nisar, H., Wu, B., & Fane, A. G. (2013). Optimization of membrane bioreactors by the addition of powdered activated carbon. *Bioresource Technology*, 138, 38–47.
- Nguyen, L. N., Hai, F. I., Kang, J., Nghiem, L. D., Price, W. E., Guo, W., Ngo, H. H., & Tung, K.-L. K. L. (2013). Comparison between sequential and simultaneous application of activated carbon with membrane bioreactor for trace organic contaminant removal. *Bioresource Technology*, 130, 412–417.
- Remy, M., van der Marel, P., Zwijnenburg, A., Rulkens, W., & Temmink, H. (2009). Low dose powdered activated carbon addition at high sludge retention times to reduce fouling in membrane bioreactors. *Water Research*, 43(2), 345–350.
- Serrano, D., Suárez, S., Lema, J. M., & Omil, F. (2011). Removal of persistent pharmaceutical micropollutants from sewage by addition of PAC in a sequential membrane bioreactor. *Water Research*, 45(16), 5323–5333. <https://doi.org/10.1016/j.watres.2011.07.037>
- Streicher, J., Sebastian, A., Gnirß, R., & Jekel, M. (2016). *Where to dose powdered activated carbon in a wastewater treatment plant for organic micro-pollutant removal*. 156, 88–94.
- Yu, J., He, C., Liu, X., Wu, J., Hu, Y., & Zhang, Y. (2014). Removal of perfluorinated compounds by membrane bioreactor with powdered activated carbon (PAC): Adsorption onto sludge and PAC. *Desalination*, 334(1), 23–28.

## The impact of graphene oxide on the methane production kinetics

Michele Ponzelli<sup>1,2,3</sup>, Jörg E. Drewes<sup>3</sup>, Jelena Radjenovic<sup>1,4</sup>, Konrad Koch<sup>3</sup>

<sup>1</sup>Catalan Institute for Water Research (ICRA), Emili Grahit 101, 17003 Girona, Spain  
(Phone: +34 972 18 33 80)

<sup>2</sup> University of Girona, 17003 Girona, Spain

<sup>3</sup> Chair of Urban Water Systems Engineering, Technical University of Munich, Am Coulombwall 3, 85748 Garching, Germany

<sup>4</sup> Catalan Institution for Research and Advanced Studies (ICREA), Passeig Lluís Companys 23, 08010 Barcelona, Spain

### Abstract

Long-term biochemical methane potential (BMP) experiments are carried out for evaluating the effects of graphene oxide (GO) addition on the degradation kinetics of two selected substrates, i.e., glucose and microcrystalline cellulose (MCC). After three subsequential feed phases, significant improvements of the hydrolysis rate, where glucose was supplied as a substrate, are noticed for GO-amended assays compared to control. Future work may include the assessment of organic micropollutants removal kinetics.

### Keywords

BMP; graphene oxide; kinetics; degradation; methane.

### INTRODUCTION

Novel anaerobic wastewater treatment technologies are attractive for upgrading WWTPs into self-sustained or even net energy producers. However, they suffer from long start-up times and low degradation removal rates due to slow interspecies electron transfer (IET) between fermenting bacteria and methanogens (Baek et al., 2018). Adding carbon-based materials to methanogenic communities may accelerate direct IET (Zhao et al., 2017). In this study low-cost GO is amended to anaerobic sludge to evaluate its impact on the degradation kinetics of two model substrates, i.e., glucose and MCC. Glucose is known as an easily degradable material. No hydrolysis is needed, and acidification is known to happen very fast, making it a substrate to identify potential impacts of GO addition on the methanogenesis step. On the other hand, MCC degradation involves all the anaerobic digestion steps, with hydrolysis as its rate-limiting step. Differentiating between these two substrates and comparing their performance allows for identifying which limiting step is favored or inhibited by the GO addition.

Compared to normal BMP batch experiment, this study aims to modify the feeding strategy to simulate continuously fed reactors in batch experiments by applying multiple refeeds once the plateau phase is reached. It is indeed assumed that the microbial community needs a certain time to adapt to the nanomaterial, which furthermore consumes electrons during its bioreduction, which are not available for methane formation. The limited methane production performance seen in literature studies (Dong et al., 2019) seems to be related to different reasons: i) the biological reduction of GO consumes electrons from the supplied substrate, which would otherwise be available for methane production (Bueno-López et al., 2020); ii) the introduction of the nanomaterial acts initially as an environmental stressor, causing the inhibition of bacterial activity (cell death, wrapping and trapping) (Zhang et al., 2017); iii) the adsorption properties of the graphene material might also contribute to lower cumulative methane production, because the soluble organic matter might be adsorbed, and are thus less available for methane production (Dong et al., 2019).

Such negative impacts on the anaerobic culture and its performance are thus limited to the initial phase when GO is amended for the first time. Extending the investigation period by subsequentially refeeding the batch reactors (or choosing a continuous system) would provide the necessary time to the anaerobic culture for adaptation.

## METHODS

### BMP Setup and operation

The inoculum used in the experiments was collected from an anaerobic digester (Garching, Germany), working at mesophilic temperature (38°C), treating a mixture of primary and secondary sludge. The experiments were conducted with glucose and MCC as substrates. The inoculum substrate ratio (ISR) was set to 2 based on VS for both substrates (Holliger et al., 2016). Stirring was applied intermittently, i.e., 5 minutes every 30 minutes. A total of three AMPTS II systems were employed. Each system comprised 15 glass bottles of 500 mL total volume and a working volume of 250 mL. Four GO levels (i.e., 0, 5, 10, and 20 mg<sub>GO</sub>/g<sub>VS</sub>) were selected and conducted in quintuplicate. Roman numerals are used to indicate the subsequent feedings, and a total of five feeds were carried out. Cumulative gas productions were calculated by subtracting the endogenous methane production obtained from blanks, i.e., assays containing only inoculum.

### Kinetic Models

Two kinetic models were adopted to estimate kinetic parameters based on the biogas profile obtained from the AMPTS systems (**Table 1**). The first order one-step for glucose and the modified Gompertz for MCC. The initial values of iteration were set according to Brulé et al. indications (2014). All variables were constrained to non-negative values ( $\geq 0$ ), and ultimate BMP ( $B_{\infty}$ ) was constrained to values less or equal to 372 and 414 mL<sub>CH<sub>4</sub></sub>/g<sub>VS</sub> for glucose (C<sub>6</sub>H<sub>12</sub>O<sub>6</sub>), and MCC ((C<sub>6</sub>H<sub>10</sub>O<sub>5</sub>)<sub>n</sub>), respectively. These two upper limits represent the maximum (100%) theoretical BMP for the two substrates.

Table 1. Kinetic models adopted.

Model	Parameters	References
<b>1<sup>st</sup> Order One-Step</b> $B(t) = B_{\infty}(1 - e^{-kt})$	$B_{\infty}$ = ultimate BMP (mL/g) k = 1 <sup>st</sup> -order rate constant (1/d) t = time (d)	(Angelidaki et al., 2009) (Brulé et al., 2014)
<b>Modified Gompertz</b> $B(t) = B_{\infty} \cdot e^{-e^{\left(\frac{R_{MAX} \cdot e}{B_0}(\lambda - t) + 1\right)}}$	$B_{\infty}$ = ultimate BMP (mL/g) $R_{MAX}$ = Maximum BMP rate (mL/g/d) $\lambda$ = lag time (d) t = time (d)	(Zwietering et al., 1990)

### Statistical parameters

Model parameters were calculated through iteration using the Excel solver function. The objective function was the relative standard square error (RSS), which was set as minimum (Min). Relative root means square error (rRMSE) and R<sup>2</sup> were used to evaluate the model fitness and model efficiency (Weinrich and Nelles, 2021). Analysis of the residuals, i.e., the differences between experimental (measured) and model data, are also used to evaluate the closeness of the model to reality.

### Analytical Methods

TS and VS were analyzed according to the Standard Methods (Baird et al., 2017).

## RESULTS AND DISCUSSION

### Kinetic parameters

As illustrated in **Figure 1**, where glucose was supplied, an initial inhibition during I. feed due to GO is noted. Also, the relatively high  $B_{\infty}$  initially seen for the control condition (i.e., 0 mg<sub>GO</sub>/g<sub>VS</sub>) during I. feed might be linked to the undegraded substrate present in the inoculum. Otherwise, no differences between GO-amended assays and control conditions for  $B_{\infty}$  are noticed during subsequent feedings (results not shown). During the V. feed, an increase of the first order degradation rate constant (k) is visible for GO-amended conditions with values above 1.2 1/d. Thus, the presence of GO at levels higher than 10 mg/g significantly improved the degradation rate compared to the control condition. However, an initial adaptation to the GO material is needed. Thereafter, an improvement in degradation kinetics is visible. Such observation might confirm the

formulated hypothesis that digestion performance inhibition occurs only during initial periods.

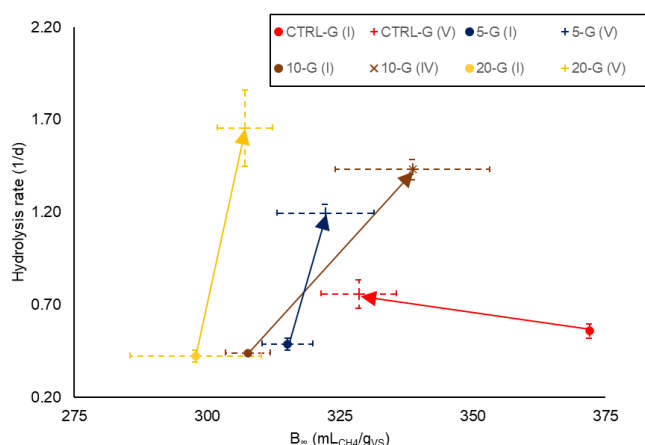


Figure 1. Kinetic parameters from 1<sup>st</sup> Order One-Step model for assays supplied with glucose at four levels of GO concentration (0, 5, 10, and 20 mg/g) (n=5), describing: the infinite methane potential ( $B_{\infty}$ ), the hydrolysis rate ( $k$ ). Only feed I and V are shown. Error bars indicate standard deviation.

In the case of MCC used as substrate, no significant improvement ( $p < 0.05$ ) of kinetics values ( $R_{MAX}$  and  $\lambda$ ) were noticed among the different GO levels.

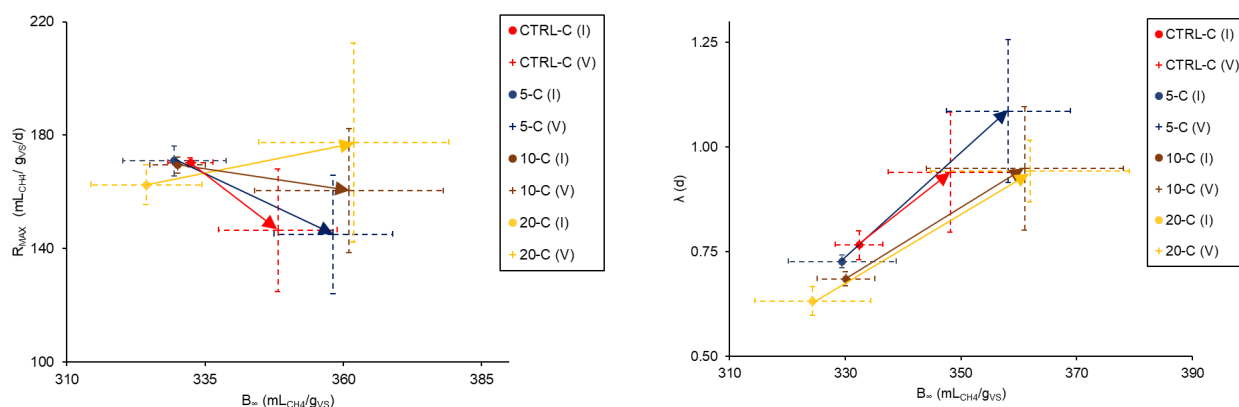


Figure 2. Kinetic parameters from modified Gompertz for assays supplied with MCC at four levels of GO concentration (0, 5, 10, and 20 mg/g) (n=5), describing: the infinite methane potential ( $B_{\infty}$ ), the maximum methane production rate ( $R_{MAX}$ ), and the lag-phase duration ( $\lambda$ ). Only feed I and V are shown. Error bars indicate standard deviation.

## CONCLUSIONS

Especially for the case of glucose, results seemed to confirm the formulated hypothesis, for which the effects of GO improvement on degradation kinetics are visible only from 1+ refeeding steps already. Otherwise, during at initial stage, an overall inhibition for GO-amended assays is noticed. Future experiments aim at implementing organic micropollutants at environmental level to discover the impact on their removal kinetics.

## ACKNOWLEDGEMENTS

This project has received funding from the MSCA-ITN-EJD – European Joint Doctorate Network NOWELTIES project (grant agreement 81288).

## REFERENCES

- Angelidaki, I., Alves, M., Bolzonella, D., Borzacconi, L., Campos, J.L., Guwy, A.J., Kalyuzhnyi, S., Jenicek, P., Van Lier, J.B., 2009. Defining the biomethane potential (BMP) of solid organic wastes and energy crops: A proposed protocol for batch assays. *Water Sci. Technol.* 59, 927–934. <https://doi.org/10.2166/wst.2009.040>
- Baek, G., Kim, Jaai, Kim, Jinsu, Lee, C., 2018. Role and Potential of Direct Interspecies Electron Transfer in Anaerobic Digestion. *energies*. <https://doi.org/10.3390/en11010107>
- Baird, R., Bridgewater, L., 2017. *Standard Methods for the Examination of Water and Wastewater*, 23rd ed, American Public Health Association. Washington, D.C.
- Brulé, M., Oechsner, H., Jungbluth, T., 2014. Exponential model describing methane production kinetics in batch anaerobic digestion: A tool for evaluation of biochemical methane potential assays. *Bioprocess Biosyst. Eng.* 37, 1759–1770. <https://doi.org/10.1007/s00449-014-1150-4>
- Bueno-López, J.I., Nguyen, C.H., Rangel-Mendez, J.R., Sierra-Alvarez, R., Field, J.A., Cervantes, F.J., 2020. Effects of graphene oxide and reduced graphene oxide on acetoclastic, hydrogenotrophic and methylotrophic methanogenesis. *Biodegradation* 31, 35–45. <https://doi.org/10.1007/s10532-020-09892-0>
- Dong, B., Xia, Z., Sun, J., Dai, X., Chen, X., Ni, B.J., 2019. The inhibitory impacts of nano-graphene oxide on methane production from waste activated sludge in anaerobic digestion. *Sci. Total Environ.* 646, 1376–1384. <https://doi.org/10.1016/j.scitotenv.2018.07.424>
- Holliger, C., Alves, M., Andrade, D., Angelidaki, I., Astals, S., Baier, U., Bougrier, C., Buffière, P., Carballa, M., De Wilde, V., Ebertseder, F., Fernández, B., Ficara, E., Fotidis, I., Frigon, J.C., De Lacroix, H.F., Ghasimi, D.S.M., Hack, G., Hartel, M., Heerenklage, J., Horvath, I.S., Jenicek, P., Koch, K., Krautwald, J., Lizasoain, J., Liu, J., Mosberger, L., Nistor, M., Oechsner, H., Oliveira, J.V., Paterson, M., Pauss, A., Pommier, S., Porqueddu, I., Raposo, F., Ribeiro, T., Pfund, F.R., Strömberg, S., Torrijos, M., Van Eekert, M., Van Lier, J., Wedwitschka, H., Wierinck, I., 2016. Towards a standardization of biomethane potential tests. *Water Sci. Technol.* 74, 2515–2522. <https://doi.org/10.2166/wst.2016.336>
- Weinrich, S., Nelles, M., 2021. *Basics of Anaerobic Digestion - Biochemical Conversion and Process Modelling*, DBFZ Report No. 40.
- Zhang, J., Wang, Z., Wang, Y., Zhong, H., Sui, Q., Zhang, C., Wei, Y., 2017. Effects of graphene oxide on the performance, microbial community dynamics and antibiotic resistance genes reduction during anaerobic digestion of swine manure. *Bioresour. Technol.* 245, 850–859. <https://doi.org/10.1016/j.biortech.2017.08.217>
- Zhao, Z., Li, Y., Quan, X., Zhang, Y., 2017. Towards engineering application: Potential mechanism for enhancing anaerobic digestion of complex organic waste with different types of conductive materials. *Water Res.* 115, 266–277. <https://doi.org/10.1016/j.watres.2017.02.067>
- Zwietering, M.H., Jongenburger, I., Rombouts, F.M., Van't Riet, K., 1990. Modeling of the bacterial growth curve. *Appl. Environ. Microbiol.* 56, 1875–1881. <https://doi.org/10.1128/aem.56.6.1875-1881.1990>

## Fabrication of composite materials using MOFs to achieve super hydrophobic materials with exceptional adsorption performance towards PFAS

*Nebojša Ilić\**, *Soumya Mukherjee\*\**, *Uwe Hübner\**, *Oliver Knoop\**, *Roland Fischer\*\**, *Jörg E. Drewes\**

*\* Chair of Urban Water Systems Engineering, Technical University of Munich, Am Coulombwall 3, D-85748 Garching, Germany  
(E-mail: [nebojsa.ilic@tum.de](mailto:nebojsa.ilic@tum.de))*

*\*\* Catalysis Research Center, Technical University of Munich, Ernst-Otto-Fischer-Straße 1, D-85748 Garching, Germany*

### Abstract

Chemically resistant per- and polyfluoroalkyl substances (PFAS) are a group of > 4730 synthetic organic chemicals. Bioaccumulation potential and toxicity of these “forever chemicals” has largely accelerated the material chemistry research on PFAS decontamination technologies. Studying the development of PFAS-selective adsorbents is a niche field with ever-increasing importance. Metal-organic frameworks (MOFs) are stable, modular porous solids with untapped potential for PFAS adsorption. Our current research aim is to develop MOFs and derived physisorbents primed to elicit high adsorption capacity towards these contaminants and to study the effect of structural differences on their adsorption performance. As part of this research, we strive to understand the potential of composite fabrication to invoke synergetic properties in the material. In this study, a composite material of increased hydrophobicity and water stability is achieved while maintaining the adsorption performance of the pristine MOF material. With such modifications we aim to improve the overall stability of the MOF allowing for multiple regeneration cycles, resulting in reusability aligned with the objective of circular economy.

### Keywords

adsorption, drinking water, metal-organic frameworks, nanomaterials, PFAS, physisorbents

### INTRODUCTION

Per- and polyfluoroalkyl substances (**PFAS**) are a class of synthetic organic chemicals that are significantly drawing public attention in the recent years due to their toxicity and bioaccumulation potential (Richardson & Kimura, 2019). Widespread use of these compounds is due to their desirable properties, which originate from the high electronegativity and small size of the fluorine atom, making the carbon-fluorine bond one of the strongest covalent bonds. PFAS are therefore thermally stable and resistant towards acids, bases and most oxidizing agents (Banks et al., 2020). Due to the simultaneous presence of a hydrophobic and a hydrophilic group, PFAS exhibit exceptional surfactant properties, making them a class of particularly relevant commercial substances and industrial tools. However, the same exceptional properties make PFAS very recalcitrant pollutants and difficult to remove using conventional (waste-)water treatment processes.

Perfluorooctanesulfonic acid (**PFOS**) and its salts have been classified as persistent, bioaccumulative and toxic chemicals and as such were added to Annex B (Restriction) of the Stockholm Convention in 2009. Perfluorooctanoic acid (**PFOA**), one of the two most studied representatives of the contaminant family, was only added to Annex A (Elimination) of the Stockholm Convention on Persistent Organic Pollutants on May 10, 2019. The European Commission has as recently as December 2020 updated the drinking water directive to limit the total amount of PFAS present in drinking water to 500 ng/L and a sum of selected 20 PFAS to 100 ng/L. As part of the early phase-out efforts, PFOA and PFOS have been substituted by new-generation PFAS, from which we selected hexafluoropropylene oxide-dimer acid (HFPO-DA, a.k.a. **GenX**) as the representative adsorbate in this study, acknowledging its steadily rising environmental footprint.

Metal-organic frameworks, popularly known as **MOFs**, are coordination networks composed of

metal nodes (or clusters) and organic ligands that feature potential voids. The combination of a) tuneable porosity ranging between nonporous and mesoporous domains, b) high stability and c) amenability to compositional modularity make MOFs one of the most promising adsorbent classes in the context of task-specific applications, including, but not limited to, pollutant removal (by selective capture) from water. Recently, the first reports of significant PFAS uptake from water harnessed a mesoporous MOF, MIL-101(Cr) (Barpaga et al., 2019), a microporous MOF, UiO-66 and its isostructural analogues (Clark et al., 2019; DeChellis et al., 2020; Sini et al., 2018), where UiO-66 has also been compared to two more MOF structures NU-1000 and ZIF-8 (Li et al., 2021). Regardless of these promising preliminary observations, this area remains significantly underexplored. Optimising adsorption kinetics, stability towards water, recycling potential and synthesis pathways in favour of green chemistry are all crucial factors to consider before a select few performance-screened MOFs can be considered viable adsorbent solutions to address PFAS remediation.

This research effort focuses on exploring how structural modification by composite fabrication affect the PFAS removal performance of a MOF material. Initial efforts are driven by the observed increased hydrophobicity with the novel structure, while the crystal structure of the MOF remains unaltered. In essence, takeaways from this study should fast-track the adoption of MOFs as reusable PFAS adsorbents with small to no reduction in capture performance between consecutive adsorption cycles.

## MATERIALS AND METHODS

### *Materials*

PFOA and PFOS were purchased from Sigma-Aldrich as solids. GenX was manufactured by Toronto Research Chemicals and purchased from Hölzel Biotech as a clear liquid. Analytical and internal standards for all three PFAS were purchased from Campro Scientific Berlin. The delay column was purchased from VWR (Agilent, ZORBAX Eclipse Plus C18, 4.6x50 mm, 3.5  $\mu\text{m}$ ). Separation and quantification of PFAS was performed with an XSelect HSS T3 column (100Å, 3.5  $\mu\text{m}$ , 2.1 mm x 100 mm).

### *MOF synthesis and characterisation*

Both the MOF and graphene-MOF composites were synthesized at room temperature through stirring in aqueous methanol followed by filtration, centrifugation and methanol washing, exemplifying simple and cost-efficient sorbent. The composite is fabricated by direct synthesis in a aqueous methanol suspension of the graphene-based foundation on which the MOF structure is synthesized directly. Two composite materials with different graphene fractions are prepared one with 12% and another with 24% of total mass being graphene-based foundation.

Powder X-ray diffraction patterns (recorded with a Rigaku MiniFlex 600 X-ray diffractometer with  $\text{CuK}\alpha$ -radiation,  $\lambda = 1.54178 \text{ \AA}$ ) was used to confirm the bulk phase purity for each of the synthesized MOFs. Thermogravimetric (TG) traces were measured on a Netzsch STA449 F5 thermogravimetric analyzer to confirm thermal stability and ensure the guest-free nature for each of the activated MOFs before PFAS sorption experiments. Brunauer-Emmett-Teller (BET) surface areas obtained from cryogenic (77 K)  $\text{N}_2$  adsorption experiments (performed on an AutosorbIQ2, Quantachrome Instruments equipped with a liquid nitrogen (77 K) Dewar vessel) confirmed the permanent porosity of each MOF.

### *Experimental design*

The initial screening of PFAS capture performance was based on batch adsorption tests. These experiments were conducted in 25 mL batches of 100  $\mu\text{g/L}$  PFAS solution with 10 mg of added adsorbent. Experiments were conducted individually for each PFAS. Validation of data was ensured by setting up each adsorption experiment in triplicate. The equilibration time was 24 hours. All experiments were done at an adjusted initial pH of 6.5.

To terminate the adsorption process immediately after sampling, samples taken from the vials

were filtered through a polypropylene syringe filter into Eppendorf vials for storage. All samples were kept refrigerated until analysed. After the experiment the MOFs were filtered out, dried, and then stored in a desiccator for future desorption and structural integrity tests. All laboratory equipment was cleaned using an ultrasound bath and by rinsing multiple times with ultrapure water and methanol.

### Analysis of samples

PFAS quantification was conducted using an LC/MS-MS system (Agilent 1260 Infinity, ABSciex Qtrap 5500). The analytical method was based on the German standard method DIN 38407-42, supported by the US Environmental Protection Agency Method 537.1. The quantification range for all three PFAS was 5 - 2,500 ng/L. Therefore, all samples acquired from experiments had to be diluted for the purpose of PFAS quantification.

## RESULTS AND DISCUSSION

The preliminary data in Figure 1 presents average values and standard deviations acquired from the triplicate series for each tested adsorbent. Labelled MOF on Figure 1 is the tested pristine MOF, whereas MOF-Graph-xx% are the two composite materials with varying fraction of graphene.

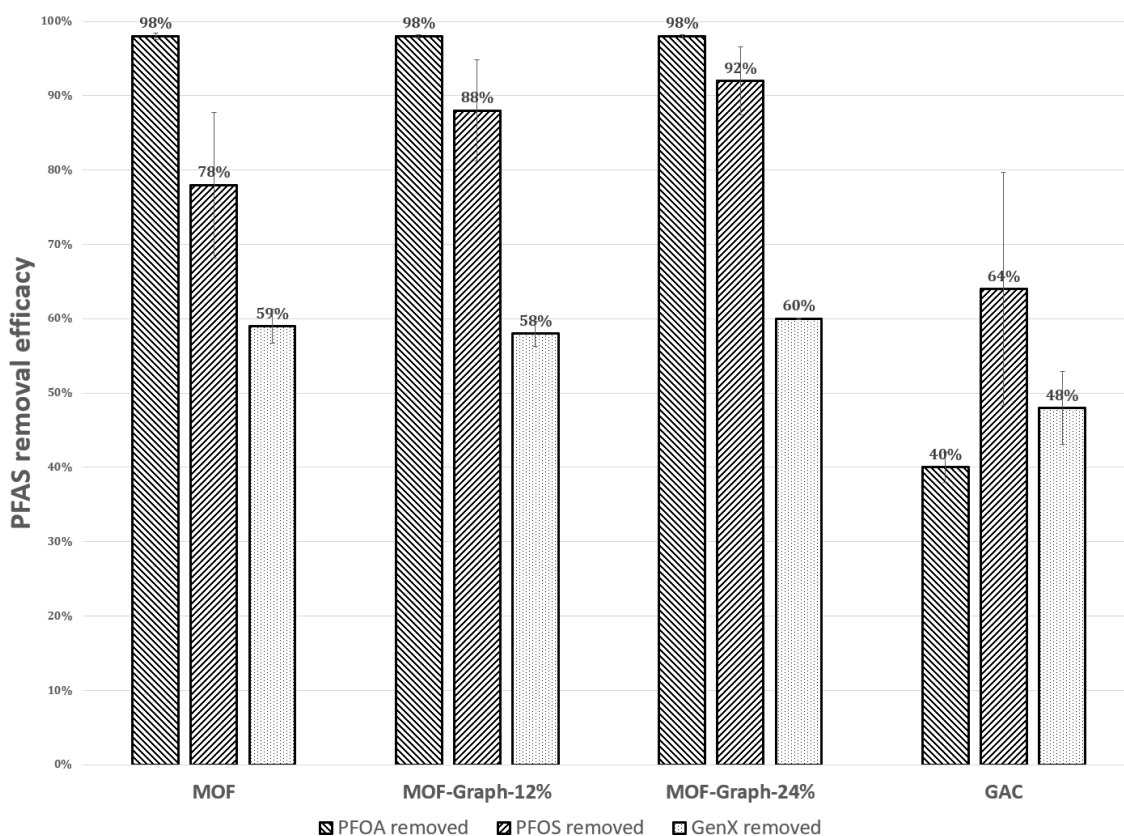


**Figure 1.** PFAS removal percentages exhibited by the three materials under identical conditions. Presented data indicates removal for 10 mg of adsorbent in 25 ml of 100  $\mu\text{g/L}$  PFAS solution. Percentage values shown on the y-axis represent PFAS removed compared to the initial PFAS concentration in individual experiments.

Notable PFAS removal performance was observed from the acquired experimental data for all three tested materials. An observation can be made that the adsorption performance between the three materials varies very slightly, with a notable increase in the removal of PFOS matching the relative increase of the hydrophobic graphene-based substrate in the composite. It is still unknown whether the substrate actively participates in the adsorption of PFAS, or if the observed increase in sorption of PFOS is merely due to fine structural differences between the materials. As PFOS is the largest of the three tested PFAS species, it is the most likely one to benefit from the finer



dispersion of the MOF material over the graphene-based substrate, as opposed to being used pristine.

The underlying force fields on the level of molecular interactions responsible for the PFAS adsorption are still being investigated by utilising solid-state nuclear magnetic resonance (SSNMR) in a first-of-its-kind study attempting to utilize this powerful technique to further characterize adsorption as a process.

## CONCLUSION

Preliminary data shows notable removal of PFAS from solutions at environmentally relevant concentrations. The presented data shows an overall best performance of tested material MOF-Graph-24%, with an increase in PFOS removal matching the increase in the graphene-based foundation. The novel graphene-based composites exhibit increased stability towards water, especially at higher pH, compared to the pristine MOF material. The significant increase in the hydrophobicity of the materials indicates longer operational times of the material, minimizing deterioration due to water molecule intrusion. Bond type formation is still under investigation with the aim of observing the difference in bonds formed between PFAS and the different adsorbents. Moving forward, we aim to explore how the materials behave at lower concentrations, in matrices containing multiple PFAS at once. Furthermore, only with regeneration studies will we truly be able to see the benefits of synthesizing composite materials to bolster the performance of an adsorbent. Synthesizing derived physisorbents using different modification techniques is an uncharted research paradigm for the adsorptive removal of PFAS that we aim to pursue in-depth in the upcoming months.

## REFERENCES

- Banks, D., Jun, B. M., Heo, J., Her, N., Park, C. M., & Yoon, Y. (2020). Selected advanced water treatment technologies for perfluoroalkyl and polyfluoroalkyl substances: A review. *Separation and Purification Technology*, 231(April 2019), 115929. <https://doi.org/10.1016/j.seppur.2019.115929>
- Barpaga, D., Zheng, J., Han, K. S., Soltis, J. A., Shutthanandan, V., Basuray, S., McGrail, B. P., Chatterjee, S., & Motkuri, R. K. (2019). Probing the Sorption of Perfluorooctanesulfonate Using Mesoporous Metal-Organic Frameworks from Aqueous Solutions. *Inorganic Chemistry*, 58(13), 8339–8346. <https://doi.org/10.1021/acs.inorgchem.9b00380>
- Clark, C. A., Heck, K. N., Powell, C. D., & Wong, M. S. (2019). Highly Defective UiO-66 Materials for the Adsorptive Removal of Perfluorooctanesulfonate. *ACS Sustainable Chemistry and Engineering*, 7(7), 6619–6628. <https://doi.org/10.1021/acssuschemeng.8b05572>
- DeChellis, D. M., Ngule, C. M., & Genna, D. T. (2020). Removal of hydrocarbon contaminants from water with perfluorocarboxylated UiO-6 X derivatives. *Journal of Materials Chemistry A*, 8(12), 5848–5852. <https://doi.org/10.1039/c9ta11144a>
- Li, R., Alomari, S., Stanton, R., Wasson, M. C., Islamoglu, T., Farha, O. K., Holsen, T. M., Thagard, S. M., Trivedi, D. J., & Wriedt, M. (2021). Efficient Removal of Per- and Polyfluoroalkyl Substances from Water with Zirconium-Based Metal–Organic Frameworks. *Chemistry of Materials*, 33(9), 3276–3285. <https://doi.org/10.1021/acs.chemmater.1c00324>
- Richardson, S. D., & Kimura, S. Y. (2019). Water Analysis: Emerging Contaminants and Current Issues [Review-article]. *Analytical Chemistry*, 92, 473–505. <https://doi.org/10.1021/acs.analchem.9b05269>
- Sini, K., Bourgeois, D., Idouhar, M., Carboni, M., & Meyer, D. (2018). Metal-organic framework sorbents for the removal of perfluorinated compounds in an aqueous environment. *New Journal of Chemistry*, 42(22), 17889–17894. <https://doi.org/10.1039/c8nj03312a>

## Degradation of pharmaceuticals with heterogeneous catalytic ozonation-membrane filtration process using modified ceramic membranes

*Nikoletta Tsiarta<sup>1,2,3</sup>, Ivana Panžić<sup>4</sup>, Lidija Ćurković<sup>3</sup>, and Wolfgang Gemjak<sup>1,5</sup>*

<sup>1</sup> *Catalan Institute of Water Research, Carrer Emili Grahit 101, 17003 Girona, Spain*

<sup>2</sup> *University of Girona, Campus de Montilivi, Girona, Catalonia, 17003 Spain*

<sup>3</sup> *Faculty of Mechanical Engineering and Naval Architecture, University of Zagreb, Ivana Lučića 5, Zagreb, Croatia*

<sup>4</sup> *Faculty of Chemical Engineering and Technology, University of Zagreb, Marulićev trg 19, 10000, Zagreb, Croatia*

<sup>5</sup> *Catalan Institution for Research and Advanced Studies (ICREA), 08010, Barcelona, Spain*

### Abstract

This study reports upon the removal of three widely used pharmaceutical compounds, namely carbamazepine (CBZ), diclofenac (DCF), and ibuprofen (IBP), by a hybrid ozonation-membrane filtration process. In addition to the selected compounds, the degradation of para-chlorobenzoic acid (pCBA) was also studied. pCBA is a hydroxyl radical (\*OH) probe compound due to its slow direct response with ozone and quick interaction with \*OH radicals. The hybrid process operates with an inside-out filtration, and the transferred ozone dose (TOD) was around 2.5 mg L<sup>-1</sup>. Four commercial ceramic membranes (CMs) with different porosity (15-200 nm) were used. The surface of the CMs was modified by the sol-gel method for the deposition of the metal oxide catalysts (CeO<sub>2</sub>, CeTiO<sub>x</sub>, and CeO<sub>2</sub>+CeTiO<sub>x</sub>). The changes in the membranes' properties were analyzed by various techniques (permeability tests, XRD, SEM-EDS, AFM). All modified CMs showed a significant decrease (>50% of the original membrane) in permeability because of the deposited layers. Results showed a better degradation of DCF and CBZ than IBP.

**Keywords:** catalytic ozonation, hybrid process, ceramic membranes, pharmaceuticals

### Introduction

Surface water quality continuously declines mainly due to anthropogenic activities. The so-called organic micropollutants (OMPs), can be found in low concentrations (ng L<sup>-1</sup>) in surface waters after their discharge into the environment. Specifically, pharmaceutical micropollutants that reach the environment through the wastewater discharged mainly by households, hospitals, and industries can cause deterioration of the natural aquatic habitats by disturbing their ecological balance. Therefore, both the drinking- and wastewater industry face many challenges regarding water treatment [1].

Wastewater is usually treated by biological wastewater treatment plants (WWTPs) that often do not have technologies targeted to remove OMPs present in wastewater. Advanced physiochemical treatment systems including oxidation processes have limited degradation efficiency towards OMPs and higher energy consumption. Thus, scientists and water authorities worldwide are investigating and developing innovative wastewater treatment techniques to tackle this issue.

Several novel technologies have emerged to convert wastewater into clean water that can be reused. These methods must be efficient and long-lasting to ensure that the water quality does not endanger the environment or human health. Ozonation has been widely used in tertiary treatment as an efficient Advanced Oxidation Process (AOP) because of its remarkable effectiveness in removing OMPs and disinfecting ability [2]. Nevertheless, ozone ( $O_3$ ) selectivity towards some functional groups is a limitation, and thus, its combination with other processes is often preferable.

Catalytic ozonation uses a catalyst to enhance the formation of hydroxyl radicals ( $\cdot OH$ ) from  $O_3$  decomposition to improve OMPs removal [3]. Heterogeneous catalytic ozonation is preferable since catalyst recovery is facilitated or needless when immobilizing the catalyst. Interestingly, when ozonation is combined with membrane separation, a membrane can act as a substrate for employing metal oxides as catalysts. In recent years we have also witnessed a growing interest in introducing ceramic membranes (CMs) in the water treatment market because of their unique advantages over the commonly used polymeric membranes.

In this study, a hybrid ozonation-membrane filtration system is proposed where modified ceramic membranes are utilized immediately after ozone to enhance the  $\cdot OH$  concentration, decrease ozone demand, and increase pharmaceuticals' removal from the secondary effluent, while at the same time reducing membrane fouling.

## Materials and Methods

### *Chemicals and materials*

Carbamazepine (CBZ), ibuprofen (IBP), and diclofenac (DCF) were used as model compounds because they are frequently detected in secondary effluents. para-chlorobenzoic acid (pCBA; was used as an  $O_3/\cdot OH$  probe compound. Single-tubular commercial CMs (10 mm outer diameter, 6 mm inner diameter, 250 mm length) with different compositions and molecular weight cut-offs (MWCO) were utilized (INSIDECÉRAM, TAMI Industries, France);  $TiO_2/ZrO_2$  composition (50-, 150-, 300 kDa MWCO) and  $TiO_2/TiO_2+ZrO_2$  composition (0.2  $\mu m$  MWCO).

### *Preparation of modified ceramic membranes and characterization techniques*

The CMs were modified by the sol-gel method in vacuum infiltration conditions to avoid clogging of the pores and to allow good dispersion of the sol-gel through the membranes. Two different sol-gels were prepared, Ceria ( $CeO_2$ ) and Ce doped Ti ( $CeTiO_x$ ), and three nanostructured films were separately deposited on the surface of each CM of particular MWCO: one layer of  $CeO_2$  [4], one layer of  $CeTiO_x$  [5], and one layer of  $CeO_2$  with an additional layer of  $CeTiO_x$  ( $CeO_2 + CeTiO_x$ ). The ceramic membranes, as well as their modified surfaces, were characterized to determine their chemical and phase composition, crystal structure, and morphology, using the following techniques: Scanning Electron Microscopy (SEM) with Energy Dispersive X-ray Spectroscopy (EDS); X-ray Diffraction Analysis (XRD); and Atomic Force Microscopy (AFM). Mercury intrusion porosimetry (MIP) was used to evaluate porosity, pore size distribution, and pore volume.

### *Hybrid ozonation-membrane filtration (HOMF) system*

All experiments were carried out at room temperature using a laboratory-scale ozone reactor (ANSEROS, COM-AD-04, Germany). Aqueous  $O_3$  concentrated stock solution was maintained at  $\sim 45 \text{ mg L}^{-1}$  and was connected to a custom-made micro- or ultrafiltration (MF/UF) filtration unit of inside-out operation (SIVA, France) (Figure 1). The initial concentration of the pollutants was 10

$\mu\text{M}$ , and the transferred ozone dose (TOD) was kept constantly at  $50 \mu\text{M}$  ( $\sim 2,5 \text{ mg L}^{-1}$ ) with a treatment time of 10 mins. The permeate was collected in specific intervals, quenched with  $\text{Na}_2\text{S}_2\text{O}_3$ , and filtrated through  $0.2 \mu\text{M}$  nylon filters (Whatman) before analysis.

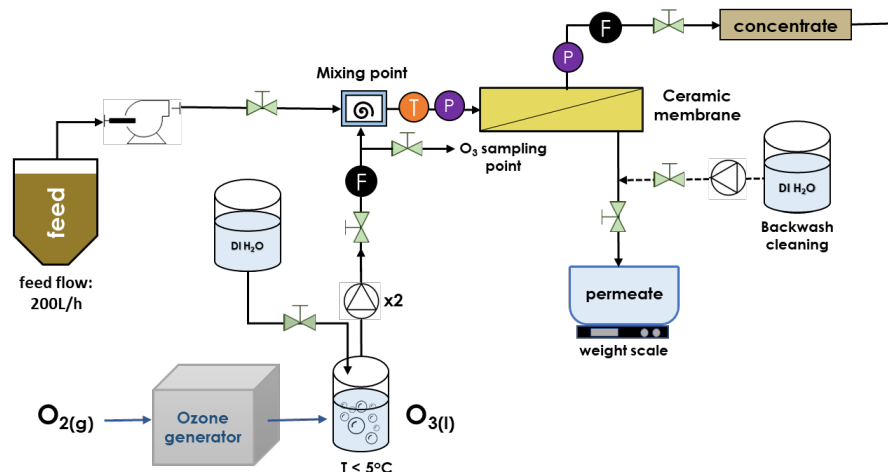


Figure 1. Experimental set-up of HOMF system

### Analytical methods

The transferred ozone dose (TOD) was determined by the indigo colorimetric method [6] with a UV-Vis spectrophotometer at 600 nm. The OMPs were identified and quantified by high-performance liquid chromatography in reversed-phase (HPLC-UV Agilent 1200). Chromatographic separation was performed using a C18 column (Microsorb-MV 100-5  $250 \times 4.6 \text{ mm}$ ) at a working temperature of  $30 \text{ }^\circ\text{C}$  and injection volume of  $200 \mu\text{L}$ .

## Results and discussion

### Ceramic membranes' modification and characterization

XRD analysis showed that pristine/unmodified CMs consist of a mixture of titania rutile (ICDD PDF#21-1276) and predominately zirconia (ICDD PDF#50-1080). The Baddeleyite zirconia phase (ICDD PDF#37-1484) was present in traces only in the lowest MWCO membranes. Regarding the modified membranes, the metal oxides of the were identified as titania anatase phase (ICDD PDF#21-1272) and ceria (ICDD PDF#34-0394). SEM images illustrated well dispersion of the metal oxides on CMs surface (Figure 2), indicating the successful use of vacuum infiltration. Additionally, the EDS elemental mappings further confirmed the successful impregnations of the metal oxides across the CMs. AFM was used to depict the topography of the CMs' surface roughness. Notable changes in the surface roughness were observed between the membrane with the lowest porosity (50 kDa) and the highest one ( $0.2 \mu\text{m}$ ).

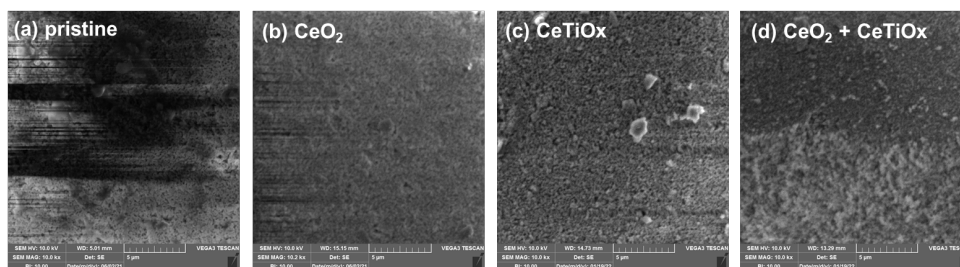


Figure 2. Surface morphologies of the inside surface of the pristine and modified  $0.2 \mu\text{m}$  MWCO CM.

### Permeability tests and OMPs removal

Permeability tests were performed to examine the changes after the deposition of the nanostructured films. The permeability ( $\text{L m}^{-2} \text{h}^{-1}$ ) of the modified CMs was dropped to less than 50% of the pristine membranes, indicating pores clogging phenomena. The CMs with two layers ( $\text{CeO}_2 + \text{CeTiO}_x$ ) showed the lowest permeability rates (Figure 3). The results suggested that surface modifications can change the commercial membranes' porosity and pore size distribution. Preliminary results using a pristine 300 kDa CM on the HOMF system showed that IBP degradation was significantly lower than CBZ and DCF (Figure 4). pCBA degradation followed a similar trend ascribed to a rather slow reaction of both compounds with  $\text{O}_3$  ( $k_{\text{O}_3} < 0.15$  and  $9.6 \text{ mol L}^{-1} \text{ s}^{-1}$ , respectively). More experiments will be performed to identify whether the modified CMs increase the yield of  $\cdot\text{OH}$  and thus, ensure increased degradation of the OMPs in synthetic wastewater while reducing membrane fouling.

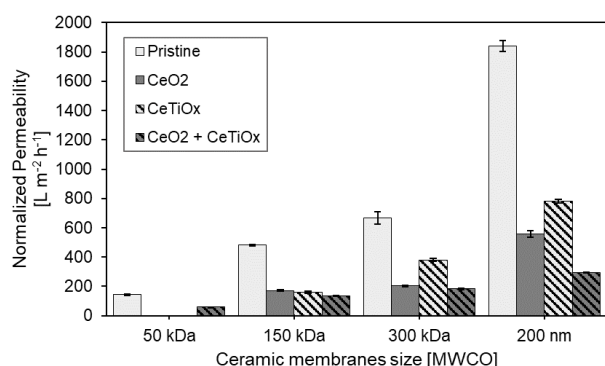


Figure 3. Permeability changes on the different CMs

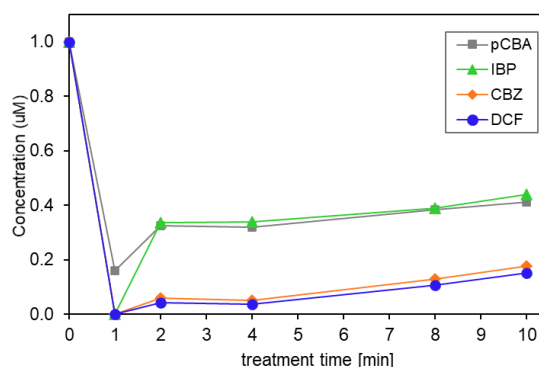


Figure 4. OMPs removal by HOMF system using a pristine 300 kDa MWCO CM.

### Acknowledgments

This research has received funding from the European Union's Horizon 2020 research and innovation program under Marie Skłodowska-Curie grant agreement No. 812880.

### References

- [1] Ratola, N., Cincinelli, A., Alves, A., Katsoyiannis, A. (2012) Occurrence of organic microcontaminants in the wastewater treatment. A mini review. *Journal of Hazardous Materials*, 239–240 18
- [2] Andreatti, R., Caprio V., Insola, A., Marotta R. (1999) Advanced oxidation processes (AOP) for water purification and recovery, *Catalysis Today* 53 (1), 51–59.
- [3] Wang, J. and Chen, H. (2020) Catalytic ozonation for water and wastewater treatment: Recent advances and perspective. *Science of the Total Environment*, 704, 135249. [online] <https://doi.org/10.1016/j.scitotenv.2019.135249>.
- [4] Lee, W. J., Bao, Y., Hu, X., and Lim, T. T. (2019) Hybrid catalytic ozonation-membrane filtration process with CeO<sub>x</sub> and MnO<sub>x</sub> impregnated catalytic ceramic membranes for micropollutants degradation. *Chemical Engineering Journal*, 378, 121670.
- [5] Ćurković, L., Ljubas, D., Šegota, S., and Bačić, I. (2014) Photocatalytic degradation of Lissamine Green B dye by using nanostructured sol-gel TiO<sub>2</sub> films. *Journal of Alloys and Compounds*, 604, 309–316.
- [6] Bader, H. and Hoigné, J. (1981) Determination of ozone in water by the indigo method. *Water Research*, 15(4), 449–456.

## POSTER PRESENTATIONS

## Study of micropollutants photocatalytic degradation using TiO<sub>2</sub> and TiO<sub>2</sub>/CNT in optimal reactor configuration

Lucija Radetić<sup>1</sup>, Igor Jajčinović<sup>2</sup>, Ivan Brnardić<sup>2</sup>, Ivana Grčić<sup>1</sup>, Jan Marčec<sup>1</sup>, Kristina Miklec<sup>1</sup>

<sup>1</sup>University of Zagreb, Faculty of Geotechnical Engineering, Varaždin, Croatia

<sup>2</sup>University of Zagreb, Faculty of Metallurgy, Sisak, Croatia

Corresponding author: [jajcinovic@simet.unizg.hr](mailto:jajcinovic@simet.unizg.hr)

### Abstract

Nowadays, efforts have been directed towards improving of existing wastewater treatment plants by application of promising advance oxidation process such as solar photocatalysis. Accordingly, an optimal reactor configuration of a semi-pilot scale compound parabolic collector (CPC) reactor was constructed to study the solar photocatalytic degradation of common organic pollutants, imidacloprid (IMI) and diclofenac (DF).

Photocatalytic oxidation was assisted either by UV photocatalytically active titanium dioxide (TiO<sub>2</sub>) or UV-Vis photocatalytically active nanocomposite of TiO<sub>2</sub> and carbon nanotubes (CNT) under simulated irradiation spectra. Both photocatalysts were immobilized on fiber glass mesh by modified sol-gel method [1].

Based on the experimental data of photocatalytic degradation, predictive mathematical models were developed including mass transfer considerations and photon absorption. The "intrinsic" photocatalytic reaction constants for the target pollutants in CPC reactor independent on irradiance levels, reactor geometry and hydrodynamics were estimated ( $k_{DF}=3.564 \times 10^{-10} \text{ s}^{-1} \text{ W}^{-0.5} \text{ m}^{1.5}$ ;  $k_{IMI}=8.9 \times 10^{-11} \text{ s}^{-1} \text{ W}^{-0.5} \text{ m}^{1.5}$ ). Results indicated that sensitization of solar photocatalysis by the addition of CNT to TiO<sub>2</sub> films, led to intensification of diclofenac and imidacloprid photocatalytic degradation.

**Keywords:** photocatalysis, imidacloprid, diclofenac, titanium dioxide (TiO<sub>2</sub>), carbon nanotubes (CNT).

### References

[1] Malinowski, I. Presečki, I. Jajčinović, I. Brnardić, V. Mandić, I. Grčić, Intensification of Dihydroxybenzenes Degradation over Immobilized TiO<sub>2</sub> Based Photocatalysts under Simulated Solar Light, Appl. Sci. 10 (2020) 7571. <https://doi.org/10.3390/app10217571>.

### Acknowledgements

This work has been supported by following project „Waste & Sun for photocatalytic degradation of micropollutants in water” (OS-Mi), KK.01.1.1.04.0006, supported by European Regional Development Fund.

## Prospecting the environmental profile of Advanced Electrochemical Oxidation according to Key Performance Indicators (KPIs) in wastewater treatment

*Sofia Estévez<sup>1</sup>, Sara Feijoo<sup>2</sup>, Mohammadreza Kamali<sup>2</sup>, Raf Dewil<sup>2</sup>, Maria Teresa Moreira<sup>1</sup>*

<sup>1</sup>Universidad de Santiago de Compostela, CRETUS, Department of Chemical Engineering, 15782 Santiago de Compostela, Spain

<sup>2</sup>KU Leuven, Department of Chemical Engineering, Process and Environmental Technology Lab, 2860 Sint-Katelijne-Waver, Belgium

The recurring presence of contaminants of emerging concern (CECs) in natural water bodies has received international attention over the past years, given the current limitations of conventional wastewater treatment plants to fully eliminate them [1]. Advanced Oxidation Processes (AOPs) are promising treatments for the degradation of recalcitrant compounds by means of highly reactive species, such as hydroxyl radicals ( $\cdot\text{OH}$ ), sulfate radicals ( $\text{SO}_4^{\cdot-}$ ) and nitrate radicals ( $\text{NO}_3^{\cdot}$ ) [2,3]. Within the treatment class of electrochemical Advanced Oxidation Processes (eAOPs), Boron-Doped Diamond (BDD) anodes enable to electrochemically generate these oxidative species at a high efficiency [4,5]. Despite the energy consumption associated with electrochemical treatments, the in-situ radical generation offered by the BDD material from water molecules and ionic species, such as sulfate and nitrate ions, is of high added value towards industrial implementation, as these radicals are formed without the addition of external precursors. The lack of supplementary chemicals minimizes the generation of secondary waste streams and hence the environmental impacts associated.

In order to evaluate the feasibility of a novel process, both process modelling and environmental aspects should be taken into consideration. In this regard, mass and energy balances, kinetic parameters, mass transport phenomena and variables for equipment design have been considered and analyzed under the Life Cycle Assessment (LCA) methodology. The reactor design selected for this analysis consisted of a vertical plate agitated tank operated in batch recycling mode. The multitude of combinations of operating conditions resulted in a set of scenarios that shed light over the influence of process variables on the environmental profile. These scenarios considered the effect of (i) the concentration of sulfate and nitrate ions in the influent, (ii) synthetic versus complex wastewater composition and (iii) the scale-up modelling. As a result, it was possible to evaluate process performance from an integrated techno-environmental perspective. The results demonstrate the potential for the development of these processes on a large scale based on technical feasibility, operational efficiency and reduced environmental impacts.

### References

- [1] N.H. Tran, M. Reinhard and K.Y.-H. Gin, "Occurrence and fate of emerging contaminants in municipal wastewater treatment plants from different geographical regions - A review", *Water Research*, vol. 133, pp. 182–207, 2018.
- [2] L. Rizzo, S. Malato, D. Antakyali, V.G. Beretsou, M.B. Đolić, W. Gernjak, E. Heath, I. Ivancev-Tumbas, P. Karaolia, A.R. Lado Ribeiro, G. Mascolo, C.S. McArdell, H. Schaar, A.M.T. Silva and D. Fatta-Kassinos, "Consolidated vs new advanced treatment methods for the removal of contaminants of emerging concern from urban wastewater", *Science of The Total Environment*, vol. 655, pp. 986–1008, 2019.
- [3] J. Wang and S. Wang, "Reactive species in advanced oxidation processes: Formation, identification and reaction mechanism", *Chemical Engineering Journal*, vol. 401, pp. 126158, 2020.
- [4] C.A. Martínez-Huitle and S. Ferro, "Electrochemical oxidation of organic pollutants for the wastewater treatment: Direct and indirect processes", *Chemical Society Reviews*, vol. 35 (12), pp. 1324–1340, 2006.
- [5] G. Divyapriya and P.V. Nidheesh, "Electrochemically generated sulfate radicals by boron doped diamond and its environmental applications", *Current Opinion in Solid State and Materials Science*, vol. 25 (3), pp. 100921, 2021.



## **Acknowledgments**

This research was supported by the HP-Nanobio project (PID2019-111163RB-I00), granted by Spanish Ministry of Science and Innovation, as well as by the European Union's EU Framework Programme for Research and Innovation Horizon 2020 under Grant Agreement No 861369 (MSCA-ETN InnovEOX) and by the KU Leuven Industrial Research Council under grant number C24E/19/040 (SO4ELECTRIC). S. Estévez thanks to the Spanish Ministry of Science, Innovation and Universities for financial support (Grant reference PRE2020-092074). M. Kamali holds a postdoctoral research grant awarded by the KU Leuven Research Council, grant number PDM/19/104.

## Effect of water constituents and scavengers on the photocatalytic degradation of anticancer drugs

Kristina Tolić Čop, Dragana Mutavdžić Pavlović

Department of Analytical Chemistry, Faculty of Chemical Engineering, University of Zagreb, Trg Marka Marulića 19, 10000 Zagreb, Croatia

Relatively newly recognized micropollutants in the environment, whose nano- and micro-scale concentrations could not be detected until recently due to the limited capabilities of instrumentation, are pharmaceuticals. Their increasing production and consumption confirms the fact that many of them are present in various parts of the environment, affecting drinking water supplies and ultimately water quality. While the parent substance is excreted into the environment, the transformation and degradation products newly formed by various biotic and abiotic processes can be more toxic. One such pharmaceutical category that is considered a potential risk to the aquatic environment is anticancer drugs. Due to their physicochemical properties leading to mobility and persistence in the aquatic environment, many of these compounds with their metabolites can cause long-term side effects on terrestrial and aquatic organisms. Classical water treatment methods are not suitable for the removal of micropollutants, so the commonly used advanced oxidation process for this purpose is photocatalysis. The simple mechanism between photocatalyst,  $\text{TiO}_2$  and light source enables the generation of highly reactive oxygen species that degrade the target compound non-selectively. The photocatalytic efficiency is controlled by various parameters such as the pH, the initial concentration of the pollutant, the light source, the dosage of the photocatalyst, etc. In addition to the above parameters, various organic and inorganic species normally found in natural waters can also greatly affect photocatalysis. Water constituents such as bicarbonate, chloride, nitrate, phosphate ions and humic substances can adsorb on the surface of the photocatalyst, scavenge hydroxyl radicals and produce less active species, absorb photons and reduce the degradation of the pollutant, or ions such as nitrates in a certain environment can promote photocatalysis by  $\cdot\text{OH}$  production. In this study, the positive or negative influence of the above water constituents on the photocatalytic degradation of crizotinib and imatinib, two anticancer drugs used in patients with lung cancer and leukemia, respectively, was investigated.  $\text{TiO}_2$  immobilized on a glass fiber mesh was used as the photocatalyst. The mechanism of the photocatalytic reaction was also investigated by adding different radical scavengers.

## Enhanced photocatalytic degradation of methylene blue by TiO<sub>2</sub>-rGO binary nanocomposites

*Martina Kocijan<sup>1</sup>, Lidija Ćurković<sup>1</sup>, Tina Radošević<sup>2</sup>, Damjan Vengust<sup>2</sup>, Matejka Podlogar<sup>2</sup>*

<sup>1</sup>*Faculty of Mechanical Engineering and Naval Architecture, University of Zagreb, Ivana Lučića 5, 10000 Zagreb, Croatia*

<sup>2</sup>*Jožef Stefan Institute, Jamova Cesta 39, SI-1000 Ljubljana, Slovenia*

The accelerated development of the dye industry in recent years contributes to an overload of wastewater, which has a negative influence on human health and aquatic ecosystems [1]. Methylene blue (MB) is a commonly used cationic dye and is very harmful to human health above a certain concentration due to its toxicity. In addition, MB is difficult to biodegrade because of its chemical persistence. Nowadays, treatment methods such as biological, physical, and chemical have been used to remove dye wastewater. However, those methods have some drawbacks like high cost as well as toxic by-products. Therefore, advanced oxidation processes, like heterogeneous photocatalytic degradation can be used as a more appropriate method for MB removal from wastewater [2], [3].

In this research, the binary TiO<sub>2</sub>-rGO nanocomposite catalyst was successfully synthesized as a mixture of pure TiO<sub>2</sub> particles and reduced graphene oxide (rGO). The graphene oxide (GO) was synthesized by Hummer's method using natural graphite flakes (particle size  $\leq 50 \mu\text{m}$ ) as a precursor. The binary TiO<sub>2</sub>-rGO nanocomposite has been self-assembled through one-pot hydrothermal synthesis followed by a calcination treatment. The structural and morphological analysis of the synthesized nanocomposites have been performed by X-ray diffraction (XRD), scanning electron microscopy (SEM), and Fourier transforms infrared spectroscopy (FTIR). Photocatalytic experiments under ultraviolet (UV) and solar-like irradiation were performed in order to evaluate the efficiency of the synthesized catalysts. Further, the influence of rGO concentration on TiO<sub>2</sub> performance for photodegradation of the MB dye was determined. It was found that the photodegradation of MB was increased as irradiation time for both sources of irradiation increased. The obtained results showed that the photocatalytic activity was increased as rGO concentration increased in the prepared nanocomposite, which can be attributed to the synergistic effect of the incorporation of rGO with TiO<sub>2</sub>.

### References:

1. Pattnaik, P.; Dangayach, G.S. Analysis of Influencing Factors on Sustainability of Textile Wastewater: a Structural Equation Approach. *Water. Air. Soil Pollut.* 2019, 230, doi:10.1007/s11270-019-4206-x.
2. Ren, G.; Han, H.; Wang, Y.; Liu, S.; Zhao, J.; Meng, X.; Li, Z. Recent Advances of Photocatalytic Application in Water Treatment: A Review. *Nanomater.* 2021, 11, doi.org/10.3390/nano11071804
3. Chen, D.; Cheng, Y.; Zhou, N.; Chen, P.; Wang, Y.; Li, K.; Huo, S.; Cheng, P.; Peng, P.; Zhang, R.; et al. Photocatalytic degradation of organic pollutants using TiO<sub>2</sub>-based photocatalysts: A review. *J. Clean. Prod.* 2020, 268, 121725, doi:10.1016/j.jclepro.2020.121725.

## Photocatalytic degradation of ciprofloxacin by sol-gel derived Ce-doped TiO<sub>2</sub> films

*Lidija Ćurković<sup>1</sup>, Debora Briševac<sup>1</sup>, Vilko Mandić<sup>2</sup>, Davor Ljubas<sup>1</sup>, Rea Veseli<sup>1</sup>*

*<sup>1</sup> Faculty of Mechanical Engineering and Naval Architecture, University of Zagreb, Croatia  
([lidija.curkovic@fsb.hr](mailto:lidija.curkovic@fsb.hr) (L.Ć.); [debora.brisevac@gmail.com](mailto:debora.brisevac@gmail.com) (D.B.); [davor.ljubas@fsb.hr](mailto:davor.ljubas@fsb.hr) (D.Lj.);  
([rea.veseli@fsb.hr](mailto:rea.veseli@fsb.hr) (R.V.))*

*<sup>2</sup> Faculty of Chemical Engineering and Technology, University of Zagreb, Croatia  
([vmandic@fkit.hr](mailto:vmandic@fkit.hr) (V.M.))*

### Abstract

Here we study the photocatalytic degradation of the antibiotic ciprofloxacin (CIP) supported by sol-gel Ce-doped TiO<sub>2</sub> photocatalyst nanoparticles. The photocatalyst samples consist of Ce in 0.08, 0.40, 0.80, 2.40 and 4.10 wt.%. For the preparing of the sols we used titanium isopropoxide and cerium (III) nitrate hexahydrate as precursors, 2-propanol as a solvent, acetylacetone as a complexation agent, distilled water as a hydrolysis agent, and nitric acid as a hydrolysis/polycondensation catalyst. The Ce-TiO<sub>2</sub> sol was deposited on borosilicate glass samples using a flow coating method. After deposition, films were dried at 100 °C for 1 hour and heat-treated at 450 °C for 2 hours at a heating rate of 3 °C/min. The activity and efficiency of Ce-TiO<sub>2</sub> films for photocatalytic degradation of the CIP under simulated solar radiation was investigated, especially the influence of the changing irradiation intensity.

The weight loss as well as exothermic and endothermic reactions during the thermal treatment, were obtained by simultaneous differential thermal and thermogravimetric analysis (DSC/TGA). The phase composition and parameters and volumes of the unit cells were determined by X-ray diffraction (XRD). Atomic force microscopy (AFM) was used to describe surface morphology and roughness parameters of the films.

Photocatalytic studies indicate that TiO<sub>2</sub> photocatalyst with 0.80 wt. % Ce showed the highest rate of degradation of ciprofloxacin using simulated solar radiation.

**Keywords:** Ce-TiO<sub>2</sub>, ciprofloxacin, characterization, photocatalysis, simulated solar radiation.

## Photolytic and Photocatalytic Degradation of Trimethoprim in Aqueous Solution

Davor Ljubas<sup>1</sup>, Sandra Babić<sup>2</sup>, Lidija Ćurković<sup>3</sup>, Alan Badrov<sup>2</sup>

<sup>1</sup>Department of Energy, Power Engineering and Environment, Faculty of Mechanical Engineering and Naval Architecture, University of Zagreb, 10000 Zagreb, Croatia

<sup>2</sup>Department of Analytical Chemistry, Faculty of Chemical Engineering and Technology, University of Zagreb, 10000 Zagreb, Croatia

<sup>3</sup>Department of Materials, Faculty of Mechanical Engineering and Naval Architecture, University of Zagreb, 10000 Zagreb, Croatia

Trimethoprim (2,4-diamino-5-(3',4',5'-trimethoxybenzyl)pyrimidine) (TMP) is an antifolate antibacterial agent used worldwide in veterinary and human medicines for the treatment of bladder infections. It is often prescribed in combination with sulfamethoxazole due to their complementary and synergistic mechanisms but may be used as a monotherapy [1]. Due to its frequent use and very low elimination rate in WWTPs, TMP has been often detected in wastewater effluents and surface waters. Previous study has shown that TMP is resistant to biodegradation and hydrolysis, while solar radiation can cause slow degradation of TMP in favourable environmental conditions and lead to a decrease in its environmental concentration [1].

In this work, the mechanism of TiO<sub>2</sub> photocatalytic and photolytic (without photocatalyst) degradation of TMP was investigated. TiO<sub>2</sub> photocatalyst was used in a form of nanostructured film on glass ring placed on the bottom of the reactor [2]. As a source of radiation a simulated solar radiation lamp was used both for photolytic and photocatalytic experiments. The photocatalytic mechanism has been elucidated by scavenger studies using isopropanol, ammonium oxalate and triethanolamine as hydroxyl radicals, positive holes and superoxide radicals scavengers, respectively [3]. The results showed strong inhibition of photocatalytic degradation of TMP in presence of isopropanol and triethanolamine, which means that •OH and superoxide radicals were the primary reactive radicals responsible for the degradation process. No inhibition of the photocatalytic degradation of TMP in presence of ammonium oxalate was observed.

**Keywords:** Trimethoprim, photolysis, photocatalysis, simulated solar radiation, mechanisms of degradation

### References:

1. Biošić M, Babić S. Trimethoprim elimination by biotic and abiotic processes, *Fresenius Environmental Bulletin*, 29 (2020) 7972 – 7979.
2. Ćizmić M, Ljubas D, Rožman M, Ašperger D, Ćurković L, Babić S. Photocatalytic Degradation of Azithromycin by Nanostructured TiO<sub>2</sub> Film: Kinetics, Degradation Products, and Toxicity, *Materials*, 12(6) 2019, 873
3. Bertagna Silva D, Buttiglieri G, Babić B, Ašperger D, Babić S. Performance of TiO<sub>2</sub>/UV-LED-Based Processes for Degradation of Pharmaceuticals: Effect of Matrix Composition and Process Variables, *Nanomaterials*, 12(2) 2022; 12(2):295.

## Production of H<sub>2</sub>O<sub>2</sub> for water treatment by photoactive functionalized carbon nitride materials

André Torres-Pinto<sup>a,b\*</sup>, Hanane Boumeriame<sup>a,b</sup>, Cláudia G. Silva<sup>a,b</sup>, Joaquim L. Faria<sup>a,b</sup>, Adrián M.T. Silva<sup>a,b</sup>

<sup>a</sup> LSRE-LCM - Laboratory of Separation and Reaction Engineering – Laboratory of Catalysis and Materials, Faculty of Engineering, University of Porto, Rua Dr. Roberto Frias, 4200-465 Porto, Portugal

<sup>b</sup> ALiCE - Associate Laboratory in Chemical Engineering, Faculty of Engineering, University of Porto, Rua Dr. Roberto Frias, 4200-465 Porto, Portugal

There is a long-lasting [1] and recent [2] interest in carbon nitride (CN) and its composites concerning photocatalytic applications owing to the intrinsic optical, electronic, and chemical features of these materials. Their main limitation arises from the fast electron/hole recombination, and, to overcome this, several modification methods have been researched in recent years [3]. The production of hydrogen peroxide (H<sub>2</sub>O<sub>2</sub>) is being more and more explored, as H<sub>2</sub>O<sub>2</sub> is a powerful oxidizing agent capable of removing organic molecules from aqueous solutions.

In this work, different functionalized materials were investigated by a facile hydrothermal method under mild conditions and without toxic solvents. The molecules of glucose (G), anthraquinone (A) and perylene (P) were selected due to their promising interaction with CN. Compared to the unmodified CN material, the evolution rates of H<sub>2</sub>O<sub>2</sub> were improved up to 1.2, 1.5 and 2.6 times (Figure 1) for CN-G, CN-P and CN-A, respectively. Optical and electrochemical characterization data showed photoluminescence quenching and enhancement of the charge carrier transfer, proving the reduced recombination. Then, studying the band structure proved that the generation of H<sub>2</sub>O<sub>2</sub> was thermodynamically favored for the functionalized materials, while H<sub>2</sub>O<sub>2</sub> decomposition was suppressed. Finally, these materials were assessed for the photocatalytic removal of phenol, resulting in enhanced mineralization of the aqueous solutions.

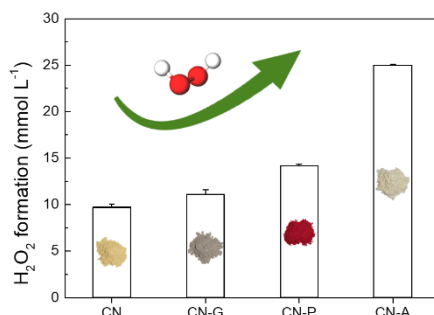


Figure 1. H<sub>2</sub>O<sub>2</sub> production after 2 h of irradiation using the CN materials in an isopropanol aqueous solution (90% v/v) under continuous air saturation.

### References

- [1] W.-J. Ong, L.-L. Tan, Y.H. Ng, S.-T. Yong, S.-P. Chai, *Chem Rev*, 116 (2016) 7159.
- [2] M. Ismael, *J. Alloys Compd.*, 846 (2020) 156446.
- [3] A. Torres-Pinto, M.J. Sampaio, C.G. Silva, J.L. Faria, A. M. T. Silva, *Catalysts*, 9 (2019) 990.

### Acknowledgments

A.T-P. acknowledges FCT for his scholarship SFRH/BD/143487/2019. This work was financially supported by projects: NORTE-01-0145-FEDER-031049 (InSpeCt) funded by the ERDF through NORTE 2020 and FCT/MCTES; NORTE-01-0145-FEDER-000069 (Healthy Waters) supported by NORTE 2020; LA/P/0045/2020 (ALiCE), UIDB/50020/2020 and UIDP/50020/2020 (LSRE-LCM), funded by FCT/MCTES.

## SPONSORS

## MASS SPECTROMETERS

PERFORM ANALYSIS WITH UNPARALLELED THROUGHPUT

- Equipped with Shimadzu's UFMS™ patented technology
- Increase specificity using the Library Screening MRM Spectrum mode
- Reduce instrument maintenance with excellent robustness
- Versatile configurations to fit your specific analysis
- Suitable for various agricultural and food contaminants analyses



## MultiNA

### Microchip

### Electrophoresis System



- Automated microfluidic device
- Wide range of amplicon detection (food allergens, pathogens, etc.)
- Higher sample throughput compared to conventional gel electrophoresis
- Compatible with 96-well PCR plates

## CHROMATOGRAPHS

### LIQUID CHROMATOGRAPHS

SIMPLIFY YOUR STARTUP

- Quick method setup for your specific applications
- Reduce method development cost



### GAS CHROMATOGRAPHS

FLEXIBLE CONFIGURATION

- (Carrier gas save) mode reduces operation costs
- Tool-free routine maintenance



### NEXERA UC

SUPERCRITICAL FLUID BASED TECHNOLOGY

- Suitable for both polar and non-polar samples
- Fully automated online sample preparation and analysis



## AXIMA Series

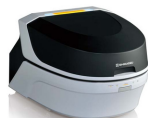
### MALDI-TOF MS

- Bacterial characterization with high discriminatory capacity
- Automated microbial identification with high accuracy



## SPECTROSCOPIES

- Routine toxic metal and foreign substance analysis



EDX



FTIR



UV-VIS



ICP

## ANALYTICAL BALANCES

SHORT RESPONSE TIME

- Accurate trace measurement with UniBloc Technology







OFFERING WHOLE ANALYTICAL SOLUTIONS IN WATER ANALYSIS

METHOD DEVELOPMENT

APPLICATION SUPPORT



Biotage-Horizon-5000



ACQUITY UPLC I-Class with Xevo TQ-S micro



Oasis Sample Extraction Products

Labtim Adria d.o.o.  
Jarušica 7/A, HR-10020 Zagreb

[www.labtim.hr](http://www.labtim.hr)

MCT LAB



# AlphaChrom

a member of Altium Group

# UVIJEK U TOKU



- | Plinska kromatografija
- | Tekućinska kromatografija
- | Spektrometrija masa - Q, QQQ, Q-TOF
- | Atomska spektroskopija - AAS, ICP-OES, MP-AES, ICP-MS, ICP-MSMS
- | Molekulska spektroskopija - FTIR, UV/Vis/NIR, fluorescencija, LDIR
- | Laboratorijska voda, mikrovalna tehnologija i analizatori žive, TOC/TN protočna analiza, termička analiza, autoklavi, klima i stabilizacijske komore, laboratorijska oprema i namještaj itd.
- | Laboratorijske kemikalije
- | Edukacije i programi osposobljavanja
- | Servis i podrška



**Agilent**

Authorized  
Distributor

**Honeywell**  
Authorized Distributor

 **starlab**

AlphaChrom d.o.o.

Karlovačka cesta 24, Blato HR-10000 Zagreb, Croatia

t: 01 550 2200 | e: prodaja@alphachrom.hr

www.alphachrom.hr

